NCHRP PROJECT 20-50 (14)

LTPP Data Analysis:
Significance of "As-Constructed" AC Air Voids to Pavement Performance

FINAL REPORT

Prepared for

National Cooperative Highway Research Program
Transportation Research Board
National Research Council

June 2002

Applied Pavement Technology, Inc.

Champaign IL • Chicago IL • Reno NV • Essex VT

TABLE OF CONTENTS

LIST OF FIGURES

LIST OF TABLES

INTRODUCTION

1.1.1 Background

Air void content, or the amount of voids in a compacted hot-mix asphalt (HMA) pavement can have a large effect on its performance. Unlike some of the other factors that affect pavement performance (e.g., surface thickness), air void content (AVC) can have a detrimental effect on the performance of the pavement if it is too high or too low. At high levels, it increases the likelihood of asphalt stripping, accelerated oxidation, and rapid deterioration. Because of consolidation under wheel loading, high AVC can also contribute to the development of rutting in the wheel paths. Low AVC, on the other hand, increases the likelihood of bleeding, shear flow, and permanent deformation (rutting) in the wheel paths. Accordingly, some control on compaction of a mix during construction is essential to achieving its maximum performance.

Most highway agencies are using AVC, along with other volumetric properties, such as voids in the mineral aggregate (VMA) or voids filled with asphalt (VFA), as measures of quality in their QC/QA specifications for HMA. Over the years, these agencies have developed statistical tolerances for AVC from historical data and set specification levels based on experience. Some state DOTs, e.g., Oregon and Washington, have actually used laboratory mix performance data to establish the effect of AVC on pavement performance (Linden, et al., 1989; and Bell, et al., 1984). The findings from these early studies indicate, for example, that for every one percent drop in AVC, there is a corresponding ten percent loss of pavement life. Despite the success of some of these studies, developing relationships between AVC and pavement performance has generally proven to be a difficult task, with no universally accepted standard available to user agencies. The lack of guidelines creates problems for agencies when changes in construction practices, test protocols, and materials lead to changes in AVC or structure. Agency efforts to implement the Superpave mix design procedure (McGennis et al. 1995) have demonstrated this particular problem.

In addition, information comparing as-designed and as-constructed AVC is generally not available in published form. Such comparisons may help quantify typical ranges in AVC variability based on normal construction practices. Data from the Federal Highway Administration (FHWA) Long-Term Pavement Performance (LTPP) program General Pavement Study (GPS) sections and especially from newly-constructed and routinely monitored test sections, e.g., LTPP Specific Pavement Study (SPS), WesTrack, and other accelerated pavement test studies, may shed some light on this subject.

By evaluating the available data in a coordinated fashion, this project has produced information to support on-going FHWA and NCHRP sponsored efforts in the area of performance-related specification (PRS) development. Thus, it will contribute to the preparation of improved construction specifications designed to enhance pavement performance.

As indicated by the project title, the primary objective of this study was to examine the significance of as-constructed AVC on HMA pavement performance. To achieve this primary objective, the following specific objectives were established:

1) Evaluate the use of LTPP data for determining the effect of in-place AVC and other

   mix volumetrics on the performance of HMA pavements.

2) Develop new or modified AVC guidelines for optimum pavement performance.

3) Examine the effect of the level of construction control between the LTPP GPS and

   SPS sections on the variability of as-constructed AVC and other volumetric

   properties.

Under the first objective, the goal was to evaluate available data in the LTPP database to develop prediction models and determine the sensitivity of pavement performance and HMA stiffness to as-constructed AVC. To satisfy the second objective, the results of the sensitivity analyses of LTPP models along with analyses of other existing models were analyzed to determine trends and, ultimately, to develop improved AVC guidelines that would optimize pavement performance. For the final objective, the goal was to evaluate available data in the LTPP database to examine the difference in AVC variability between pavement sections constructed with a level of quality control and quality assurance (GPS sections) associated with typical agency practice and those constructed with an anticipated higher level (SPS sections) because of the known experimental nature at the time of construction.

RESEARCH APPROACH

Accomplishment of the project objectives called for a coordinated research effort involving four key tasks, as summarized below.

1) <u>Develop prediction models for pavement performance and HMA stiffness using data available from the current FHWA LTPP program</u>. This purpose of this task, which is documented in Chapter 2, was to develop statistically sound prediction models that related certain measures of pavement performance, i.e., fatigue life and rutting life, and HMA stiffness to as-constructed AVC. The LTPP database was selected primarily because of its potential to provide a substantial amount of field data that could be used to establish a meaningful connection between pavement performance and AVC. Data from other notable field experiments (WesTrack, Mn/ROAD, FHWA-ALF, Louisiana TRC, and Austroads) were also examined; however, analyses were not conducted for two primary reasons. In the case of Mn/ROAD, FHWA-ALF and Louisiana TRC, the experiments were not designed to treat AVC as an independent variable; consequently, there was no basis to evaluate the effects of AVC

variability.   In the case of WesTrack and Austroads, analyses had already been performed and suitable models were available to evaluate their sensitivity to AVC.

The LTPP database contains thousands of pavement sections and is subdivided according to pavement type, experiment type and type of data.   Consequently, before any statistical analyses were performed, four basic steps were required to process the raw data into three separate project databases, one for fatigue life, one for rutting life and one for HMA stiffness. These steps are basically the same for all three databases:

- Screening and section selection – Under this step, candidate pavement sections from

  throughout the LTPP database were identified based primarily upon the availability of

  HMA test results which could be used to calculate the as-constructed AVC.   Other

  criteria for section selection depended upon the type of prediction model.   In the case of

  both fatigue life and rutting life models, past traffic information as well as performance

  data had to be available.   In addition, limiting criteria were established on certain

  pavement structural characteristics to avoid complications brought about by behavioral

  and performance differences in different pavement combinations.   For example, overlaid

  sections were excluded in the fatigue database because of the likely effect that the

  original asphalt surface would have on the rate of fatigue crack progression.

- Section classification – After screening, all the selected sections were classified within a

  matrix in order to establish the range of inference associated with any developed

  prediction model.   The two primary factors included in the classification were HMA

  surface thickness and environmental region (based on temperature and moisture).

- Calculation of AVC – For each selected LTPP section, AVC was calculated using a

  standardized formula and the laboratory test results available in the LTPP database.

  During this step of the process, it was found that much of the testing had been performed

  on samples obtained well after initial pavement construction.   Accordingly, 18 months

(after initial construction) was established as a cut-off point and all sections tested

beyond that point were eliminated from the database.

- Calculation of dependent variable – In this step, values for the dependent variable in the

  three databases were calculated.   In the case of fatigue life and rutting life, failure criteria

  were established and the number of ESAL applications required to achieve those levels

  was estimated based upon traffic information in the LTPP database.   In the case of HMA

  stiffness, the resilient modulus of the HMA surface was estimated through a process

  involving backcalculation analysis of nondestructive test data and an adjustment for mix

  temperature.

Once the three databases were completed, it was anticipated that statistical regression analyses
would be performed to produce the desired prediction models that would relate pavement
performance and HMA stiffness to as-constructed AVC.   Unfortunately, graphs of the data for
all three targeted models indicated that either no correlation existed or that the derived
relationship would not pass the test of reasonableness.   Thus, no LTPP-based prediction models
were produced.

2) Evaluate the sensitivity of pavement performance and HMA stiffness to AVC through the
analysis of available relationships.   The purpose of this task, which is documented in Chapter 3,
was to use available information from the literature (and any prediction models that might have
been derived from analysis of LTPP data) to evaluate the sensitivity of pavement performance
and HMA stiffness to AVC.   This effort required four basic steps:

- Literature search – An extensive search of the literature was conducted to identify any

  available prediction models that related pavement performance (in terms of fatigue

  cracking or permanent deformation) or HMA stiffness to AVC.   Initially, the focus of the

  search was on field performance and as-constructed AVC; however, because of limited

  past work, the search was expanded to include data from laboratory experiments.

- Development of sensitivity statistic – The sensitivity of the dependent variable (in this

  case, performance or HMA stiffness) in a prediction relationship to any one of the

  independent variables (in this case, AVC) is best represented by the change in the value

of the dependent variable as a result of a change in the value of the independent variable. For a linear relationship in which the independent variable appears in only one term, this sensitivity is represented by the coefficient on the independent variable. Graphically, it is depicted by the slope of the line in a graph of the dependent variable versus the independent variable. This approach to characterizing sensitivity was adopted for this study, since almost all the prediction models examined either exhibited this simple linear relationship or were adequately represented by it. To provide additional meaning to the sensitivity statistic, it was mathematically related to a term that has more engineering significance, i.e., the percent change in performance (or stiffness) versus the change in AVC. With this additional feature, it becomes possible to make statements about the sensitivity of an individual model such as: "It indicates that a one percent increase in AVC will result in a 10 percent decrease in fatigue life."

- Develop method to account for uncertainty – To provide an indication of the variability or uncertainty associated with the sensitivity of each model, all available measures of the statistical accuracy were reported. In addition, a rating of the overall reliability of each model is included. This rating is based on a subjective consideration of the quantity and quality of data used to develop the original model, the accuracy of the original fit, and how well it is represented by the sensitivity statistic.

- Determine sensitivity for each prediction model – Under this step, each prediction model was evaluated to determine its sensitivity to AVC and to characterize its uncertainty. The results were summarized in tabular form and then examined as a whole to identify trends and draw conclusions about the overall sensitivity.

3) <u>Examine the variability in air void content between select GPS and SPS sections from the LTPP experiment</u>. All SPS sections were constructed after the initiation of the SHRP LTPP

program in the late 1980s.   Most of the GPS sections, on the other hand, had been constructed before the experiment began.   Since the SPS sections were constructed to satisfy certain LTPP experimental design criteria, and since they constructed with a certain amount of LTPP oversight, it was believed that they would have experienced better quality control and exhibited lesser variability than their GPS counterparts.   Accordingly, the primary purpose of this task was to evaluate the LTPP GPS and SPS data and determine if these differences in variability did indeed exist.   These analyses were performed using standard statistical analysis approaches from several data perspectives.   The results are documented in Chapter 4.

4) <u>Develop guidelines for AVC in construction specifications</u>.   It is widely acknowledged that proper AVC is critical to achieving the maximum performance of an HMA surface layer.   What is not known is if there exists optimum ranges of AVC for performance in terms of fatigue cracking and permanent deformation and, to what extent do deviations from the target AVC actually affect performance.   The primary purpose of this task, therefore, was to use the information gathered from the analysis of LTPP data and other sources to develop improved AVC selection guidelines for use in pavement construction specifications.   This was accomplished (to the extent possible) through analysis of findings of the three tasks above.   The results are documented in Chapter 5.

analysis of ltpp data

2.1 OVERVIEW

This chapter summarizes the result of the analyses of LTPP data to develop prediction models that relate pavement performance and HMA stiffness to AVC.   Three separate analyses were conducted to produce models for fatigue cracking, permanent deformation, and HMA stiffness and are described in that order.   This chapter begins first with a description of the equation used to calculate AVC from LTPP data.

2.2 CALCULATION OF AIR VOID CONTENT

Air void content was determined from bulk and maximum specific gravity data in the IMS database.   Specifically, air void content was calculated using the following equation:

$$\text{AVC} = 100 \left(1 - \frac{G_{MB}}{G_{MM}} \right) \tag{1}$$

where:

AVC   = air void content (percent).

G_{MB} = bulk specific gravity of compacted HMA mixture from IMS table TST_AC02.

G_{MM} = maximum theoretical specific gravity of mixture from IMS table TST_AC03.

For most test sections, several samples were taken for testing of bulk specific gravity but only one sample was measured for maximum specific gravity.   In such a case, the maximum specific gravity was used to compute AVC for all locations of the section where samples were taken for testing of bulk specific gravity.

2.3 FATIGUE CRACKING ANALYSES

2.3.1 Selection of Test Sections

The LTPP IMS Database Release 10.9 (November 2000) was used for this project.   There were a total of 2,522 test sections in the database.   To select sections that were most suitable for

evaluating the effect of as-constructed AVC on pavement performance in terms of fatigue cracking, the following criteria were applied:

- Pavements with a HMA structural layers over granular base.

- Core samples (from which bulk and maximum specific gravity measurements were made) obtained within 18 months after construction.

- AVC data available for the bottom of the HMA structural layer.

- Traffic, pavement structure, and distress survey data available.

The following LTPP experiment types were included for section selection:

- GPS-1 Asphalt Concrete on Granular Base

- SPS-1 Strategic Study of Structural Factors for Flexible Pavements

- SPS-8 Study of Environmental Effects

- SPS-9 Superpave Asphalt Binder Study

As a result of this screening, only 15 sections, as shown in Table 1, were potentially useful for further fatigue analysis.

Table 1.   Summary of data availability for sections identified for fatigue analyses.

State Code	SHRP_ID	Experiment Type		Air Void Data	Monitored Traffic (years)	Fatigue Data (years)
4	0113	SPS	1	-	4	5
4	0114	SPS	1	-	5	5
4	0161	SPS	1	+	5*	4
4	0162	SPS	1	-	5	4
12	0101	SPS	1	+	3	1
12	0102	SPS	1	-	3	2
31	0113	SPS	1	-	2	2
31	0114	SPS	1	-	2	2
35	0101	SPS	1	+	1	3
35	0102	SPS	1	+	1	3
37	1992	GPS	1	+	2	1
39	0101	SPS	1	+	1	1
39	0102	SPS	1	-	1	1

| 42 | 1618 | GPS | 1 | + | 6 | 1 |
| 48 | 3835 | GPS | 1 | + | 7 | 5 |

*Estimated traffic from section 40162.
+ Section has air void content measured in the laboratory from core samples.
- Section does not have measured air void content. Data is from adjacent section of the same project.

2.3.2 Computation of Total Fatigue

The extent of pavement fatigue for a test section was determined from a combination of fatigue and longitudinal crack data stored in the IMS database.   To convert longitudinal cracking in the wheel path to an area, the linear extent was multiplied by 0.15 m (0.5 ft).   The following formula was used to compute the total fatigue area (m^2) on a test section:

Total Fatigue = AlligatorCrack(L, M, H) + LongitudinalCrack(L, M, H) * 0.15   (2)

Where:

AlligatorCrack(L, M, H)   = Areal sum (m^2) of measured alligator crack with low,

medium, and high severity levels.

LongitudinalCrack(L, M, H) = Linear sum (m) of measured longitudinal crack length

in wheel path with low, medium and high

severity levels.

The percentage of fatigue on a test section was determined from the total fatigue divided by the total area of the test section, as shown below:

Percent fatigue = Total fatigue / (Section Length * Section Width)   (3)

LTPP Sections are typically 152.4 m (500 ft) in length and 3.7 m (12 ft) in width, respectively. A 10 percent fatigue would roughly equal 56 m^2 (600 ft^2) for a typical test.

2.3.3 Findings

Since LTPP test sections were constructed at various times, experienced different traffic loadings, and exhibited various level of surface distress, some processing of the data was required to provide a basis for evaluating the effect of as-constructed AVC at the same fatigue cracking level.   This was accomplished by first determining the ESAL applications for all

sections reaching a 10 percent of fatigue cracking and then developing a relationship between ESAL applications and AVC.   Initially, there were a total of 15 sections identified for this purpose.   However, only five of the sections exhibited noticeable fatigue cracking by the last survey date.   Consequently, these were the only sections that could be considered in developing a relationship between ESAL applications and AVC.

Table 2 shows the classification matrix for sections identified for the fatigue analyses by environmental (climate and moisture) zone and pavement types for various HMA thickness and AVC levels.   The environmental zone for each section was determined using the environmental zone map contained in the *AASHTO Guide for Design of Pavement Structures* (AASHTO 1993).

Table 2.   Classification matrix for LTPP sections identified for fatigue cracking analysis.

| HMA Thickness (in) | Air Void Content (%) | Environmental Zone | | | | Total |
| | | Hot | | Freeze | | |
		Wet	Dry	Wet	Dry	
<4	<5	≤				
	≥5, ≤7	≥		1		1
	>7, ≤9					
	>9					
≥4, ≤6	<5					
	≥5, ≤7		1			1
	>7, ≤9		1			1
	>9					
>6, ≤8	<5					
	≥5, ≤7		1			1
	>7, ≤9					
	>9					
>8	<5	1				1
	≥5, ≤7					
	>7, ≤9					
	>9					
Total		1	3	1	0	5

To estimate the ESAL applications for a test section to reach 10 percent fatigue cracking, a linear regression equation between traffic loading and measured fatigue cracking was developed for the section.   The equation was then used to interpolate the ESAL applications for each section for the 10 percent fatigue cracking level.

With estimated ESAL applications and AVC, the basis for a correlation between the two was established.   Table 3 shows ESAL applications for all sections reaching the 10 percent fatigue cracking level, while Figure 1 graphically illustrates the relationship.

Table 3. Projected ESALs for sections with new HMA exhibiting 10 percent fatigue cracking.

State Code	SHRP ID	Experiment Type		HMA Thickness (in)	Initial Air Void Content (%)	Projected ESALs (1000)
42	1618	GPS	1	2	5.72	102
35	0102	SPS	1	4.8	6.39	16,129
4	0161	SPS	1	5.7	8.71	1,775
35	0101	SPS	1	7.2	6.82	18,138
48	3835	GPS	1	8.7	4.8	1,737
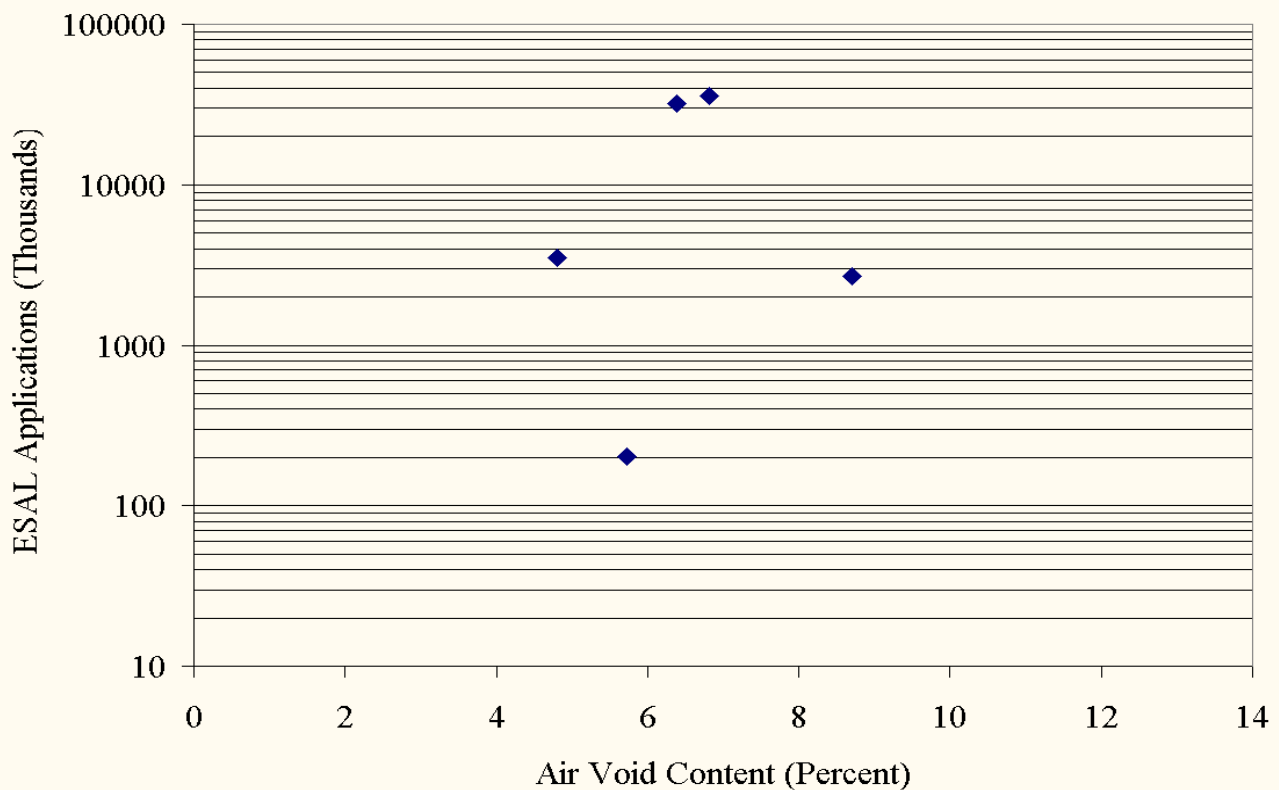
Figure 1. Relationship between estimated ESAL applications and air void content for
HMA sections exhibiting 10 percent fatigue cracking.

As can be seen, the data from the five test sections do not provide any indication of a relationship between AVC and fatigue cracking. While the data shown in Figure 1 is suggestive that peak performance is obtained with AVC in the 6 to 7 percent range, these results are considered inconclusive and the development of prediction model was deemed inappropriate. Some of the factors contributing to this finding from the LTPP data include:

- Test sections with no fatigue related cracking had been excluded from this analysis. Since many of the LTPP test sections in which as-constructed AVC data are available are still relatively young (less than 8 years), fatigue cracking is not yet evident and a valid assessment of the sensitivity is not possible.

- The fatigue cracking mechanism is more complicated than a direct relation to compaction expressed in terms of AVC. Other factors affect this relationship, with ESAL applications, pavement structure, and subgrade soil being the most significant.

2.4 PERMANENT DEFORMATION ANALYSES

2.4.1 Selection of Test Sections

To select sections suitable for the evaluating the effect of as-constructed AVC on pavement performance in terms of permanent deformation, the following criteria were applied:

- All types of HMA surfaced pavement structures were included.

- Core samples (from which bulk and maximum specific gravity measurements were made) obtained within 18 months after construction.

- AVC data available for the uppermost HMA structural layer.

- Traffic, pavement structure, and rut depth computations from transverse profile data available.

The following LTPP experiment types were included for section selection:

- GPS-1 Asphalt Concrete (AC) on granular base

- GPS-2 AC on bound Base

- GPS-6 AC Overlay on AC Pavement

  o 6A – AC overlay placed before LTPP monitoring

- o 6B – Conventional AC overlay

- o 6C – Modified asphalt AC overlay

- o 6D – Second or third AC overlay

- o 6S – AC overlay with structural milling of existing surface

- GPS-7 AC Overlay on PCC Pavement

  - o 7A – AC overlay placed before LTPP monitoring

  - o 7B – Conventional AC overlay

  - o 7C – Modified asphalt AC overlay

  - o 7D – Second or third AC overlay

  - o 7S – AC overlay with structural milling of existing surface

- SPS-1 Strategic Study of Structural Factors for Flexible Pavements

- SPS-5 Rehabilitation of AC Pavements

- SPS-6 Rehabilitation of Jointed PCC Pavements

- SPS-8 Study of Environmental Effects

- SPS-9 Superpave Asphalt Binder Study

After applying these criteria, the 100 sections listed in Table 4, were found to be candidates for the permanent deformation investigation.

Table 4. Summary of data availability for sections identified for rutting analyses (continued).

State Code	SHRP_ID	Experiment Type		Air Void Content Data	Monitored Traffic (years)	Rut Data (number of measurements)
2	1004	GPS	6B	+	2	5
4	0115	SPS	1	+	5	3
4	0116	SPS	1	+	5	3
4	0117	SPS	1	-	5	3
4	0118	SPS	1	-	5	3
4	0119	SPS	1	-	5	3
4	0120	SPS	1	-	5	3

Table 4. Summary of data availability for sections identified for rutting analyses (continued).

State Code	SHRP_ID	Experiment Type		Air Void Content Data	Monitored Traffic (years)	Rut Data (number of measurements)
4	0121	SPS	1	-	5	3
4	0122	SPS	1	+	5	3
4	0123	SPS	1	-	5	3
4	0124	SPS	1	+	5	3
5	3058	GPS	2	+	6	3
6	8534	GPS	6B	+	7	4
6	8535	GPS	6B	+	7	3
8	6002	GPS	6C	+	2	2
9	4020	GPS	7B	+	5	4
17	5151	GPS	7B	+	7	4
24	1634	GPS	6C	+	1*	1
26	0603	SPS	6	+	8	5
26	0604	SPS	6	-	8	5
26	0606	SPS	6	-	8	4
26	0607	SPS	6	-	8	5
26	0608	SPS	6	-	8	5
29	5403	GPS	6B	+	8	5
29	5413	GPS	6B	+	9	4
30	0502	SPS	5	+	5	3
30	0503	SPS	5	-	5	3
30	0504	SPS	5	-	5	3
30	0505	SPS	5	+	5	2
30	0506	SPS	5	-	5	3
30	0507	SPS	5	-	5	3
30	0508	SPS	5	-	5	3
30	0509	SPS	5	-	5	3
30	7066	GPS	6B	+	6	3
30	7076	GPS	6B	+	6	3
30	7088	GPS	6B	+	6	3
31	0115	SPS	1	-	2	3
31	0116	SPS	1	-	2	2
31	0117	SPS	1	-	2	3
31	0118	SPS	1	-	2	2
31	0119	SPS	1	-	2	3
31	0120	SPS	1	+	2	2
31	0121	SPS	1	+	2	3
31	0122	SPS	1	-	2	2
31	0123	SPS	1	-	2	3
31	0124	SPS	1	-	2	3

Table 4.   Summary of data availability for sections identified for rutting analyses (continued).

State Code	SHRP_ID	Experiment Type		Air Void Content Data	Monitored Traffic (years)	Rut Data (number of measurements)
34	0502	SPS	5	-	7	5
34	0503	SPS	5	+	7	5
34	0504	SPS	5	+	7	5
34	0505	SPS	5	-	7	5
34	0506	SPS	5	-	7	5
34	0507	SPS	5	+	7	5
34	0508	SPS	5	+	7	5
34	0509	SPS	5	-	7	5
34	0559	SPS	5	+	7	5
35	0103	SPS	1	-	1	2
35	0104	SPS	1	-	1	2
35	0105	SPS	1	+	1	2
35	0106	SPS	1	-	1	2
35	0107	SPS	1	-	1	2
35	0108	SPS	1	-	1	2
35	0109	SPS	1	+	1	2
35	0110	SPS	1	-	1	2
35	0111	SPS	1	+	1	2
35	0112	SPS	1	+	1	1
39	0103	SPS	1	+	1	3
39	0104	SPS	1	-	1	2
39	0105	SPS	1	+	1	3
39	0106	SPS	1	-	1	3
39	0107	SPS	1	-	1	1
39	0108	SPS	1	-	1	3
39	0109	SPS	1	-	1	3
39	0110	SPS	1	-	1	3
39	0111	SPS	1	+	1	2
39	0112	SPS	1	-	1	2
39	0160	SPS	1	-	1	3
39	5010	GPS	7B	+	4	3
40	4086	GPS	6B	+	3	5
40	4161	GPS	2	+	2	5
42	1617	GPS	7B	+	8*	3
42	1618	GPS	6B	+	6	5
42	1691	GPS	7B	+	6	4
48	1119	GPS	6B	+	9	6
48	A502	SPS	5	-	8	5
48	A503	SPS	5	-	8	5

Table 4. Summary of data availability for sections identified for rutting analyses (continued).

State Code	SHRP_ID	Experiment Type		Air Void Content Data	Monitored Traffic (years)	Rut Data (number of measurements)
48	A504	SPS	5	-	8	5
48	A505	SPS	5	-	8	5
48	A506	SPS	5	-	8	5
48	A507	SPS	5	-	8	5
48	A508	SPS	5	-	8	5
48	A509	SPS	5	+	8	5
51	1419	GPS	6B	+	7	5
51	1419	GPS	6D	+	2	2
53	1008	GPS	6B	+	4	4
81	1805	GPS	6B	+	4*	3
83	6450	GPS	6B	+	4	3
83	6451	GPS	6B	+	3	3
89	1125	GPS	6B	+	2	2
90	6410	GPS	6B	+	7	3
90	6412	GPS	6B	+	7	3

* Traffic applications were from estimated information stored in the LTPP database.
+ Section has air void content measured in the laboratory from core samples.
- Section does not have measured air void content. Data is from adjacent section of the same project.

2.4.2 Computation of Permanent Deformation

In LTPP, permanent deformation (rutting) is available from three types of measurements.   One of the first rut measurement devices was a 1.2-m (3.9-ft) long straight edge, similar to the device used at the AASHO Road Test.   The other two sources are based on measurement of the transverse profile across the test lane.   To obtain rutting information, the transverse profile shapes had to be interpreted.   This interpretation was performed under one of the LTPP sponsored data analysis efforts (Simpson 1999).

A variety of transverse profile distortion indices are stored in LTPP database that can be used to characterize rutting. Quantification of rutting is complex and much more difficult than is apparent to a casual observer.   While LTPP has not yet developed indices that capture all aspects of rut characterization, one relatively simple measure of total rut depth was used on this project. The two measures of rut depth considered for this project are based on a 1.83-m (6-ft) straight edge and lane width wire line reference.

The straightedge rut depth method is based on positioning the straight edge at various locations in each lane half, until the maximum displacement from the bottom of the straightedge to the

pavement surface is found.   As shown in Figure 2, at each measurement location, three surface profile distortion indices are computed for each lane half.   These include rut depth, offset from lane edge to the point of maximum depth, and depression width.
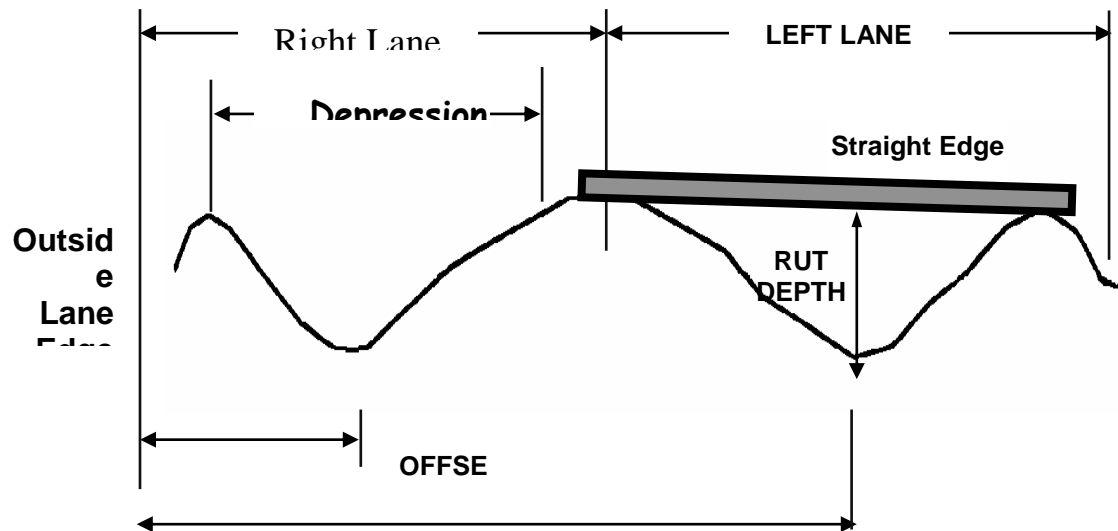
Figure 2.   Illustration of LTPP transverse pavement distortion indices based on 1.8-m (6-ft) straightedge reference.   Distortion indexes computed for each lane half include depth, offset to point of maximum depth, and depression width.

The lane width wire rut indices are based on anchoring an imaginary wire line at each lane edge. The wire reference connects any peak elevation points which extend above the lane edges with straight lines.   The wire line reference method is illustrated in Figure 3, the same type of pavement surface profile distortion indices as those for the straightedge are computed.
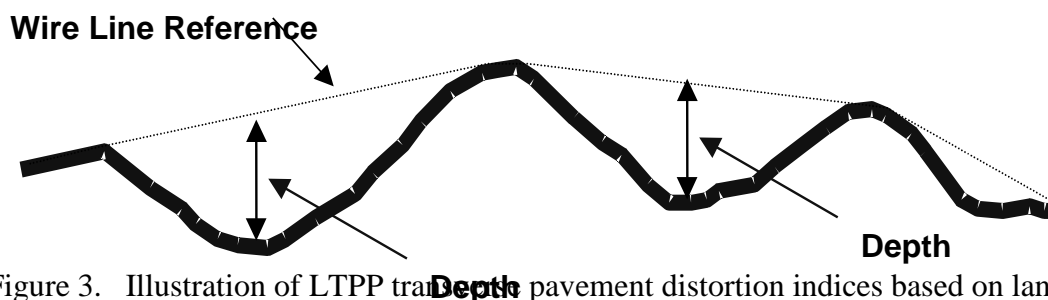
Figure 3.   Illustration of LTPP transverse pavement distortion indices based on lane width wire line reference.   Distortion indexes computed for each lane half include depth, offset, and depression width.

In many cases, the wire line and straightedge techniques produced identical results, however, there is a subset of sections where they did not. If all of the points between the lane edges fall below the datum between the lane edge elevations, then the wire reference method will produce rut depths greater than those from the straightedge. Thus, the wire line method is very sensitive to the lane edge end point locations. Observation of many LTPP transverse profile plots suggests that the lane edge endpoints are variable along a test section. The relationship between the straightedge and wire reference depth is shown in Figure 4. As suspected, the wire reference depth is always either equal to or greater than the straightedge depth.

For this study, the 1.8-m (6-ft) straightedge indices were used since distortions in the transverse profile relative to the wheel path locations and not to the lane edges were of primary interest. These indices should provide a better measure of the HMA mix stability subject to wheel load effects.
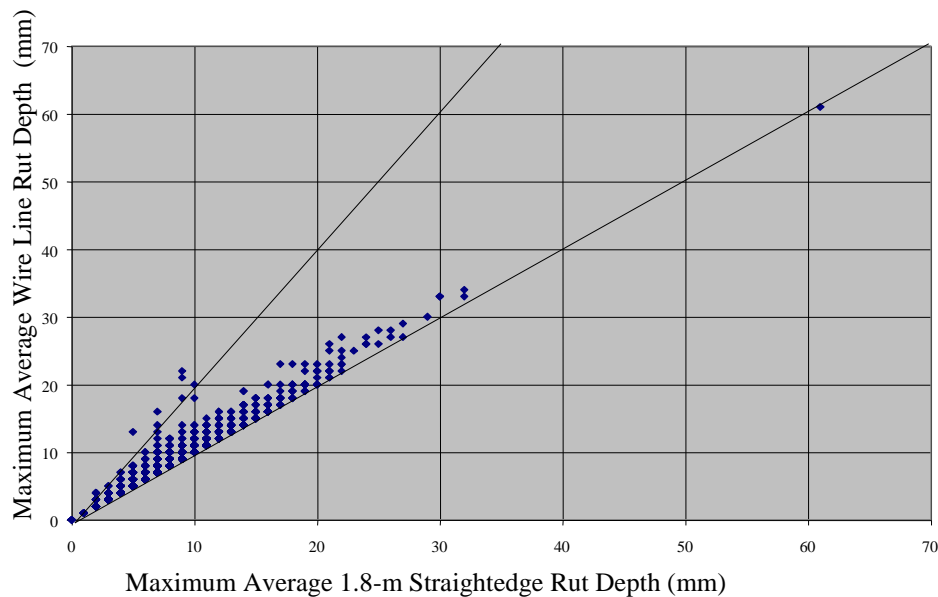
Figure 4. Relationship between straightedge and wire line rut depths for GPS 1 and 2 test sections. Lines represent 1:1 and 2:1 ratios.

2.4.3 Findings

Since LTPP test sections were constructed at various times, experienced different ESAL traffic levels, and exhibited various levels of surface distress, the use of raw rut depth measurements in the evaluations would be misleading. Instead, it was decided that to investigate the relationship of AVC to permanent deformation, rutting performance would be expressed in terms of the number of projected ESAL applications to a specified rut depth. This approach requires interpolation within or extrapolation of the data. To avoid over-extrapolation, a rut depth of 6-mm (0.25-in) was selected, due to the relatively young age (less than 10 years) of the LTPP sections that had the necessary data available.

There were initially 100 sections identified for this purpose.   Further examination of the data indicated that AVC data for many SPS sections were not directly measured and were also shared with the same AVC data from an adjacent section (thereby creating the potential to confound the analysis).   After excluding these types of sections, only 51 sections remained.

Table 5 shows the classification matrix for those sections identified for permanent deformation analyses by environmental (climate and moisture) zone and pavement type for various HMA thicknesses and AVC.   (Note: The pavement type labeled as COMP refers to AC overlays on PCC pavements).

Table 5.   Classification matrix for LTPP sections identified for rutting analysis.

HMA Thickness (in)	Air Void Content (%)	Environmental Zone								Total
		Hot				Freeze				
		Wet		Dry		Wet		Dry		
		Pavement Type								
		HMA	Comp	HMA	Comp	HMA	Comp	HMA	Comp	
<4	<5			1			2			3
	≥5, ≤7						1			1
	>7, ≤9									
	>9					1				1
≥4, ≤6	<5			1			2	1		4
	≥5, ≤7			1			1	2		4
	>7, ≤9	1		3				1		5
	>9			1		2				3
>6, ≤8	<5					1		2		3
	≥5, ≤7					1		4		5
	>7, ≤9	1		2		3				6
	>9			1						1
>8	<5	1				7		3		11
	≥5, ≤7	1						1		2
	>7, ≤9	1								1
	>9							1		1
Total		5		10		15	6	15		51

To estimate ESAL applications for each test section reaching a 6-mm (0.25-in) rut depth, a linear regression equation between ESAL applications and measured rut depth was developed.   The equation was then used to estimate ESAL applications for each section based upon a 6-mm (0.25-in) rut depth.

Because of the different pavement type combinations, the analyses of the rutting data were divided into three categories. The first two categories are classified as HMA in Table 5.

- Newly constructed HMA pavements.

- HMA overlays on HMA pavements.

- HMA overlays on PCC pavements.

The findings are discussed below.

Newly Constructed HMA Pavements

With the estimated ESAL applications and AVC, a correlation between traffic application and AVC was performed. Table 6 presents the ESAL applications for the 15 newly constructed HMA sections reaching 6-mm (0.25-in) rut depth. Most of these test sections are located on SPS-1 projects with a mixture of base material types.

Figure 5 graphically illustrates the relationship between ESAL applications and AVC. Inexplicably, the relationship suggests better rut performance for mixtures with an in-place AVC of 10 percent, compared to an expected value in the range of 5 to 8 percent. Interestingly, the test sections with the better rut-resistant mixtures are located in relatively hot regions of Arizona and New Mexico.

Table 6. Estimated ESAL applications to reach a 6-mm (0.25-in) rut depth for newly constructed HMA sections.

State Code	SHRP_ID	Experiment Type		HMA Thickness (in)	Air Void Content (%)	Projected_ESAL (1000)
40	4161	GPS	2	2.8	1.36	63.5
39	0103	SPS	1	3.9	11.17	327.7
39	0105	SPS	1	4	11.8	213.2
39	0111	SPS	1	4	9.76	696.2
4	0116	SPS	1	4.1	9.75	1439.6
4	0122	SPS	1	4.2	10.52	1302.3
31	0120	SPS	1	4.7	5.8	259.0
35	0111	SPS	1	5	7.5	767.4
35	0112	SPS	1	5.1	7.5	750.0
31	0121	SPS	1	5.3	5.8	321.3
35	0105	SPS	1	5.9	7.23	674.8
5	3058	GPS	2	6	7.63	792.0
4	0115	SPS	1	6.6	9.75	2119.7
4	0124	SPS	1	6.7	9.75	1385.4
35	0109	SPS	1	8	7.5	654.9
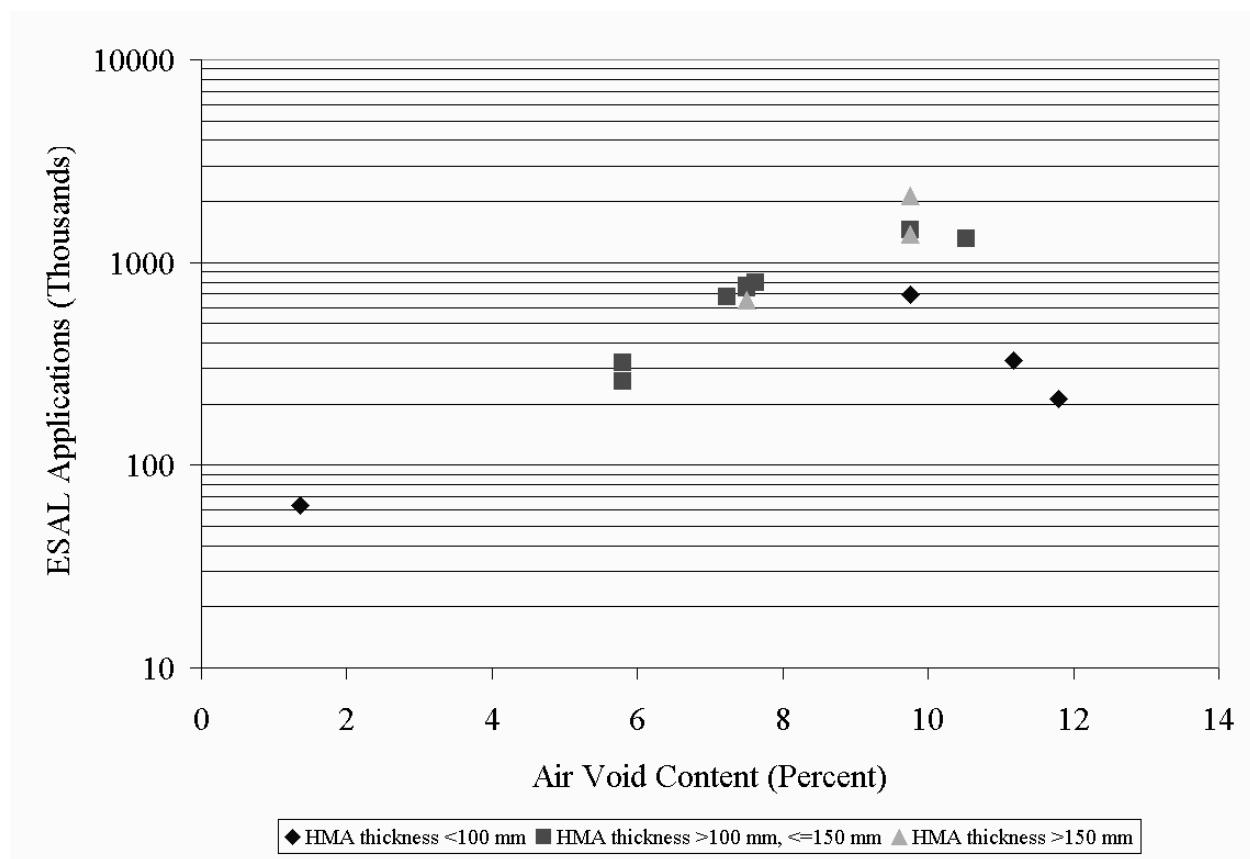
Figure 5. Relationship between estimated ESAL applications to reach 6-mm (0.25-in) rut depth and AVC for newly constructed HMA pavement sections.

HMA Overlays on HMA Pavements

Table 7 presents the estimated ESAL applications to reach a 6-mm (0.25-in) rut depth for the 30 sections having an HMA overlay on a pre-existing HMA pavement. Most of these test sections are from the GPS-6B experiment, which are HMA mixtures using non-modified binders placed on a HMA surface with no prior cold milling. The two pavement sections in the GPS-6C experiment have overlay mixes with a modified binder. The HMA thickness shown is the total for both the HMA overlay and original HMA layer.

Figure 6 graphically illustrates the relationship between ESAL applications and the AVC of the HMA overlay. As can be seen, there are no discernable trends in the relationships between AVC and HMA rutting performance. This may be due to a combination of different mix types. (For example, the two overlays containing the modified HMA mixtures (GPS-6C sections) have the poorest resistance to permanent deformation. However, it could also be due to uncertainty in the estimated ESAL applications and the influence of the underlying pavement.

HMA Overlays on PCC Pavements

Table 8 shows the estimated ESAL applications to reach a 6-mm (0.25-in) rut depth for the 6 sections having an HMA overlay on an existing PCC pavement.   Figure 7 graphically illustrates the relationship of rutting performance with respect to AVC.

While there is an apparent trend for improved rut performance with AVC increasing from 2 to 7 percent, a model developed from so few data points and with such variablilty would be statistically insignificant.   Furthermore, no observations exist for AVC values above 8 percent, where the rutting trend would likely reverse.

Table 7. Estimated ESAL applications to reach 6-mm (0.25-in) rut depth for HMA overlay sections on HMA pavements.

State Code	SHRP_ID	Experiment Type		HMA Thickness (in)	Air Void Content (%)	Projected_ESAL (1000)
2	1004	GPS	6B	5.4	3.97	205.0
40	4086	GPS	6B	5.5	1.56	589.2
53	1008	GPS	6B	5.6	8.33	447.7
29	5403	GPS	6B	6.2	8.89	1497.4
30	7088	GPS	6B	6.6	6.68	1083.6
83	6451	GPS	6B	6.7	5.33	2255.3
24	1634	GPS	6C	6.8	7.71	70.3
30	0505	SPS	5	6.8	3.19	1543.8
29	5413	GPS	6B	6.9	6.97	1328.0
48	1119	GPS	6B	6.9	8.46	319.5
30	0502	SPS	5	6.9	5.62	861.1
30	7066	GPS	6B	7.1	5.61	1072.6
89	1125	GPS	6B	7.1	7.25	456.5
30	7076	GPS	6B	7.6	0.93	213.9
42	1618	GPS	6B	7.9	4.08	134.4
6	8534	GPS	6B	8.2	6.65	1047.1
51	1419	GPS	6B	9.5	4.88	404.2
83	6450	GPS	6B	10.3	4.24	1850.3
6	8535	GPS	6B	10.4	7.65	1889.2
8	6002	GPS	6C	10.5	5.96	206.9
34	0559	SPS	5	11	3.42	2374.2
51	1419	GPS	6D	11.1	4.23	397.9
48	A509	SPS	5	12.1	4.49	804.4
34	0504	SPS	5	13.2	3.86	1970.7
90	6410	GPS	6B	13.6	3.03	443.8
34	0503	SPS	5	13.7	3.8	2729.3
34	0507	SPS	5	14.2	3.75	2249.7
34	0508	SPS	5	14.9	3.86	2594.3
81	1805	GPS	6B	16.3	9.1	1043.0
90	6412	GPS	6B	16.8	2.96	1086.5
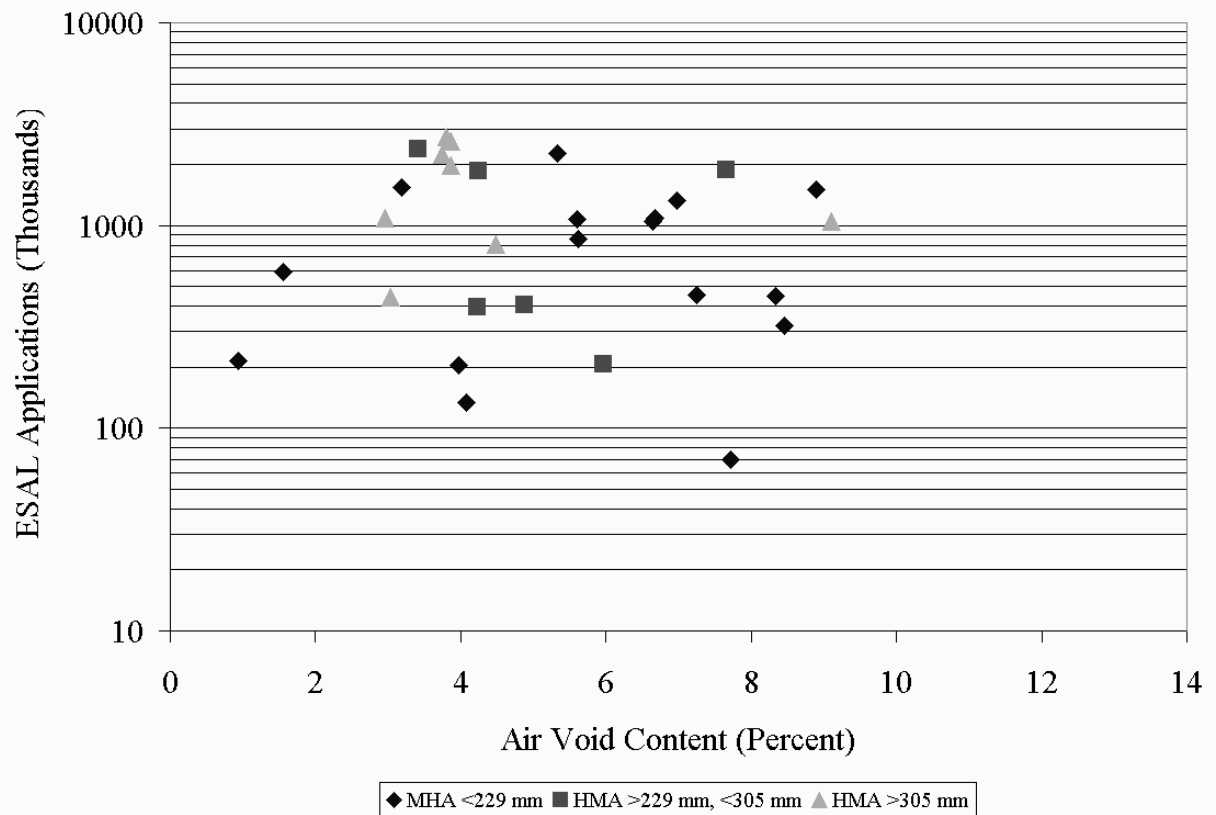
Figure 6. Relationship between estimated ESAL applications and AVC for HMA overlay sections (on existing HMA pavements) exhibiting 6-mm (0.25-in) rut depth.

Table 8. Estimated ESAL applications for HMA overlaid sections on existing PCC pavements reaching a 6-mm (0.25-in) rut depth.

State Code	SHRP_ID	Experiment Type		HMA Thickness (in)	Air Void Content (%)	Projected_ESAL (1000)
9	4020	GPS	7B	3.4	6.97	1093.2
17	5151	GPS	7B	3.3	4.29	7805.3
26	0603	SPS	6	5.1	1.79	2012.6
39	5010	GPS	7B	2.8	3.16	570.2
42	1617	GPS	7B	4.7	6.8	9362.6
42	1691	GPS	7B	4	2.09	443.6
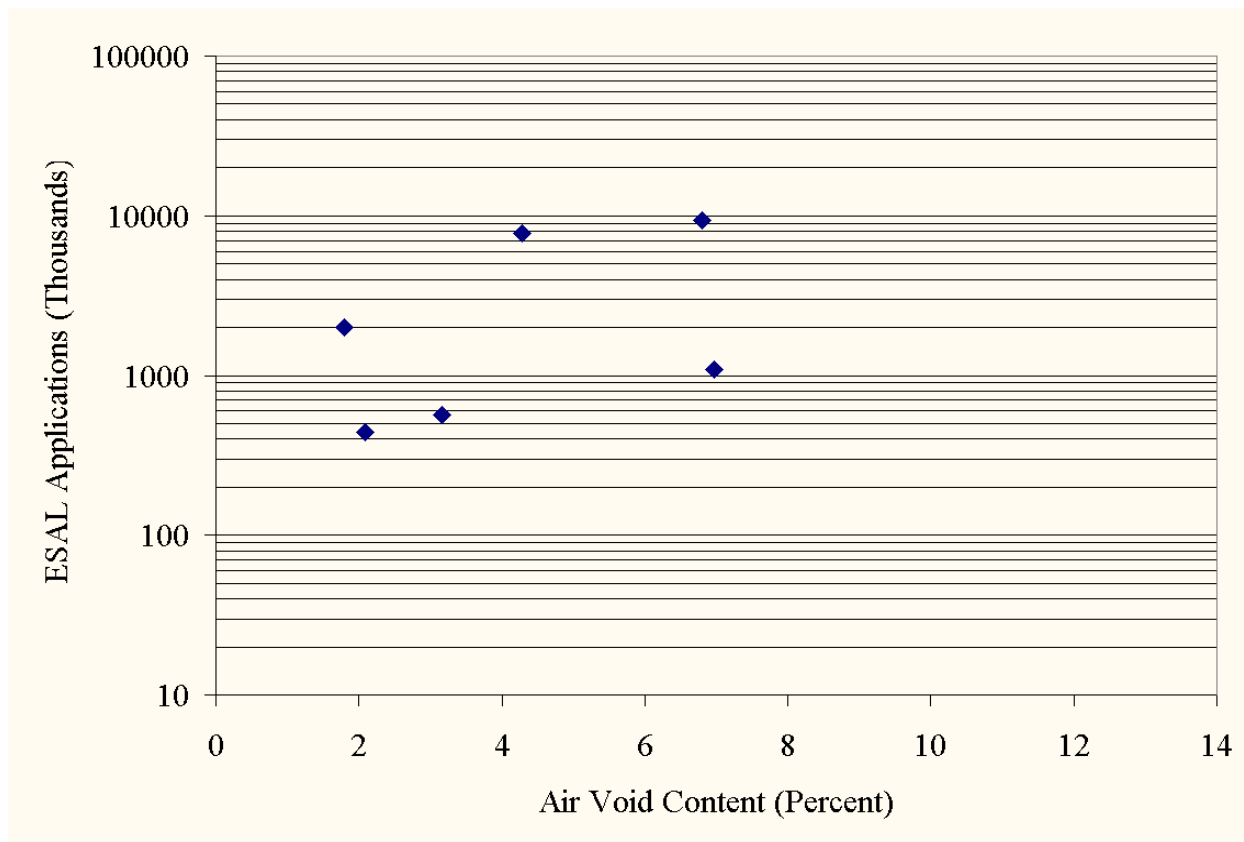
Figure 7.   Relationship between estimated ESAL applications and AVC for HMA overlay sections (on existing PCC pavements) exhibiting 6-mm (0.25-in) rut depth.

2.5 HMA STIFFNESS ANALYSES

2.5.1 Selection of Test Sections

All test sections identified for fatigue cracking and permanent deformation analyses were used as data for evaluating the effect of AVC on HMA stiffness.   However, review of the current LTPP database found only a few sections having HMA stiffness information from deflection measurement backcalculation.   Thus, to complete this analysis, a simplified backcalculation analysis was performed using the available deflection measurements for each section.

2.5.2 Estimation of HMA Stiffness

The BOUSDEF backcalculation program (Zhou et al. 1990) was selected as the tool to estimate the HMA stiffness (in-situ elastic modulus) for each section.   BOUSEF was selected because of its simplicity, accuracy, and the speed at which it can be used to process the data from all the

sections.   The deflection data collected closest to the date of laboratory bulk and maximum specific gravity tests were used in backcalculation.   Raw deflection data, obtained from the outer wheel path, near 40-kN (9000-lb) FWD load and from the third load drop, were used in the backcalculation analyses.

Pavement structural data were obtained directly from the LTPP database.   During backcalculation, the following simplifications were made:

- Layers with similar materials were combined. (For example, a granular base was combined with a granular subbase).

- Thin layers directly beneath a thick HMA or PCC were basically treated as a support layer and combined with the next uppermost layer.

- Typical Poisson's ratios for the various layer materials were used.

To correlate HMA modulus with AVC at the same temperature, the backcalculated HMA moduli for each section were averaged and adjusted to 20 °C (68 °F) using the following equation (Lukanen et al. 2000):

$$\text{ATAF} = 10^{\text{slope}*(T_r - T_m)} \tag{4}$$

Where:

ATAF = Asphalt temperature adjustment factor.

Slope = Slope of the log modulus versus temperature equation (-0.0195 for the wheel path and -0.021 for mid-lane are recommended).

T_r = Reference mid-depth HMA temperature (^{o}C).

T_m = Mid-depth HMA temperature at time of measurement (^{o}C).

The estimated modulus at 20 °C was obtained by multiplying the unadjusted modulus by ATAF.

For this project, measured surface temperatures, rather than mid-depth HMA temperatures, were used for correction purposes.   The mid-depth HMA temperature was preferred, however, the effort required to estimate this temperature from other inputs such as exact timing of the deflection test, the depth for predicting the asphalt temperature, and average air temperature for five days prior to deflection test, made its use prohibitive.   Furthermore, measured surface

temperature has often been used in pavement design projects as a first-order correction. (Considering the positive outcome of this effort, this may be an area where more attention should be given in future research to developing a better relationship).

2.5.3 Findings

Initially, there were a total of 56 sections (five for fatigue cracking and 51 for permanent deformation analyses) that could be used in the investigation. During the backcalculation analysis, however, six sections either did not have deflection data or the backcalculation program did not yield a solution from a measured deflection basin. As a result, only 50 sections were included in the remaining analyses.

Table 8 shows the classification matrix for sections identified for stiffness analyses by environmental (climatic and moisture) zone and pavement type for various HMA thicknesses and AVC.

Table 8. Classification matrix for LTPP sections identified for stiffness analysis.

HMA Thickness (in)	Air Void Content (%)	Hot Wet HMA	Hot Wet Comp	Hot Dry HMA	Hot Dry Comp	Freeze Wet HMA	Freeze Wet Comp	Freeze Dry HMA	Freeze Dry Comp	Total
<4	<5			1			2			3
	≥5, ≤7					1	1			2
	>7, ≤9									
	>9									
≥4, ≤6	<5			1			1			2
	≥5, ≤7			2			1	2		5
	>7, ≤9	1		4					1	6
	>9			1						1
>6, ≤8	<5	1							2	3
	≥5, ≤7			1					4	5
	>7, ≤9	1		2			3			6
	>9			1						1
>8	<5	2					7		3	12
	≥5, ≤7	1							1	2
	>7, ≤9	1								1
	>9								1	1
Total		7		13		1	15	2	12	50

The HMA layer moduli were first backcalculated for all the selected LTPP sections from the raw deflection data. Figure 8 illustrates the general correlation between the backcalculated HMA layer modulus and the measured pavement surface temperature during testing. The high-low points for the range of backcalculated moduli are shown for each point. Considering the fact that a multitude of mixes is represented, this graph indicates that a strong relationship between HMA modulus and temperature does exist.
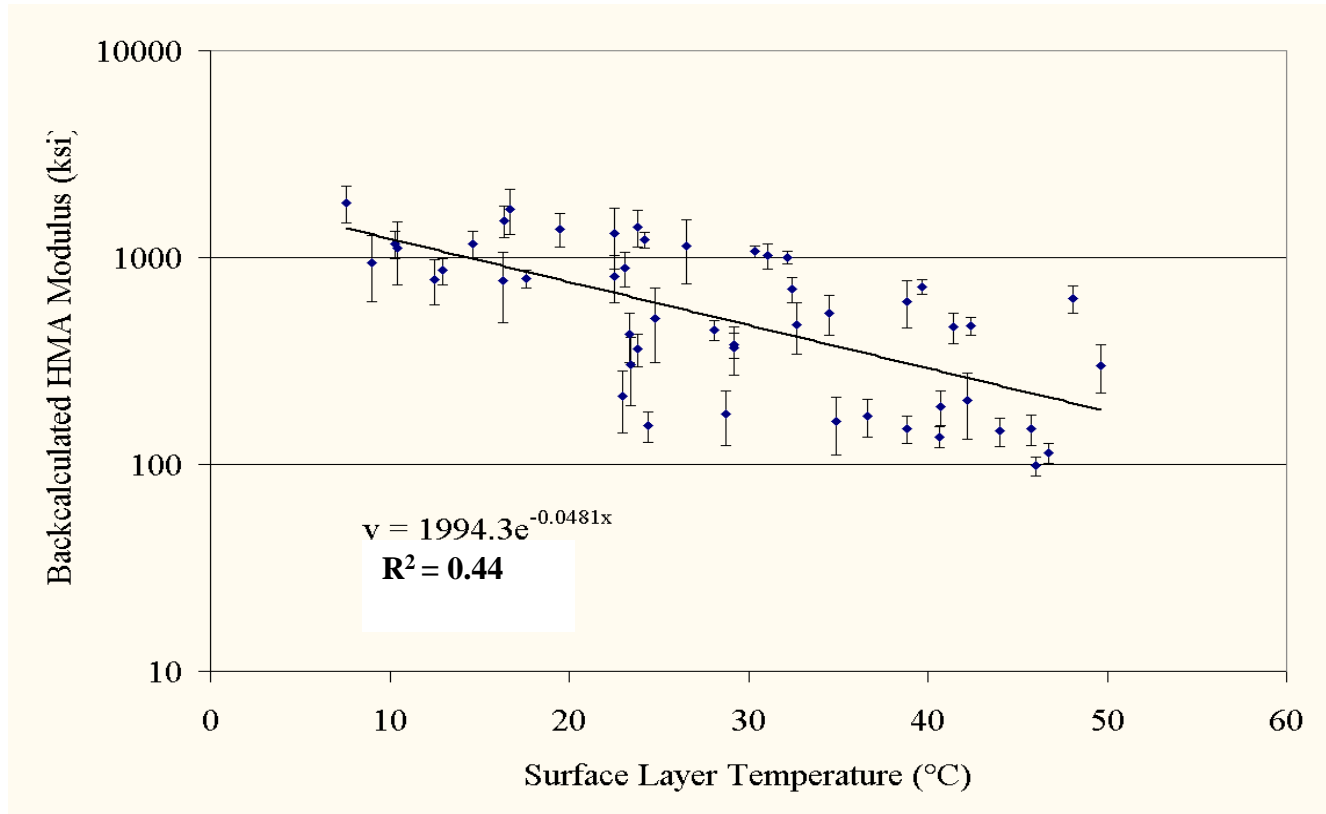
Figure 8. Relationship between HMA modulus versus pavement surface temperature for the selected LTPP sections.

Since HMA stiffness is temperature sensitive, it is necessary to extract its effect if an accurate assessment of the sensitivity of HMA stiffness to as-constructed AVC is to be conducted. Consequently, a standard temperature of 20 °C (68 °F) was chosen as a basis for correction.

The preferred method for temperature correction is to develop a modulus-temperature relationship for each LTPP section and use this relationship as the basis to adjust to the 20 °C (68 °F). However, not all the LTPP test sections have enough data collected at different temperatures to develop this type of site-specific relationship. Accordingly, the relationship between modulus-temperature developed using data from the LTPP database by other researchers (equation 4) was used for adjustment purposes.

Table 9 presents the AVC versus HMA layer stiffness (adjusted to the 20 °C temperature) while Figure 9 graphically illustrates their relationship. Figure 9 indicates that there is a slight tendency for the HMA stiffness (elastic modulus) to increase with increasing AVC; however, the relationship is not significant and no prediction model could be developed.

2.6 SUMMARY

This chapter presents the results of analyses of LTPP data for the ultimate purpose of developing prediction models that related fatigue performance, rut performance, and HMA stiffness to as-constructed air void content. Based upon the data analyses, the results can be summarized as follows:

1. Fatigue Cracking: Because of limited number of pavement sections (5) that satisfied the selection criteria and the scatter of the data, no relationship between fatigue performance and AVC could be established.

2. Rutting: Rut performance was evaluated for three principal pavement types in the LTPP database.

   - The analysis of data from newly constructed HMA pavements showed unreasonable results (i.e., an optimum AVC of about 10 percent). However, only limited number of pavement sections (15) satisfied the selection criteria.

Table 9. HMA layer stiffness adjusted to 20 °C standard temperature.

State Code	SHRP_ID	Experiment Type		HMA Thickness (in)	Air Void Content (%)	Modulus Adjusted to 20°C (1000 psi)
37	1992	GPS	1	2.4	5.27	1,675.2
40	4161	GPS	2	2.8	1.36	259.4
39	5010	GPS	7B	2.8	3.16	361.3
17	5151	GPS	7B	3.3	4.29	653.4
9	4020	GPS	7B	3.4	6.97	494.3
42	1691	GPS	7B	4	2.09	633.0
4	0116	SPS	1	4.1	9.75	725.1
4	0122	SPS	1	4.2	10.52	558.8
31	0120	SPS	1	4.7	5.8	243.2
42	1617	GPS	7B	4.7	6.8	1477.4
35	0102	SPS	1	4.8	6.39	1031.8
35	0111	SPS	1	5	7.5	376.8
35	0112	SPS	1	5.1	7.5	315.9
31	0121	SPS	1	5.3	5.8	314.2
40	4086	GPS	6B	5.5	1.56	836.8
53	1008	GPS	6B	5.6	8.33	1746.4
4	0161	SPS	1	5.7	8.71	574.9
35	0105	SPS	1	5.9	7.23	424.8
5	3058	GPS	2	6	7.63	2237.5
29	5403	GPS	6B	6.2	8.89	1459.4
30	7088	GPS	6B	6.6	6.68	1527.8
4	0115	SPS	1	6.6	9.75	1051.0
83	6451	GPS	6B	6.7	5.33	711.2
4	0124	SPS	1	6.7	9.75	1470.8
30	0505	SPS	5	6.8	3.19	551.6
12	0101	SPS	1	6.8	4.98	1706.9
24	1634	GPS	6C	6.8	7.71	640.7
30	0502	SPS	5	6.9	5.62	352.4
48	1119	GPS	6B	6.9	8.46	555.3
30	7066	GPS	6B	7.1	5.61	1674.9
89	1125	GPS	6B	7.1	7.25	429.3
35	0101	SPS	1	7.2	6.82	573.1
30	7076	GPS	6B	7.6	0.93	1024.1
35	0109	SPS	1	8	7.5	482.0
6	8534	GPS	6B	8.2	6.65	1280.4
48	3835	GPS	1	8.7	4.8	1223.9
51	1419	GPS	6B	9.5	4.88	911.1
83	6450	GPS	6B	10.3	4.24	629.7
6	8535	GPS	6B	10.4	7.65	1734.8
8	6002	GPS	6C	10.5	5.96	471.1
34	0559	SPS	5	11	3.42	1136.9
51	1419	GPS	6D	11.1	4.23	1430.2
48	A509	SPS	5	12.1	4.49	1346.8
34	0504	SPS	5	13.2	3.86	1209.9
90	6410	GPS	6B	13.6	3.03	187.3
34	0503	SPS	5	13.7	3.8	915.8
34	0507	SPS	5	14.2	3.75	752.4
34	0508	SPS	5	14.9	3.86	1285.2
81	1805	GPS	6B	16.3	9.1	343.1
90	6412	GPS	6B	16.8	2.96	348.4
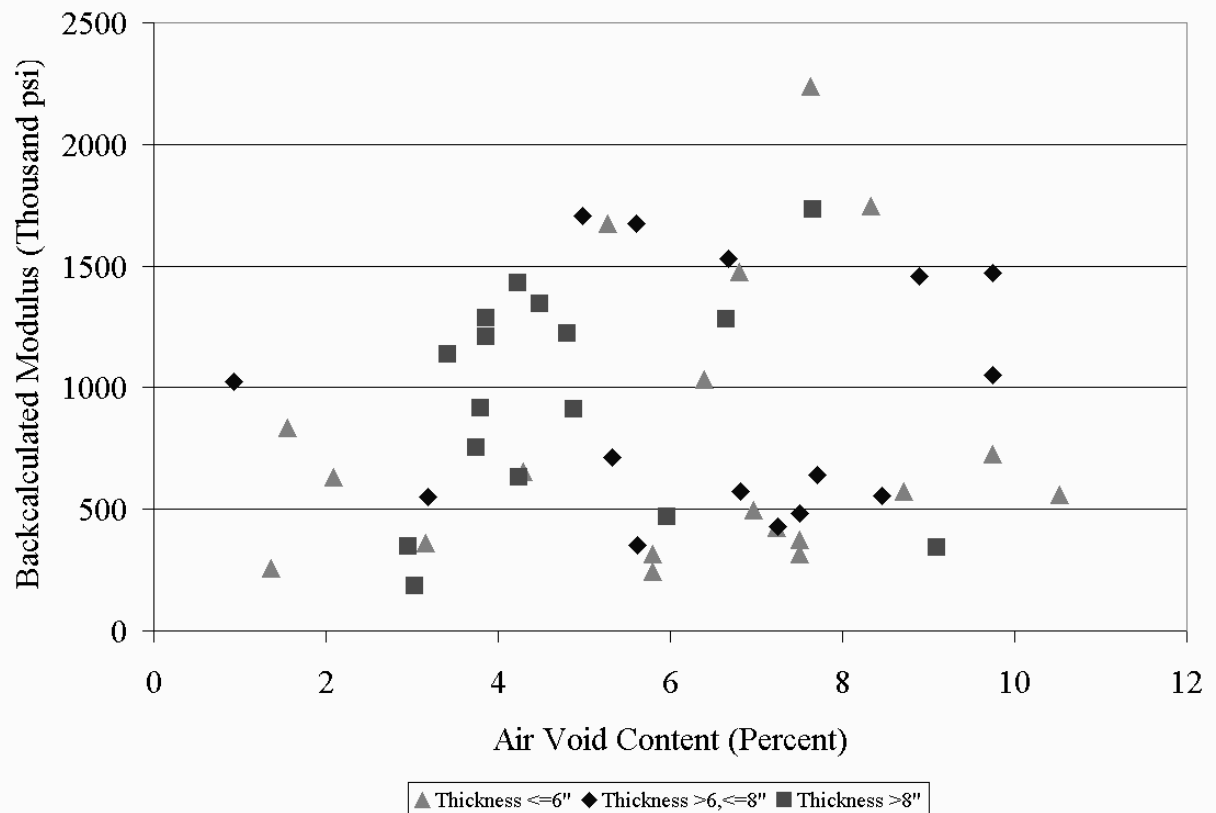
Figure 9.   Relationship between HMA layer stiffness (at 20°C) and AVC.

- The analysis of data from HMA overlays on pre-existing HMA pavements produced no apparent sensitivity and no correlation.   In this case, the 30 sections that satisfied the selection criteria exhibited wide scatter.

- The analysis of data from HMA overlays on pre-existing PCC pavements showed a possible trend of improved rut performance in an AVC range of 2 to 7 percent.   However, only 6 sections satisfied the criteria and considerable scatter did exist.

Other factors that likely contributed to the variability of the results include a) a limited

range of AVC in some of the data, 2) uncertainty in the calculated AVC and estimated

ESAL applications, and 3) unquantified variability in the underlying support conditions.

HMA Stiffness: Fifty (50) pavement sections were identified, processed, and evaluated in an effort to develop a relationship between HMA stiffness and as-constructed AVC.   The findings basically indicated that there is no apparent relationship between HMA stiffness and AVC. Although uncertainty exists in the estimation of HMA stiffness and AVC, the number of data points and the fact that a wide variety of pavements was represented, suggests that the results of these analyses are meaningful.

CHAPTER 3

effect of air void content on

pavement performance and stiffness

A number of different relationships exist in the literature that relate, among other factors, air void content (AVC) to HMA pavement performance and stiffness. By mathematically evaluating these relationships, it was possible to develop a numerical indication of the sensitivity of HMA fatigue cracking, permanent deformation, and stiffness to changes in AVC. As previously stated, the benefit of this analysis is that it provides pavement engineers and contractors with a strong indication of the importance of achieving the AVC specification during the construction process.

3.1 SELECTION OF SENSITIVITY STATISTIC

To examine the sensitivity of pavement performance and stiffness to AVC, it was necessary to establish a statistic (or measure) that represents the effect of a change in AVC on the dependent variable. During this study, several different mathematical forms were investigated with the goal of identifying one that best captured the sensitivity over the widest range of AVC. In the end, a relatively simple model form was selected that was equally applicable to fatigue cracking, permanent deformation and stiffness. The equation for this sensitivity statistic is as follows:

$$S_{PAV} = \frac{Log(\varphi)_x - Log(\varphi)_t}{AV_x - AV_t} \tag{5}$$

where:

S_{PAV} = Statistic indicating the sensitivity of some measure of pavement performance

(i.e., fatigue cracking or permanent deformation) or HMA stiffness to AVC.

AV_t = Target AVC (percent).

AV_x = As-constructed (or off-target) AVC (percent)

$(\varphi)_t$ = Either the predicted pavement life (in ESAL applications) or HMA stiffness

associated with the target AVC.

$(\varphi)_x$ = Either the predicted pavement life (in ESAL applications) or HMA stiffness

associated with the as-constructed AVC.

This relationship basically represents the slope of the line on a graph of the log (base 10) of

predicted pavement life (or HMA stiffness) versus AVC.   This relationship was chosen because,

in evaluating the sensitivity of pavement performance for several different models, it provided an

exact mathematical representation of the sensitivity of pavement performance (and HMA

stiffness) for almost every model evaluated.

To provide a more meaningful indication of the sensitivity of the S_{PAV} statistic, it was related
mathematically to the percent effect on pavement life (or HMA stiffness) for different deviations
in AVC (from the target percentage).   This relationship is shown in Figure 10.   As an example,
for an S_{PAV} of -0.10 and a deviation in AVC from it target of +2 percent, the percent effect on
pavement life would be −50 percent.   In terms of effect, it should be noted that for negative
values of S_{PAV} (i.e., a negative slope), positive increases in AVC will always result in a reduction
if pavement life (or HMA stiffness).

Figure 10.   Effect of sensitivity statistic (S$_{PAV}$) and deviation AVC (from target) on pavement life.

Sensitivity Statistic for Any Given Prediction Model (S$_{PAV}$)
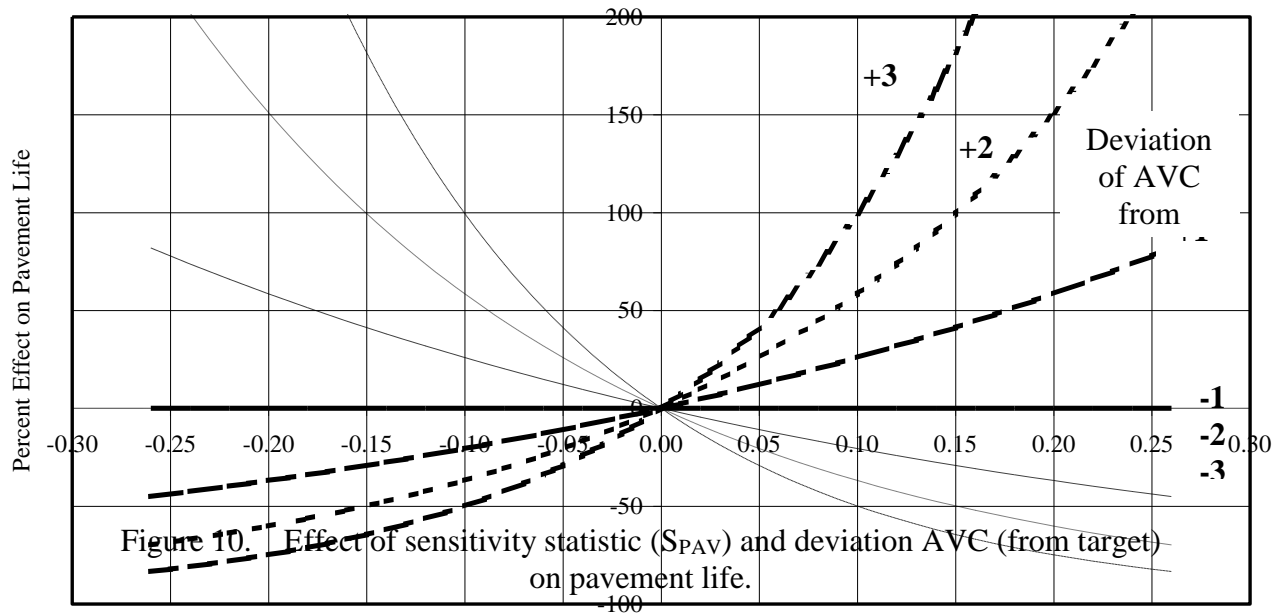
3.2 TREATMENT OF UNCERTAINTY

In almost every prediction model developed from analysis of experimental data, there is a certain amount of variability or uncertainty associated with its predictive ability.   This uncertainty is derived primarily from the lack-of-fit between the prediction model (equation) and the data used to develop it; however, there are other factors such as limited data and/or extrapolation beyond the range of the data that can have large impacts as well.   Uncertainty in pavement performance and material property prediction has a definite impact on accurately quantifying the effect of AVC.   In fact, there are many cases where the variability of the model is so great that it overwhelms the effect of AVC.

Because of its significance in interpreting the effect of AVC, a "two-prong" approach was selected for characterizing uncertainty.   First, wherever possible, typical statistical measures of model lack of fit, i.e., coefficient of determination (r^2) and standard error of estimate (SEE), are provided so that the reader can interpret the results of the analysis at "face value."   The problem with this approach is that some of the models gathered from the literature do not have documented statistics or their statistics are difficult to compare.   Consequently, a second approach, based on the judgment of the research team, was used to develop a subjective rating of the overall reliability of each model.   This rating is in the form of a letter grade (A, B+, C−, etc.) and takes into consideration the available information on statistical accuracy, the type of mathematical model, the quantity of data, and whether the model is based on laboratory of field test results.

3.3 EFFECT OF AVC ON FATIGUE PERFORMANCE

Through a comprehensive review of the literature, ten models from four different sources were identified that related fatigue life to initial AVC.   Eight models were derived from fatigue testing of HMA mixes in the laboratory.   The remaining two models were based on the fatigue

performance of HMA mixtures under field loading conditions.   Each model is identified below, followed by a summary table indicating their individual sensitivity to AVC.

3.3.1 The Asphalt Institute

The Asphalt Institute published a research report that documents the development of a component fatigue performance model that was incorporated into one of the early mechanistic-empirical design procedures for flexible pavements (The Asphalt Institute 1982).   The report describes a model to estimate the fatigue life of a pavement that relates allowable axle load repetitions to maximum tensile strain in the HMA layer, stiffness of the HMA layer, asphalt content and AVC.   The model is based primarily on the results of laboratory testing to simulate the effects of the different factors.   It is also based upon the AASHO Road Test, which was used as a basis to calibrate laboratory fatigue test results to field performance through the use of a shift factor (SF).   The component of the model that accounts for the effect of AVC is actually based on earlier laboratory fatigue testing (Pell and Cooper 1975 and Epps 1968).

$$N_f = C \cdot SF (4.325 \cdot 10^{-3} \cdot \varepsilon_t^{-3.29} \cdot E*^{-0.854}) \qquad (6)$$

where:

N_f = Number of 80-kN (18,000 lb) equivalent single axle loads applications.

C = Function of volume of voids and volume of asphalt.

SF = Shift factor for level of fatigue cracking (relative to wheel path area):

= 18.4 for 45 percent fatigue cracking.

= 13.0 for 10 percent fatigue cracking.

ε_t = Tensile strain in asphalt layer.

$E*$ = Asphalt mixture dynamic modulus (psi).

C is the term accounts for the effects of both asphalt content and air void content:

$$C = 10^M \qquad (7)$$

$$M = 4.84 \left(\frac{V_b}{V_v + V_b} - 0.69 \right) \qquad (8)$$

where:

V_b = Volume of asphalt (percent).

V_v = Volume of air voids (percent).

Based upon the levels of the factors selected for the original experiment, $C = 1$, when $V_b = 11$ percent and $V_v = 5$ percent.

The component nature of the prediction model made it impossible for the original researchers to identify any real measures of statistical accuracy. Furthermore, we could not determine from the available literature the inherent accuracy of the component of the model that accounts for the effect of AVC. Nevertheless, the model is based on an extensive amount of testing and calibration and, accordingly, was assigned an overall reliability rating of C–.

The inherent sensitivity of fatigue performance to AVC in the model is depicted in Figure 11. As the AVC increases from it target, there is a reduction in the predicted fatigue life of the pavement. In contrast, as the AVC decreases from it target, there is a corresponding increase in the predicted pavement life. The fact that the C-term is made up of both AVC and asphalt content means that the two interact. Thus, the four lines shown all represent the sensitivity of fatigue performance to AVC for different combinations of target AVC and target asphalt content. Close consideration of these results shows that the effect of AVC on pavement performance does not change significantly with different target levels of asphalt content. On the other hand, the effect of AVC does change with different target levels of AVC. Not surprisingly, the effect of deviations in AVC becomes greater as the target AVC becomes lower.

As previously indicated, the sensitivity statistic (S_{PAV}) is represented by the slope of the line between the deviation in HMA fatigue life with respect to the deviation in AVC from its target. In this instance, the lines are slightly nonlinear, so the sensitivity statistic for each

combination (shown in Figure 11) was calculated as the average slope. Overall, for AVC = 5 percent, $S_{PAV} = -0.246$ and for AVC = 8 percent, $S_{PAV} = -0.144$.
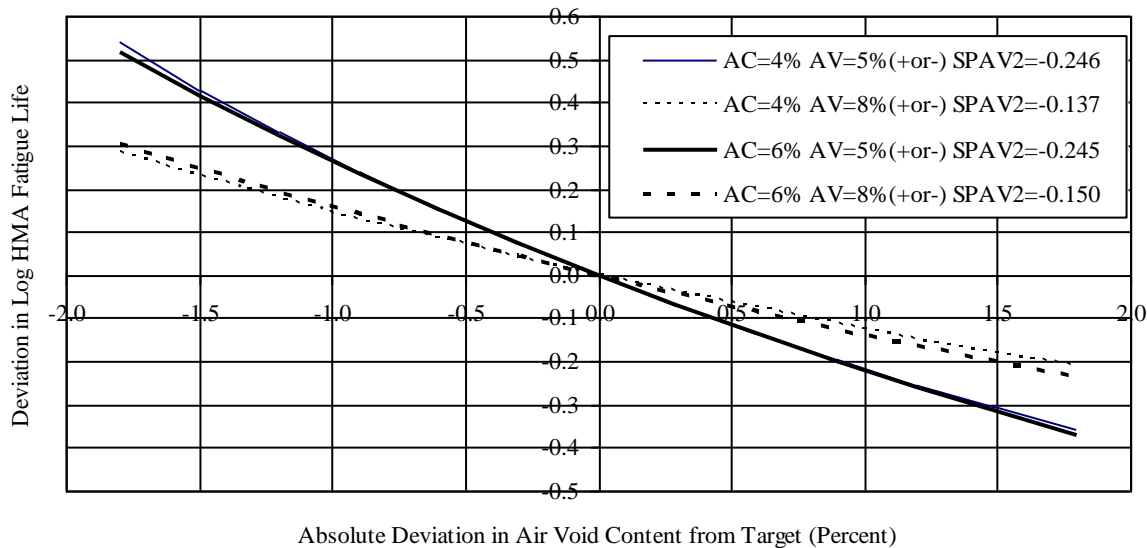
Figure 11. Graph illustrating the sensitivity of HMA pavement fatigue performance to deviations in AVC from its target.

3.3.2 University of California at Berkeley

This report documents the results of fatigue testing that was performed on three different mixes to determine the effect of AVC on fatigue performance (Epps et al. 1969). The results are depicted in Figure 12. The significant details for each of the mixes are provided below:

1. British Standard 594 Grading, 7.9 percent asphalt content, 4 to 14 percent range in AVC: $S_{PAV} = -0.100$, n = 26 data points, $r^2 = 0.47$, SEE = 0.317, and reliability rating = C+.

2. California Fine Grading, 6 percent asphalt content, 5 to 8 percent range in AVC: $S_{PAV} = -0.250$, n = 22 data points, $r^2 = 0.40$, SEE = 0.263, and reliability rating = C+.

3. California Coarse Grading, 6 percent asphalt content, 2.5 to 7 percent range in AVC: $S_{PAV} = -0.179$, n = 20 data points, $r^2 = 0.76$, SEE = 0.171, and reliability rating = B.

Unlike the AI model, S_{PAV} is constant for these three models, regardless of the initial AVC.
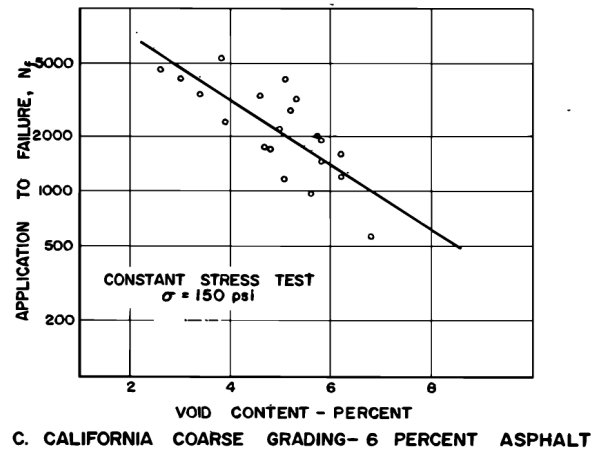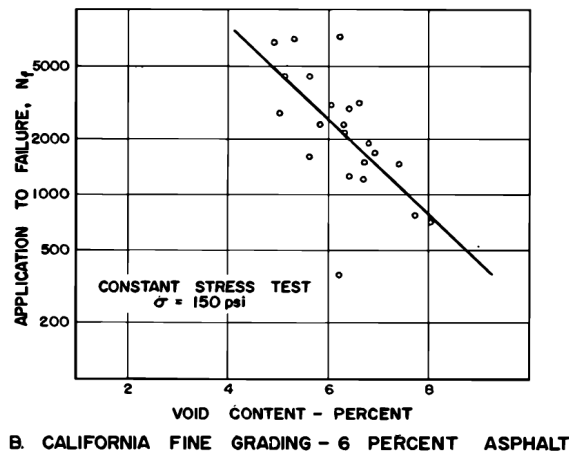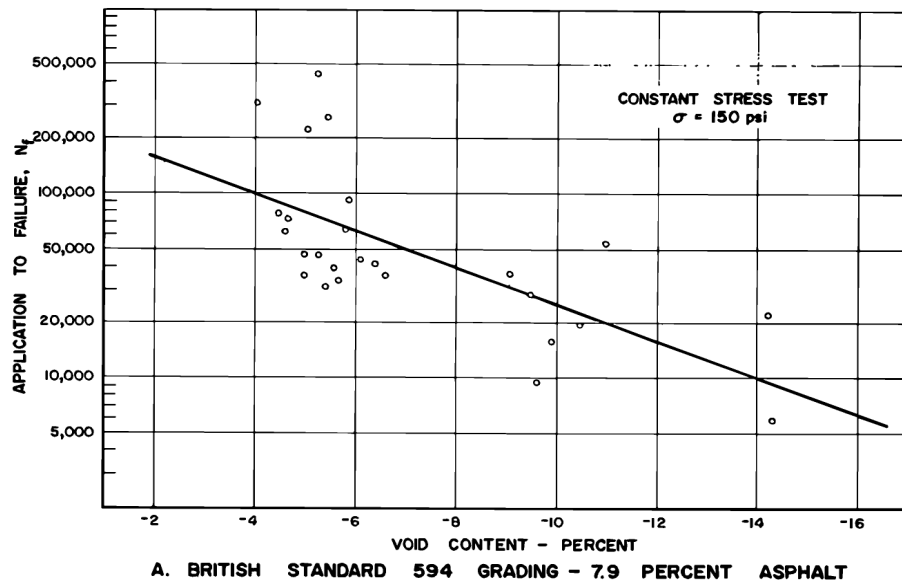
Figure 12.   The effect of AVC on fatigue life (Epps et al. 1969).

It should be noted that neither the coefficient of determination (r^2) or standard error of estimate (SEE) were provided in the documentation for these models. Instead, they were estimated based upon visual extraction and re-analysis of the graphical data in Figure 12. It should be further noted that both r^2 and SEE are based on the log (base 10) transformation of fatigue applications.

3.3.3 University of California at Berkeley

The following relationship was developed at UCB based on a recent extensive laboratory-based fatigue experiment (Harvey et al. 1996). The experiment involved the study of a single dense-graded mix with a crushed aggregate and an AR-4000 asphalt binder. However, a full factorial experiment design with three levels of AVC and five levels of asphalt content was conducted. The following relationship was developed:

$$\ln(N_f) = -22.191 - 0.164 \cdot AVC + 0.594 \cdot AC - 3.729 \cdot \ln(\varepsilon_t) \tag{9}$$

where:

$\ln(N_f)$ = Natural (Naperian) log of the HMA fatigue life.

$\ln(\varepsilon_t)$ = Natural log of the tensile strain at the bottom fiber of the HMA layer.

AVC = Air void content (percent).

AC = Asphalt content (percent).

The pertinent statistics on this model are: $n = 97$ data points and $r^2 = 0.92$. No SEE was identified in the documentation. The calculated sensitivity of fatigue life to AVC (S_{PAV}) is equal to -0.071. Based on the size of the experiment and the accuracy of the fit, the overall reliability rating assigned to the relationship is A–.

The primary objective of the WesTrack project (Epps et al. 2002) was to develop a procedure to account for the effect that contractor non-conformance to specifications has on pavement performance and, in turn, provide a basis for adjusting the contractor's payment based upon the magnitude of the deviation from the specification.   Asphalt content, air void content, and aggregate gradation were the key experimental factors and their effects were evaluated both in the laboratory and in the field.   The focus of the experiment was on three HMA mixtures having different aggregate gradations: the *fine*, *fine-plus* (slightly higher fines content than the fine mix) and *coarse* mixes.   Each mix had seven possible treatment combinations depending on the level of asphalt content (high, medium and low) and level of AVC (high, medium, and low).

WesTrack Laboratory Models

Three separate fatigue models were developed based on laboratory testing of fatigue beams extracted from the field.   The equations and associated statistics are provided below.

The variables in each equation are defined as follows:

N_f = Fatigue life (load repetitions to crack failure).

AC = Asphalt content (percent).

T = Mix temperature at 150 mm (6 in) depth (^{o}C).

ε_t = Maximum HMA tensile strain.

Fine Mixes:

$$\ln(N_f) = -27.0265 - 0.1439 \cdot AVC + 0.4148 \cdot AC - 4.6894 \cdot \ln(\varepsilon_t) \tag{10}$$

For this relationship, S_{PAV} = -0.063, the number of data points, n = 9 (based on seven unique mix combinations plus two replicates) and $r^2 = 0.88$.   No SEE was documented.   Based on the accuracy of the fit and the fact that multiple samples were tested to determine an average fatigue life for each data point, the overall reliability rating assigned to the model is B+.

<u>Fine-Plus Mixes</u>:

$$\ln(N_f) = -27.3409 - 0.1431 \cdot AVC + 0.4219 \cdot AC + 0.0128 \cdot \ln(T) - 4.6918 \cdot \ln(\varepsilon_t) \quad (11)$$

For this relationship, S_{PAV} = -0.062, n = 8 (based on seven unique mix combinations plus one replicate) and r^2 = 0.88.   No SEE was documented.   Based on the accuracy of the fit and the fact that multiple samples were tested to determine an average fatigue life for each data point, the overall reliability rating assigned to the model is B+.

<u>Coarse Mixes</u>:

$$\ln(N_f) = -27.6723 - 0.0941 \cdot AVC + 0.6540 \cdot AC + 0.0331 \cdot T - 4.5402 \cdot \ln(\varepsilon_t) \quad (12)$$

For this relationship, S_{PAV} = -0.041, n = 9 (based on seven unique mix combinations plus two replicates) and r^2 = 0.92.   No SEE was documented.   Based on the accuracy of the fit and the fact that multiple samples were tested to determine an average fatigue life for each data point, the overall reliability rating assigned to the model is B+.

WesTrack Field Models

Two separate fatigue models were developed based upon the observed field performance of the pavement sections at WesTrack: one for the *fine* and *fine-plus* mixes (combined) and the second for the *coarse* mixes.   Since the performance of the WesTrack sections varied considerably and some of the sections never exhibited fatigue cracking, a probabilistic-based regression approach was used to develop the prediction models.   This probabilistic regression approach accounted for (in a statistically rigorous fashion) the effect of the sections that "survived" the experiment.

The original models were formulated to predict the probability of fatigue cracking based upon the levels of load applications, AVC, asphalt content, and fines content. However, for application purposes, the models were reconfigured to predict the number of 80-kN (18,000-lb) ESAL applications (W_{18}) to 10 percent fatigue cracking. The only (as yet) undefined term in these relationships is P_{200}, the percent of aggregate finer than the 0.074 mm (No. 200) sieve.

Fine and Fine-Plus Mixes:

$$\log(W_{18}) = 4.490 + 0.4757 \cdot AC - 0.1041 \cdot AVC + 0.2087 \cdot P_{200} \tag{13}$$

There were 17 mixes that fell under this category (14 unique mixes plus three replicates). The calculated S_{PAV} for this relationship is -0.104, while the r^2 is 0.56. No SEE was reported. Considering these factors plus the fact that it was a field test, the assigned overall reliability rating for this model is B.

Coarse Mixes:

$$\log(W_{18}) = 3.8686 + 0.4920 \cdot AC - 0.03692 \cdot AVC \tag{14}$$

There were nine mixes that fell under this category (seven unique mixes plus two replicates). The calculated S_{PAV} for this relationship is –0.037, while the r^2 is 0.51. No SEE was reported. Accordingly, the assigned overall reliability rating for this model is B–.

3.3.5 Summary of Fatigue Sensitivity

Table 10 summarizes the sensitivity to AVC of all the HMA fatigue performance models studied. As can be seen, S_{PAV} ranges from -0.037 to -0.246. The corresponding range in effect on fatigue life (for a one percent increase in AVC) is -8 to -44 percent. There does not appear to

be any trends related to the type of mix or whether the model is based on field or laboratory

testing.   With the exception of the Asphalt Institute model, all the models have a reasonable

overall reliability rating.   Considering these results, along with the overall reliability ratings, the

recommended "rule of thumb" for sensitivity of fatigue cracking to AVC is an S_{PAV} of -0.10.

This corresponds to a 20 percent reduction in fatigue life for a one percent increase in AVC

above the target.

Table 10.   Summary of findings on sensitivity of HMA fatigue performance to AVC.

Model or Data Source	Based on Field or Lab Testing	Description of Mix(es)	Initial AVC (%)	Sensitivity Statistic, S_{PAV}	Effect on Fatigue Life for 1% Increase in AVC	Measures of Statistical Accuracy			Overall Reliability Rating
						n	r^2	SEE	
Asphalt Institute (TAI 1982)	Lab	Information not available	5	-0.246	-43.2%	-	-	-	C-
			8	-0.144	-28.2%				
UCB (Epps et al. 1969)	Lab	British Std 594, AC=7.9%	N/A	-0.100	-20.6%	26	0.47	0.317	C+
		California Fine, AC=6%	N/A	-0.250	-43.8%	22	0.40	0.263	C+
		California Course, AC=6%	N/A	-0.179	-33.8%	20	0.76	0.171	B
UCB (Harvey et al. 1996)	Lab	Dense-graded crushed aggr., AR-4000 binder	N/A	-0.071	-15.1%	97	0.92	-	A-
WesTrack (Epps et al. 2002)	Lab	Fine Mix	N/A	-0.063	-13.5%	9	0.88	-	B+
		Fine-Plus Mix	N/A	-0.062	-13.3%	8	0.88	-	B+
		Coarse Mix	N/A	-0.041	-9.0%	9	0.92	-	B+
	Field	Fine & Fine-Plus Mix	N/A	-0.104	-21.3%	17	0.56	-	B
		Coarse Mix	N/A	-0.037	-8.2%	9	0.51	-	B-

Note: n = number of data points, r^2 = coefficient of determination, SEE = standard error of estimate.

3.4 EFFECT OF AVC ON RUTTING PERFORMANCE

As a result of a review of the literature, only five models from two

different sources were identified that related rutting life to initial AVC.

One model was derived from rut testing of HMA mixes in the laboratory.

The remaining four models were based on the rutting performance of HMA

mixtures under field loading conditions at WesTrack. Each model is described

below, followed by a summary table indicating their individual sensitivities to

AVC.

3.4.1 National Center for Asphalt Technology

This primary objective of this study, initiated in 1987, was to identify the material properties and mix design parameters that affect rutting.   Additional objectives were to provide information necessary to 1) produce HMA mixtures that perform satisfactorily and 2) identify those mixes with a tendency to rut under heavy traffic loading (Brown et al. 1992).   Forty pavement sections in 14 states were surveyed, sampled and tested.   The sections represented covered a wide range of environments, HMA thicknesses, mix types, traffic levels, and underlying support layer (including PCC, HMA and base).   The pavement age at time of sampling ranged from 0.6 to 18 years.   Thus, as was the case with most of the pavement sections in the LTPP database, there is only limited data on as-constructed AVC.

The results of this field study, with regard to the effect of AVC on rutting performance, are graphically depicted in Figure 13.
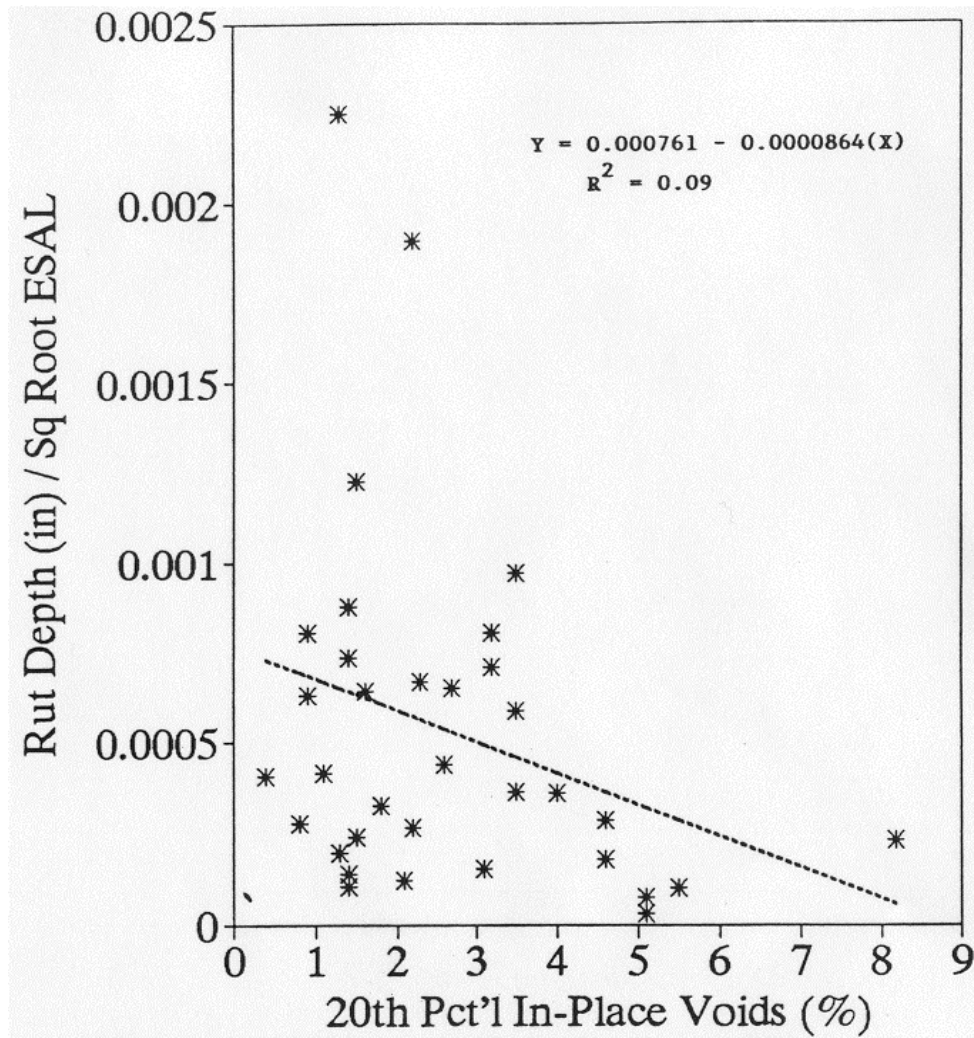
Figure 13.   Twentieth percentile in-place voids versus rate of rutting (Brown et al. 1992).

The linear regression equation resulting from the analysis of the data is as follows:

$$Y = 0.000761 - 0.0000864 * X \tag{15}$$

where:

X = Twentieth percentile in-place AVC.

Y = Rate of rutting, rut depth (in) per (ESAL applications)$^{0.5}$.

The equation is based on 34 data points and has an r^2 is 0.09.   No SEE was reported.

For purposes of determining the sensitivity to AVC, the equation was rearranged to solve for the log of ESAL applications. Our analysis of the resultant equation yielded average S_{PAV} values of +0.184 and +0.331 for target AVCs of 4 and 6 percent, respectively. The positive S_{PAV} values indicate that an increase in AVC would, contrary to expectation, result in increased rut life. Thus, although this model is based on field data and covers a wide range of mixes in different environments, the poor fit, the positive S_{PAV} values, and the fact that most of the AVCs do not represent as-constructed values meant that only an overall reliability rating of D could be assigned.

3.4.2 WesTrack

In introducing the WesTrack fatigue models, section 3.3.4 provided background information on the overall objectives and the experiment design that is also applicable here. As was the case in the WesTrack fatigue cracking models, performance data for the four different HMA mixes was gathered through field observation. Unlike the cracking models, no models were developed based solely upon laboratory performance testing.

Three approaches were used in the development of the rutting models (Epps et al. 2002):

- Level 1A models involved a direct regression between rut depth and traffic, environment (temperature), and mix parameters.

- Level 1B models involved a regression analysis of data generated by the application of the Level 2 mechanistic-empirical model.

- Level 2 models involved a rigorous mechanistic-empirical analysis of all the data in which incremental rut behavior was characterized on an hour-by-hour basis during the life of each pavement section.

Since the Level 1B model is a simplification of the Level 2 mechanistic-empirical model and should, therefore, reflect the same sensitivity to AVC, the Level 2 models were not included in this analysis.

For each prediction model, the dependent variable is rut depth. Consequently, each model was mathematically re-arranged to establish rutting life as the dependent variable in order to evaluate the sensitivity of performance to AVC in a manner consistent with the other models. (Unfortunately, these transformations do reduce the meaningfulness of the reported lack-of-fit for each model).

WesTrack Level 1A Rutting Models

Three separate rutting models were developed through linear regression analyses of the field performance data from WesTrack, one for the *fine* and *fine-plus* mixes (combined), one for the *original coarse* mix, and one for the *coarse mix in the replacement* sections. The analysis was based on the performance of sections through the first 2 million 80-kN (18-kip) ESAL applications. Although some of the sections (particularly the fine mixes) exhibited very good performance, they did rut enough such that they could still be included in the analysis. The only (as-yet) undefined variables in these equations are:

rd   = Rut depth (in).

ESAL = Estimated cumulative 80-kN (18-kip ESAL) applications required to achieve a selected rut depth.

P_{200} = Percent aggregate finer than 0.074 mm (No. 200) sieve.

T   = Ninetieth percentile air temperature (^{o}F) during the period in which rutting occurred.

Fine and Fine-Plus Mixes

$$\ln(\text{rd}) = -5.257 + 0.357 \cdot \ln(\text{ESAL}) + 0.185 \cdot \text{AC} + 0.041 \cdot \text{AVC} \\ + 0.916 \cdot P_{200} + 0.005 \cdot T \tag{16}$$

For this relationship, $S_{PAV} = -0.053$, the number of data points, n = 17 (based on 15 unique mix combinations plus three replicates) and $r^2 = 0.67$. SEE was not documented. Taking into consideration the accuracy of the fit, the fact that the equation needed to be re-arranged, the number of test sections and the field nature of the experiment, the overall reliability rating assigned to the model is B–.

Original Coarse Mixes

$$\ln(\text{rd}) = -4.939 + 0.212 \cdot \ln(\text{ESAL}) + 0.439 \cdot \text{AC} + 0.044 \cdot \text{AVC} + 0.034 \cdot \text{T} \qquad (17)$$

For this relationship, $S_{PAV} = -0.044$, the number of data points, n = 9 (based on seven unique mix combinations plus two replicates) and $r^2 = 0.80$. SEE was not documented. Considering the accuracy of the fit, the number of test sections, the fact that the equation had to be re-arranged to solve for rutting life, and the field nature of the experiment, the overall reliability rating assigned to the model is B.

Replacement Coarse Mixes

$$\ln(\text{rd}) = -6.204 + 0.190 \cdot \ln(\text{ESAL}) + 0.829 \cdot \text{AC} + 0.207 \cdot \text{AVC} \qquad (18)$$

In this relationship, $S_{PAV} = -0.630$, the number of data points, n = 8 (based on seven unique mix combinations plus one replicate) and $r^2 = 0.63$. No SEE was reported. Considering the accuracy of the fit, the number of test sections, the fact that the equation had to be re-arranged to solve for rutting life, and the field nature of the experiment, the overall reliability rating assigned to the model is C+.

WesTrack Level 1B Model

The rut prediction model below is basically a simplification of the Level 2 rutting model developed through a rigorous mechanistic-empirical (M-E) analysis of the WesTrack field performance data. It was derived through linear regression analysis of simulated data generated by the Level 2 M-E model for 23 of the 34 WesTrack pavement sections, i.e., those that did not exhibit any significant fatigue cracking. Although the model was derived from the same basic data as the Level 1A model, the differences in model development approach make it valid to

evaluate the model independent of the Level 1A model. The model has two sources of lack-of-fit error, that associated with the predictive accuracy of the Level 2 model and that associated with the error in simplifying the M-E model.

$$
\begin{aligned}
\ln(\text{rd}) = &-6.1651 + 0.309941 \cdot \ln(\text{ESAL}) + 0.00294305 \cdot \text{AVC}^2 \\
&+ 0.0688276 \cdot \text{AC}^2 - 0.0657803 \cdot \text{AC} \cdot \text{P}_{200} \\
&+ 0.600498 \cdot (\textit{fine} - \textit{plus}) \\
&- 1.59167 \cdot (\textit{coarse}) + 2.35276 \cdot (\textit{replace}) \\
&+ 0.21327 \cdot \ln(\text{ESAL}) \cdot (\textit{coarse}) \\
&- 0.140386 \cdot \ln(\text{ESAL}) \cdot (\textit{replace})
\end{aligned}
\tag{19}
$$

In this equation, *fine-plus*, *coarse*, and *replace* are dummy variables designed to account for the effect of mix type on rut performance. In application, one of the three variables is assigned a value of 1 to specify the type of mix, while the other two variables are assigned a value of 0. This term is intended to account for the effect of mix type on rutting performance. All other variables in the model are as previously defined.

Analysis of the re-arranged form of the model indicates that the sensitivity of the model is dependent upon the target AVC. Thus, for target AVC values of 4 and 6 percent, the respective S_{PAV} values are -0.033 and -0.050. Because of the complexity of the process used to generate the model, no estimate of r^2 or SEE could be determined. Because of this, the number of test sections considered, and other unique developmental factors associated with the model, it was assigned an overall reliability rating of C+.

3.4.3 Summary of Rutting Sensitivity

Our review of the literature produced only two sources of information upon which to evaluate the sensitivity of rutting performance to AVC. A summary of the sensitivity findings is presented in Table 11.

Table 11.   Summary of findings on sensitivity of HMA rutting performance to AVC.

Model or Data Source	Based on Field or Lab Testing	Description of Mix(es)	Initial AVC (%)	Sensitivity Statistic, S_{PAV}	Effect on Rutting Life for 1% Increase in AVC	Measures of Statistical Accuracy			Reliability Rating
						n	r^2	SEE	
NCAT (Brown et al. 1992)	Field	Information not available	4	0.184	52.8%	34	0.09	-	D
			6	0.331	114.3%				
WesTrack (Epps et al. 2002)	Field Level 1A	Fine & Fine-Plus Mixes	N/A	-0.053	-11.5%	17	0.67	-	B-
		Original Course Mix	N/A	-0.044	-9.6%	9	0.80	-	B
		Replacement Course Mix	N/A	-0.473	-66.3%	8	0.63	-	C+
	Field Level 1B	Fine, Fine-Plus, Coarse, and Replacement Mixes	4	-0.033	-7.3%	23	-	-	C
			6	-0.050	-10.9%				

Note: n = number of data points, r^2 = coefficient of determination, SEE = standard error of estimate.

Because of the fact that the initial AVC is unknown for any of the sections in the NCAT study, the sensitivity results resulting from that project are ignored.   The remaining models, all derived from field performance data, have a fair to good reliability rating.

Based upon the sensitivity results from the WesTrack models, the S_{PAV} values range from -0.033 to -0.473.   The corresponding range in effect on rutting life (for a one percent increase in AVC) is -7 to -66 percent.   With the exception of the model for the replacement mixes, there seems to be some consistency amongst the mixes in terms of sensitivity.   Given that the replacement mixes rutted heavily during their first month of loading, the focus of this analysis was on the sensitivity of rutting to AVC for the fine, fine-plus, and coarse mixes.   Considering the results, along with the overall reliability ratings, the recommended "rule of thumb" value for rutting is an

S_{PAV} value of -0.05.   This corresponds to a 10 percent reduction in rutting life for a one percent increase in AVC above the target.   It should be noted, however, that because WesTrack was an accelerated load test, the mixes did not experience the level of age-hardening associated with longer-life pavements.   Consequently, the effects of increased AVC on rutting life may be exaggerated.

3.5 EFFECT OF AVC ON HMA STIFFNESS

As a result of the literature review, seven models from six different sources were identified that related some measure of HMA stiffness (i.e., resilient modulus, dynamic modulus, or flexural stiffness) to initial AVC. Some models were based on a limited number of tests for a specific mix (or mixes) while another was based the analysis of over 2,700 data points.   Each model is described below, followed by a summary table indicating their individual sensitivities to AVC.

3.5.1 ARRB Transport Research, Ltd.

As part of a larger study involving research on asphalt mixes using the accelerated load facility (ALF), researchers at the Australian Road Research Board (Oliver 2000) conducted resilient modulus testing to examine the effect of AVC on two mixes identified as C1 and C2. Unfortunately, information on the type and gradation of the mixes could not be obtained.   The results of the resilient modulus testing are depicted in Figure 14.
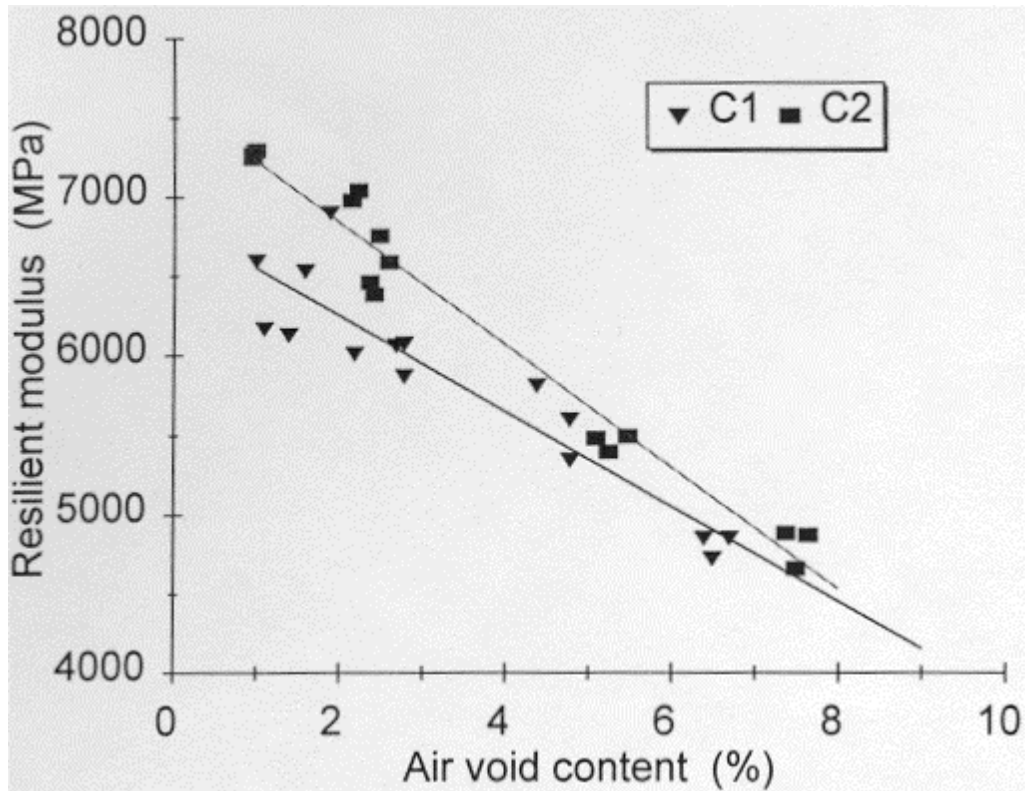
Figure 14. Relationship between AVC and resilient modulus for mixes C2 and C2 (Oliver 2000).

Both relationships shown are based on the analysis of 15 tests (five levels of AVC combined with three specimens per AVC level). The r^2, standard error of estimate (SEE), overall reliability rating, and S_{PAV} for mix C1 are 0.91, 0.015, B, and -0.0231, respectively. Similarly, the values for mix C2 are 0.99, 0.005, B+, and -0.0283, respectively.

3.5.2 University of Maryland

The (as yet) unpublished stiffness model presented below was developed by researchers at the University of Maryland (Andrei et al. 1999) from a database of dynamic modulus test results generated over a 30-year period at the university, the Asphalt Institute, and the Federal Highway Administration.   The database contains 2,750 test results from 205 different asphalt mixtures, 171 with unmodified binders, 34 with modified binders.   The experiment covered 39 different

aggregates and testing was over a wide range of temperatures (0 to 130 °F) and loading frequencies (0.1 to 25 Hz).

$$\log E = -1.249937 + 0.02932 \cdot P_{200} - 0.001767(P_{200})^2 - 0.002841 \cdot P_4$$
$$- 0.058097 \cdot AVC - 0.802208 \cdot \left(\frac{AC_{eff}}{AC_{eff} + AVC}\right) \tag{20}$$
$$+ \frac{3.871977 - 0.0021 \cdot P_4 + 0.003958 \cdot P_{38} - 0.000017 \cdot (P_{38})^2 + 0.005470 \cdot P_{34}}{1 + e^{(-0.603313 - 0.313351 \cdot \log(f) - 0.393532 \cdot \log(\eta))}}$$

where:

E	= Dynamic modulus (10^5 psi).
η	= Bitumen viscosity (10^6 Poise).
f	= Loading frequency (Hz).
AVC	= Air void content (percent).
AC_{eff}	= Effective asphalt content (percent by volume).
P_{34}	= Cumulative percent retained on the 19-mm (3/4 in) sieve.
P_{38}	= Cumulative percent retained on the 9.5-mm (3/8 in) sieve.
P_4	= Cumulative percent retained on the 4.76-mm (No. 4) sieve.
P_{200}	= Percent passing the 0.075-mm (No. 200) sieve.

The model has a very high accuracy of fit ($r^2 = 0.96$), but because of an interaction with asphalt content, is dependent upon the target AVC. For example, the S_{PAV} is -0.0077 when the target AVC is 5 percent and -0.0150 when the target AVC is 8 percent. Because of the size of the database and the accuracy of fit, this model was assigned an overall reliability rating of A.

3.5.3 Transportation and Road Research Laboratory

As part of a larger study on compaction of bituminous materials, researchers at TRRL (Powell et al. 1975) examined laboratory test results from various sources. One, in particular, provided a basis for a relationship between dynamic stiffness modulus and AVC for four mixes with varying asphalt content and maximum size aggregate. The relationship is depicted in the top half of Figure 15. It is based on 14 separate test results (data points).

Regression analysis of the data presented in the graph results in an S_{PAV} value of -0.0340, an r^2 of 0.83, and an SEE of 0.051 (on the log of the dynamic modulus).   Based on the number of mixes, the number of samples, and the accuracy of the fit, an overall reliability rating of B– was assigned to the model.
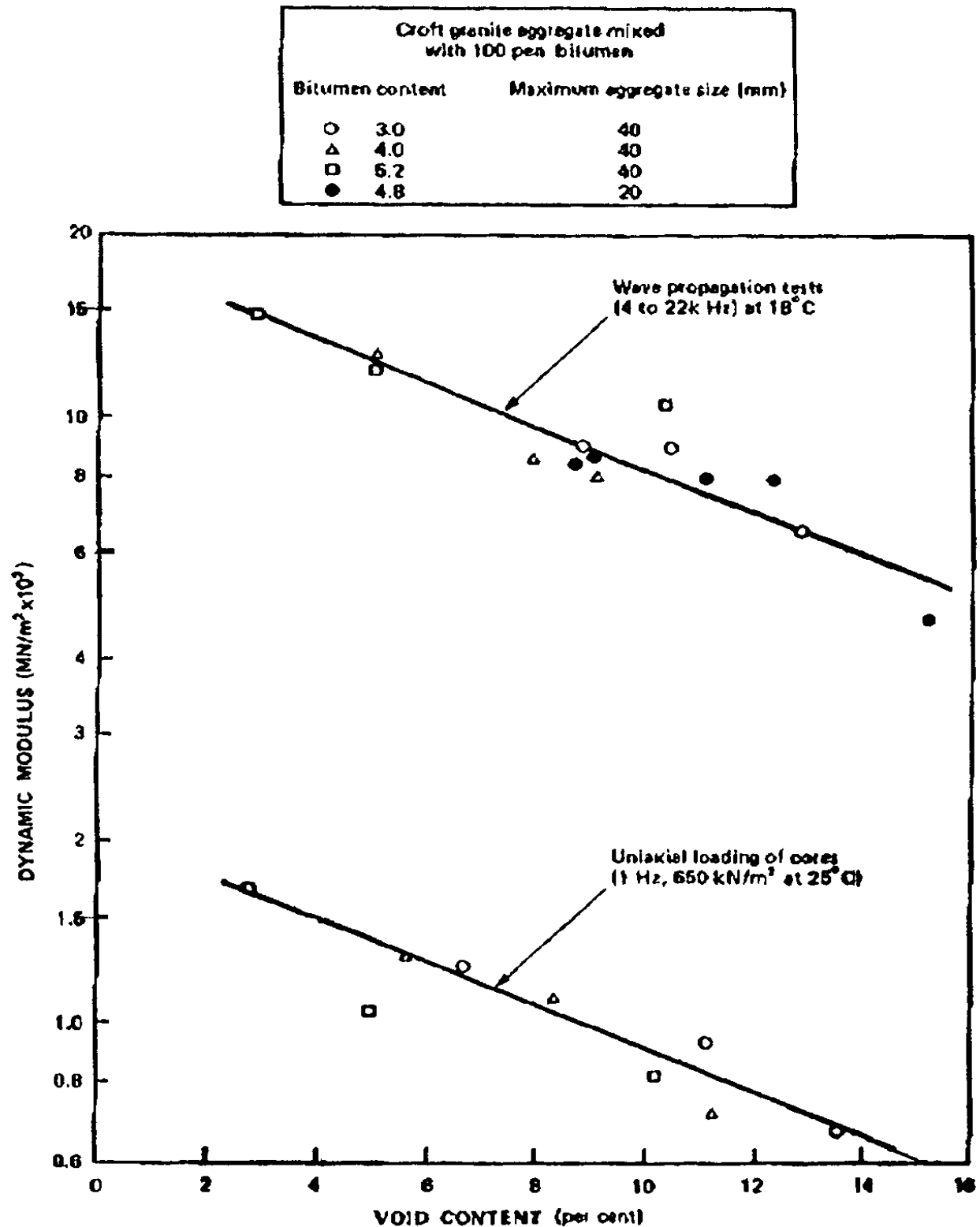
Figure 15.   Variation of dynamic modulus with air void content
(from a literature search by Powell et al. 1975)

3.5.4 University of California at Berkeley

The stiffness model shown below was developed at UCB as part of an extensive laboratory-based fatigue experiment (Harvey et al. 1996).   The experiment involved the study of a single dense-graded mix with a crushed aggregate and an AR-4000 asphalt binder.   However, a full factorial experiment design with three levels of AVC and five levels of asphalt content was conducted.

$$\ln(S_o) = 10.725 - 0.076 \cdot AVC - 0.171 \cdot AC \tag{21}$$

where S_o is equal to the initial mix stiffness (MPa) and the remaining variables are as previously defined.

The pertinent statistics on this model are: n = 97 data points and $r^2 = 0.684$.   The SEE was not identified in the documentation.   The calculated sensitivity of HMA stiffness to AVC (S_{PAV}) for this model is equal to -0.0330.   Based on the size of the experiment and the accuracy of the fit, the overall reliability rating assigned to the relationship is B+.

3.5.5 University of Nottingham

The dynamic stiffness versus AVC relationship depicted in Figure 16 is the result of a small study to characterize the effect of AVC on stiffness for a single HMA mix.   The study was conducted by researchers at the University of Nottingham as part of a larger case study to implement an analytical pavement design procedure for a local agency in the United Kingdom (Brown 1980).   The HMA is basically a dense-graded mix with a crushed limestone aggregate.
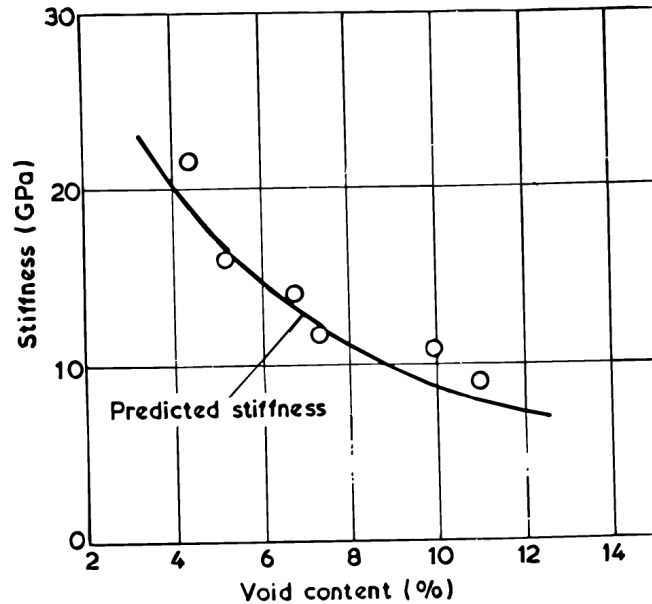
Figure 16.   Relationship between dynamic stiffness and void content (Brown 1980).

Regression analysis of the data presented in the graph results in an S_{PAV} value of -0.0492, an r^2 of 0.86, and an SEE of 0.051 (on the log of the dynamic stiffness).   Based on the number of mixes, the number of samples, and the accuracy of the fit, an overall reliability rating of B– was assigned to the model.

3.5.6 WesTrack

In introducing the WesTrack data for evaluating the effect of AVC on fatigue performance, section 3.3.4 provides background information on the objectives, nature, and overall experiment design for the WesTrack project (Epps et al. 2002).   That information relative to the types of mixes and their basic properties is applicable here.

Two stiffness models were developed from laboratory test results on WesTrack mixes for use in developing the mechanistic-empirical performance prediction models.   One model combined the data from the *fine* and *fine-plus* mixes.   The second combined the data from the *coarse* mixes. In these models, the independent variable, T, represents the temperature of the mix (ºC) and the dependent variable, Stiff, is the flexural fatigue mix stiffness (MPa).   The remaining independent variables are all as previously defined.

Fine and Fine-Plus Mixes

$$\ln(\text{Stiff}) = 11.4677 - 0.0827 \cdot \text{AVC} - 0.2285 \cdot \text{AC} - 0.0579 \cdot \text{T} \tag{22}$$

The pertinent statistics for this model are the number of data points, n, equal to 127 and the r^2 equal to 0.85. SEE was not reported in the documentation. The sensitivity of HMA stiffness to AVC for this model, S_{PAV}, is -0.0359. Based on the number of data points and the predictive accuracy of the model, an overall reliability rating of B+ was assigned.

Coarse Mixes

$$\ln(\text{Stiff}) = 11.4707 - 0.0576 \cdot \text{AVC} - 0.2142 \cdot \text{AC} - 0.0606 \cdot \text{T} \qquad (23)$$

The pertinent statistics for this model are the number of data points, n, equal to 59 and the r^2 equal to 0.79. SEE was not reported in the documentation. The sensitivity of HMA stiffness to AVC for this model, S_{PAV}, is -0.0250. Based on the number of data points and the predictive accuracy of the model, an overall reliability rating of B was assigned.

3.5.7 Summary of HMA Stiffness Sensitivity

Table 12 summarizes the sensitivity to AVC of all the HMA stiffness models studied. As can be seen, S_{PAV} ranges from -0.0077 to -0.0492. The corresponding range in effect on HMA stiffness (for a one percent increase in AVC) is -1.8 to -10.7 percent. This is a relatively small range and there does not appear to be any trends related to the type of mix. All the models have a relatively high overall reliability rating. Considering these results, along with the overall reliability ratings, the recommended "rule of thumb" for the sensitivity of HMA stiffness to AVC is an S_{PAV} of -0.023. This corresponds roughly to a five percent reduction in stiffness for a one percent increase in AVC above the target.

Table 12.   Summary of findings on sensitivity of HMA stiffness to AVC.

Model or Data Source	Measure of Stiffness	Description of Mix(es)	Initial AVC (%)	Sensitivity Statistic, S_{PAV}	Effect on Stiffness for 1% Increase in AVC	Measures of Statistical Accuracy			Overall Reliability Rating
						n	r^2	SEE	
ARRB	Resilient	C1 (Control)	N/A	-0.0231	-5.2%	15	0.91	0.015	B
(Oliver 2000)	Modulus	C2 (AUSTROADS)	N/A	-0.0283	-6.3%	15	0.99	0.005	B+

chapter 4

differences in variability and

volumetric properties

4.1 INTRODUCTION

The chapter describes the work conducted to examine the differences in variability and volumetric properties between LTPP SPS and GPS test sections.   Since the LTPP database encompasses such a large number of sections constructed over a number of years, it was possible examine within section variability and make comparisons between SPS and GPS sections.   The investigation of differences in variability and volumetric properties was not limited to just the LTPP data.   The findings from the following studies were also examined:

- WesTrack, Epps, et al. 2002

- FHWA Demo Project 74, Aschenbrener 1994a

- Colorado DOT Study, Aschenbrener 1992 and 1994b

- Aurilio et al. 1995

- Brakey et al. 1997

- Benson et al. 1995

- Kandahl et al. 1984

- Linden et al. 1989

- Weed et al. 1995

Details of the investigations and summaries of the findings of these investigations are provided herein.

4.2 LTPP TEST SECTIONS

The SPS and GPS sections utilized for investigation of variability and volumetric properties include those from GPS-1, GPS-2, GPS-6B, GPS-6C, GPS-6D, GPS-7B, SPS-1, SPS-5, SPS-6, and SPS-8 experiments.   In total, 108 test sections were identified as being appropriate for investigation.

The LTPP SPS and GPS data were analyzed to determine the variability of AVC within each test section and the differences of AVC between groups of tests sections. Test sections were grouped according to the two broad LTPP experiments (GPS or SPS) to determine within section AVC variability and according to specific types of experiments (e.g., GPS-6B) to make comparisons amongst groups of test sections. The statistical method of analysis of variance (ANOVA) was employed to determine the variance of AVC data within each test section and to determine if the AVC of groups of test sections were statistically significantly different from one another.

Within Section Variability

To determine within section variability of AVC, the data from individual test sections were first grouped as being either GPS or SPS. This resulted in 38 GPS test sections and 62 SPS test sections. Eight test sections had single observations of AVC and, therefore, could not be used in the ANOVA (i.e., more than one observation is needed to determine variance). Once grouped in this way, a single-factor (one-way) ANOVA was conducted to determine within section variance of the AVC and to determine the mean square error (MSE), which is an unbiased estimate of the variance of the population AVC. It should be noted that the standard deviations from within each GPS or SPS section were pooled to determine the overall standard deviation. In the process, the individual group standard deviations were weighted according to the number of samples within each group.

Differences Between Groups of Test Sections

To determine if differences in AVC exist among groups of test sections, the data from individual test sections were first grouped as being in a specific type of experiment. The specific types of experiments included:

GPS-1 – Asphalt Concrete (AC) on Granular Base

GPS-2 – AC on Bound Base

GPS-6B – New AC Overlay on AC Pavements

GPS-6C – AC Overlay With Modified Binder

GPS-6D – AC Overlay on Previously Overlaid Pavement

GPS-7B – New AC Overlay on PCC Pavements

SPS-1 – Strategic Study of Structural Factors for Flexible Pavements

SPS-5 – Rehabilitation of Asphalt Concrete Pavements

SPS-6 – Rehabilitation of Jointed Portland Cement Concrete Pavements

SPS-8 – Study of Environmental Effects in the Absence of Heavy Loads

Once the test sections were grouped by specific experiment, single factor ANOVAs were conducted at a level of significance of 0.05 (i.e., 95 percent confidence level) to determine if differences in AVC existed between the certain groups of data. Tests were conducted with a null hypothesis of no difference in mean AVC and an alternative hypothesis of a difference in mean AVC. Since comparisons between certain groups would not provide intuitively useful information (e.g., GPS-1 versus SPS-6), only certain groups of data were compared. The analysis matrix shown in Table 13 indicates the groups of data that were compared. Although it is recognized that comparing the average AVC of all GPS test sections with the average AVC of all SPS test sections does not provide for a like-for-like comparison, it was included simply to obtain the average and variance of the respective groups of data.

The data were also grouped according to thickness and comparisons were made between certain groups of data to determine if thickness played a role in the variability of AVC. The analysis matrix shown in Table 14 indicates the groups of data that were compared.

Table 13.   Analysis matrix for broad comparisons.

GPS Experiment	SPS Experiment				
	SPS	SPS-1	SPS-5	SPS-6	SPS-8
GPS	√				
GPS-6		√	√		√
GPS-6B		√	√		√
GPS-6C		√	√		√
GPS-6D		√	√		√
GPS-7B				√	

Table 14.   Analysis matrix for comparisons grouped by HMA thickness.

GPS Experiment	SPS Experiment									
	SPS		SPS-1		SPS-5		SPS-6		SPS-8	
	< 4 in.	≥ 4 in.	< 4 in.	≥ 4 in.	< 4 in.	≥ 4 in.	< 4 in.	≥ 4 in.	< 4 in.	≥ 4 in.
GPS	√	√								
GPS-6B			√	√	√				√	√
GPS-6C			√		√				√	
GPS-6D			√		√				√	
GPS-7B							√			

Within Section Variability

The results of the ANOVA to determine within section variability in AVC are summarized in Table 15. The results indicate that when all data from GPS sections is considered as a single group and all data from SPS sections is considered as a single group, the estimate of the population variance (mean square error) for the GPS sections is nearly double that of the estimate for the SPS sections. In terms of standard deviation, these results indicate that the data from the GPS sections had a standard deviation that was approximately 35 percent greater than that of the data from the SPS sections.

Table 15. Summary of variability in AVC for the GPS and SPS sections analyzed.

Statistic	Experiment	
	GPS	SPS
Mean Square Error (MSE)	2.03	1.11
Minimum Variance	0.00	0.00
Maximum Variance	18.9	20.1
Overall Standard Deviation	**1.42**	**1.05**
Minimum Standard Deviation	0.00	0.00
Maximum Standard Deviation	4.35	4.49

Differences Between Groups of Test Sections

The results of the ANOVA to determine if differences in AVC exist among certain groups of data are summarized in Table 16. The table shows whether or not the null hypothesis (i.e., no difference in means) should be rejected at the significance level $\alpha = 0.05$ (95 percent confidence level) and the p-value, which indicates the smallest level of significance at which the null hypothesis can be rejected.

Table 16. Summary of comparisons of certain data groups.

Data Group Comparison	Significant Difference at $\alpha = 0.05$?	p-value
GPS vs. SPS	*No*	0.82
GPS-6B, 6C, and 6D vs. SPS-1	Yes	0.010
GPS-6B vs. SPS-1	Yes	0.0040
GPS-6C vs. SPS-1	No	0.83
GPS-6D vs. SPS-1	No	0.84
GPS-6B, 6C, and 6D vs. SPS-5	Yes	0.0012

GPS-6B vs. SPS-5	Yes	0.022
GPS-6C vs. SPS-5	No	0.082
GPS-6D vs. SPS-5	Yes	0.00085
GPS-6B, 6C, and 6D vs. SPS-8	No	0.49
GPS-6B vs. SPS-8	No	0.92
GPS-6C vs. SPS-8	No	0.31
GPS-6D vs. SPS-8	Yes	0.046
GPS-7B vs. SPS-6	No	0.39

The results indicate that the mean AVC from GPS-6B sections was significantly different from the mean AVC from SPS-1 and SPS-5 sections but not the SPS-8 sections at the 95 percent confidence level. They also indicate that the mean AVC from GPS-6D sections was significantly different from the mean AVC from SPS-5 and SPS-8 sections but not the SPS-1 sections at the 95 percent confidence level. Also, the mean AVC from the GPS-7B sections was not significantly different from the mean AVC from the SPS-6 sections at the 95 percent confidence level.

Although these comparisons are interesting to make, they do not provide information about the variability in the data groups. However, in ANOVA, the variance within each data group is determined prior to determining significance. Table 17 summarizes the standard deviation (the square root of the variance) for each data group compared in Table 16. It indicates that, in all but three cases, the standard deviations (and, hence, the variances) of the SPS data groups were greater than those for the GPS data groups.

Table 17. Summary of standard deviations of certain data groups.

Data Group Comparison	Standard Deviation of AVC (Percent)	
	GPS Sections	SPS Sections
GPS vs. SPS	2.22	2.63
GPS-6B, 6C, and 6D vs. SPS-1	2.24	2.70
GPS-6B vs. SPS-1	2.44	2.70
GPS-6C vs. SPS-1	1.04	2.70
GPS-6D vs. SPS-1	1.29	2.70
GPS-6B, 6C, and 6D vs. SPS-5	2.24	2.29
GPS-6B vs. SPS-5	2.44	2.29
GPS-6C vs. SPS-5	1.04	2.29
GPS-6D vs. SPS-5	1.29	2.29
GPS-6B, 6C, and 6D vs. SPS-8	2.24	2.06
GPS-6B vs. SPS-8	2.44	2.06
GPS-6C vs. SPS-8	1.04	2.06
GPS-6D vs. SPS-8	1.29	2.06
GPS-7B vs. SPS-6	1.79	2.05

The results of the ANOVA to determine if differences in AVC exist among certain groups of data categorized by thickness are summarized in Table 18. The table shows whether or not the

null hypothesis (i.e., no difference in means) should be rejected at the significance level $\alpha = 0.05$ (95 percent confidence level) and the p-value, which indicates the smallest level of significance at which the null hypothesis can be rejected.

The results indicate that significant differences exist for the majority of comparisons at the 95 percent confidence level ($\alpha = 0.05$). In the comparisons where there are significant differences, the results provide evidence that thickness is an important factor in the variability of AVC when comparing GPS versus SPS test sections. In addition, it can be seen from Table 19 that the SPS sections had greater variability in AVC in all but three of the comparisons.

Table 18. Summary of certain data groups categorized by thickness.

Data Group Comparison	HMA Thickness			
	< 4 in.		≥ 4 in.	
	Sig. Diff. at $\alpha = 0.05$?	p-value	Sig. Diff. at $\alpha = 0.05$?	p-value
GPS vs. SPS	No	0.14	Yes	0.0059
GPS-6B vs. SPS-1	Yes	1.8×10^{-8}	*Yes*	0.0016
GPS-6C vs. SPS-1	Yes	0.0080		
GPS-6D vs. SPS-1	Yes	2.2×10^{-5}		
GPS-6B vs. SPS-5	Yes	0.015		
GPS-6C vs. SPS-5	No	0.088		
GPS-6D vs. SPS-5	Yes	0.0010		
GPS-6B vs. SPS-8	No	0.088	No	0.36
GPS-6C vs. SPS-8	Yes	0.003		
GPS-6D vs. SPS-8	Yes	0.00011		
GPS-7B vs. SPS-6	No	0.39		

Table 19. Summary of standard deviations of certain data groups categorized by thickness.

Data Group Comparison	Standard Deviation			
	< 4 in.		≥ 4 in.	
	GPS	SPS	GPS	SPS
GPS vs. SPS	2.25	2.94	1.38	2.33
GPS-6B vs. SPS-1	2.49	2.65	*1.70*	2.00
GPS-6C vs. SPS-1	1.04	2.65		
GPS-6D vs. SPS-1	1.29	2.65		
GPS-6B vs. SPS-5	2.49	2.34		
GPS-6C vs. SPS-5	1.04	2.34		
GPS-6D vs. SPS-5	1.29	2.34		
GPS-6B vs. SPS-8	2.49	1.21	1.70	1.96
GPS-6C vs. SPS-8	1.04	1.21		
GPS-6D vs. SPS-8	1.29	1.21		

GPS-7B vs. SPS-6	1.79	2.05		

4.3 OTHER STUDIES

In addition to examining LTPP data, the findings from several other studies were reviewed. These are summarized below.

4.3.1 WesTrack Project

During the WesTrack project, a substantial number of cores were taken during and immediately following construction of the various test sections (Epps et al. 2000a, Epps et al. 2000b).   In most cases, five cores from each test section were tested for bulk specific gravity and loose mixtures sampled from trucks were tested for theoretical maximum specific gravity.   AVCs calculated from these test results were grouped according to the three gradations utilized in the WesTrack study—fine, fine-plus, and coarse—and analyzed to determine variance in AVC by test section and the mean square for error (estimate of population variance).

Table 20 summarizes the results of ANOVA conducted on the data from the WesTrack test sections (Epps et al. 2002).   It indicates that although differences in variability existed between test sections grouped by aggregate gradation, the standard deviation of AVC was, in all but one case, less than 1 percent.   The mean square error (the unbiased estimate of population variance) when considering all data as a single sample was 0.70 with a corresponding standard deviation of 0.84 percent.

4.3.2 Colorado DOT Studies

FHWA Demo Project 74

Aschenbrener documented a variety of mixture characteristics from pavements in Colorado that were part of the FHWA Demonstration Project No. 74 (Aschenbrener 1994a).   Table 21 summarizes the variability in lab-measured AVC for these projects.   As indicated, the standard deviations ranged from 0.44 to 0.64 percent.

Table 20.   Summary of variability in AVC data from WesTrack sections (Epps et al. 2002).

Data Group	Variance	Standard Deviation (Percent)
Fine Mixture, Bottom Lift, Before Placement of Top Lift	0.61	0.78
Fine Mixture, Bottom Lift, After Placement of Top Lift	1.8	1.3
Fine Mixture, Top Lift	0.42	0.65
Fine Plus Mixture, Bottom Lift, Before Placement of Top Lift	0.90	0.95
Fine Plus Mixture, Bottom Lift, After Placement of Top Lift	0.80	0.89
Fine Plus Mixture, Top Lift	0.25	0.50
Coarse Mixture, Bottom Lift, Before Placement of Top Lift	0.62	0.79
Coarse Mixture, Bottom Lift, After Placement of Top Lift	0.94	0.97
Coarse Mixture, Top Lift	0.46	0.68
Replacement Sections, Bottom Lift	0.56	0.75
Replacement Sections, Top Lift	0.38	0.61
Overall (All Above Data Groups)	**0.70**	**0.84**

Table 21.   Summary of variability in AVC from HMA pavements in Colorado
(Aschenbrener 1994a).

Project	AVC Data		
	Mean (Percent)	Standard Deviation (Percent)	Number of Samples Tested
I-70, Silverthorne to Copper Mtn.	2.95	0.64	40
Arapahoe Road, Galena to Parker	3.77	0.54	14
6th Avenue, Knox Ct. to Wadsworth	2.61	0.44	22

Rutting Study

Colorado DOT (CDOT) conducted a study of rutting performance on 33 HMA pavements in various locations throughout Colorado (Aschenbrener 1992). As part of the study, CDOT measured various mixture properties including AVC. A summary of the variability in AVC from samples taken between the wheel paths from these pavements is shown in Table 22. As indicated, the *study* standard deviation in AVC varied over a fairly wide range. It should be noted, however, that the AVCs were determined after the pavements had been in service for as many as 33 years.

Table 22.   Summary of variability in AVC from HMA pavements in Colorado
(Aschenbrener 1992).

Project Site	AVC Data		Pavement

	Mean (Percent)	Variance	Standard Deviation (Percent)	Number of Samples Tested	Age (Years)
3	4.35	2.62	1.62	4	Unknown
4	3.97	0.12	0.35	3	6
5	5.93	4.62	2.15	3	7
6	4.90	5.16	2.27	3	17
7	5.38	1.54	1.24	4	18
8	3.90	0.50	0.71	2	12
9	8.17	3.12	1.77	3	9
10	3.57	0.41	0.64	3	13
11	6.80	4.44	2.11	3	8
13	7.87	6.92	2.63	3	6
14	3.93	1.08	1.04	3	23
15	3.55	5.45	2.33	2	15
17	3.10	3.92	1.98	2	15
18	4.95	0.85	0.92	2	31
19	9.95	55.13	7.42	2	Unknown
21	7.85	12.01	3.46	2	12
25	6.17	1.82	1.35	3	25
26	6.55	29.65	5.44	2	25
27	5.23	2.65	1.63	3	5
28	3.00	0.03	0.17	3	33
29	5.73	2.04	1.43	3	9
30	5.70	0.39	0.62	3	9
32	8.53	0.17	0.42	3	Unknown
33	4.95	0.85	0.92	2	Unknown
34	2.40	0.64	0.80	3	21
35	3.65	1.81	1.34	2	8
36	5.30	2.00	1.41	2	29
37	5.87	5.45	2.34	3	4

Interstate 25 Study

Aschenbrener documented a variety of mixture characteristics from nine overlay projects constructed on I-25 in Colorado in 1994 (Aschenbrener 1994b). Table 23 summarizes the results of AVC determined from field cores on these projects. As indicated, the standard deviations ranged from 0.31 to 0.75 percent.

Table 23.   Summary of variability in AVC from HMA pavements in Colorado

(Aschenbrener 1994b).

Project Location	Grading	AVC Data		
		Mean (Percent)	Standard Deviation (Percent)	Number of Samples Tested
New Mexico State Line	CX	4.1	0.42	4
	C	2.7	0.49	7
Trinidad	C	4.6	0.60	7
North of Walsenburg	CX	3.8	0.75	6
Colorado City	CX	3.4	0.42	55
	C	3.8	0.58	59
Colorado Springs	CX	3.2	0.44	7
Air Force Academy	C (5.1% AC)	2.2	0.39	5
	C (4.9% AC)	3.6	0.54	8
Monument	C	4.0	0.54	46
Denver	C	2.7	0.31	6
Longmont	C	2.7	0.70	64

4.3.3 Voids Acceptance Specification Study

Brakey summarized various mixture characteristics of several HMA pavements investigated during a study on voids acceptance specifications (Brakey 1997). Table 24 summarizes the results of AVCs determined from cores taken from the projects in the study. As indicated, the standard deviations in AVC ranged from 0.40 to 0.76 percent.

Table 24. Summary of variability in AVC from HMA pavements in Colorado

(Brakey 1997).

Project	Standard Deviation of AVC (Percent)	Number of Samples Tested
CX 11-0006-17	0.40	24
STRS 0835-031	0.52	36
C 0361-046	0.53	29
STA 0451-003	0.59	73
IM 0252-279	0.53	40
IM 0704-179	0.48	39
IM 0292-293	0.57	21
HB 0703-234	0.76	26

Table 25 summarizes the compaction data compiled by Aurilio and Raymond from 1697 pavement lots constructed during 1992 in Ontario (Aurilio et al. 1995).   Although it is not possible to determine AVC from the data shown (the data were adjusted using a correction factor if core thickness was less than 40 mm), the standard deviations reported for relative compaction are indicative of standard deviations in AVC.   As indicated, these range from 1.1 to 2.2 percent.

Table 25.   Analysis of 1992 compaction data (Aurilio et al. 1995).

Mix Type[1]	Lot Mean (Percent)	Std. Dev. of Lot Means (Percent)	Coefficient of Variation (Percent)	Minimum Lot Mean (Percent)	Maximum Lot Mean (Percent)	Number of Lots Analyzed
DFC	90.9	1.78	2.0	85.6	96.6	193
HDBC	91.6	1.65	1.8	87.6	96.6	324
HL1	93.9	1.54	1.6	89.7	98.3	94
HL3	92.8	1.46	1.6	87.0	95.8	78
HL4	93.7	1.57	1.7	88.1	98.9	741
HL8	93.7	2.24	2.4	88.3	97.6	90
MDBC	94.7	1.30	1.4	91.7	96.9	47
RHM	93.6	1.07	1.1	90.1	96.1	130
Total	93.0	1.97	1.2	85.6	98.9	1697

[1]DFC = Dense Friction Course, HDBC = Heavy Duty Binder Course, HL = Hot Laid,

MDBC = Medium Duty Binder Course, and RHM = Recycled Hot Mix

4.3.5 Benson

Benson reported on a study conducted by Caltrans that compared various mixture properties of HMA pavements placed using end result and method specifications (Benson et al. 1995).   In the paper the results of ANOVA utilizing pooled data are presented and indicate the standard deviation of AVC was 1.94 percent.

4.3.6 Kandahl

Kandhal and Koehler reported on a study conducted in Pennsylvania to investigate premature pavement distress in the form of raveling on several HMA pavements between 1974 and 1977 (Kandhal et al. 1984).   In the study, cores were obtained from the distressed areas of eight projects and tested for a variety of mixture and materials properties.   The in-place AVC data

from this study is summarized in Table 26.   As indicated, the standard deviations in AVC ranged from 1.35 to 2.78 percent.

Table 26.   Summary of AVC data from the Pennsylvania study (Kandhal et al 1984).

Project	In-Place AVC Data (Percent)		
	Mean	Standard Deviation	Range
1 (Area 1)*	16.0	1.60	14.0 to 18.3
1 (Area 2)*	13.6	1.38	11.6 to 15.4
2 (Area 1)*	16.3	2.78	Not given
2 (Area 2)*	14.2	1.49	Not given
2 (Area 3)*	12.0	1.86	Not given
3	11.7	2.18	8.2 to 15.5
4	12.1	2.12	8.9 to 15.3
5	13.2	1.69	9.5 to 15.8
6	10.9	1.35	8.8 to 12.6
7	9.9	1.60	7.8 to 11.6
8	9.8	2.09	6.3 to 13.0

*Projects divided into areas based on extent of raveling.

4.3.7 Linden

From their own review of literature and data sources, researchers at the University of Washington presented findings on how compaction influences the performance of dense asphalt concrete pavement surfaces (Linden et al. 1988).   The relevant information provided in the paper regarding variability in AVC is summarized in Table 27.   As indicated, it includes only means and ranges.

Table 27.   Summary of AVC data (Linden et al. 1988)

	Pavement AVC Data (Percent)*	
	Average	Range
Maximum	9.9	5 – 15
Minimum	3.5	1 – 6
Average	6.5	2.8 – 10

*Range and average of field AVC in pavements constructed in the past (from 1988) years.

4.3.8 Weed

Weed reported on the development of a New Jersey DOT specification for AVC (Weed 1995). Two jobs were selected as pilot projects to test the implementation of the new specification. Table 28 summarizes the variability in AVC from these projects.   As indicated, the standard

deviations ranged from 0.61 to 1.59 percent for the base course mixtures and from 0.82 to 4.12 percent for the surface course mixtures.

Table 28.   Summary of variability in AVC from HMA pavements in New Jersey
(Weed 1995).

LOT	MIXTURE TYPE	AVC DATA	
		MEAN (PERCENT)	STD. DEVIATION (PERCENT)
PROJECT #1			
1	SURFACE	8.06	1.61
	BASE	5.66	0.75
2	SURFACE	6.88	1.43
	BASE	5.34	0.61
3	SURFACE	7.56	1.68
	BASE	5.26	0.98
4	SURFACE	7.22	1.54
	BASE	5.74	1.36
5	SURFACE	7.04	1.79
	BASE	4.38	0.69
6	SURFACE	7.12	2.52
	BASE	5.72	1.17
7	SURFACE	8.06	2.09
	BASE	5.72	1.18
8	SURFACE	7.30	2.13
	BASE	4.92	0.89
9	SURFACE	6.26	0.82
	BASE	5.06	1.02

10	**SURFACE**	**9.66**	**2.44**
	BASE	**5.48**	**0.79**
11	**SURFACE**	**5.90**	**1.14**
	BASE	**5.32**	**0.73**
12	**SURFACE**	**8.10**	**1.62**
	BASE	**6.74**	**1.59**
PROJECT #2			
1	**SURFACE**	**6.12**	**1.38**
	BASE	**5.16**	**0.62**
2	**SURFACE**	**8.00**	**4.12**
	BASE	**5.48**	**0.87**
3	**SURFACE**	**9.38**	**3.01**

4.4 SUMMARY

A thorough statistical analysis of the LTPP AVC database was conducted to examine the differences in variability and volumetric properties (i.e., AVC) between the SPS and GPS test sections.   In addition, data from several other studies were compiled in an effort to characterize field variability.   The ultimate goal of this effort is develop some improved guidelines for specifying AVC control requirements in future HMA construction specifications.

Following is a summary of the findings.

1. When all data from the LTPP sections analyzed were grouped according to the broad

    LTPP experiments (i.e., GPS or SPS), the estimate for the population standard deviation

    for AVC for GPS sections was 1.42 percent whereas that for the SPS sections was 1.05

    percent.

2. In testing certain groups of data categorized by specific experiment (e.g., GPS-6B versus SPS-1), significant differences existed between the mean AVC of the GPS sections and the mean AVC of the SPS sections in only 6 of the 14 comparisons made. In addition, in these comparisons the standard deviation in AVC of the SPS sections was greater than that of the standard deviation in AVC of the GPS sections in 11 of the 14 comparisons.

3. When the data from specific SPS and GPS experiments (e.g., GPS-6B, SPS-1, etc.) were grouped by thickness (i.e., less than 4 in. or greater than or equal to 4 in.), significant differences existed between the mean AVC of the GPS sections and the mean AVC of the SPS sections in 9 of the 14 comparisons made. These results provide evidence that thickness is an important factor in the variability of AVC when comparing GPS versus SPS test sections. In addition, in these comparisons the standard deviation in AVC of the SPS sections was greater than that of the standard deviation in AVC of the GPS sections in 11 of the 14 comparisons.

4. Analysis of the AVC data from the WesTrack project, where emphasis was placed on quality control, indicated that the standard deviation of AVC ranged from 0.50 to 1.3 percent for test sections grouped by gradation (i.e., fine, fine plus, and coarse) and that the overall standard deviation (when all data was considered as a single sample) was determined to be 0.84 percent.

5. AVC standard deviation from various studies in Colorado ranged from a low of 0.17 percent to a high of 7.4 percent for pavements that had been in service for as many as 33 years. However, for those projects where data was collected immediately following construction, AVC standard deviation ranged from 0.31 to 0.76 percent.

6. A study conducted by the Ontario Ministry of Transportation involving investigation of the volumetric properties of samples obtained from 1697 pavement lots indicated that the standard deviation of AVC ranged from 1.07 to 2.24 percent.

7. A study conducted by Caltrans that involved investigating deviations in AVC (and other mixture properties) in projects constructed in accordance with end result and method specifications showed that the overall (pooled) standard deviation in AVC was 1.94 percent.

8. A study conducted by the New Jersey DOT that investigated in-place AVCs from several pavement lots in two pilot projects indicated that the standard deviations in AVC ranged from 0.61 to 1.59 percent for base course mixtures and from 0.82 to 4.12 percent for surface course mixtures.

Figure 17 presents a graphical summary of these findings.
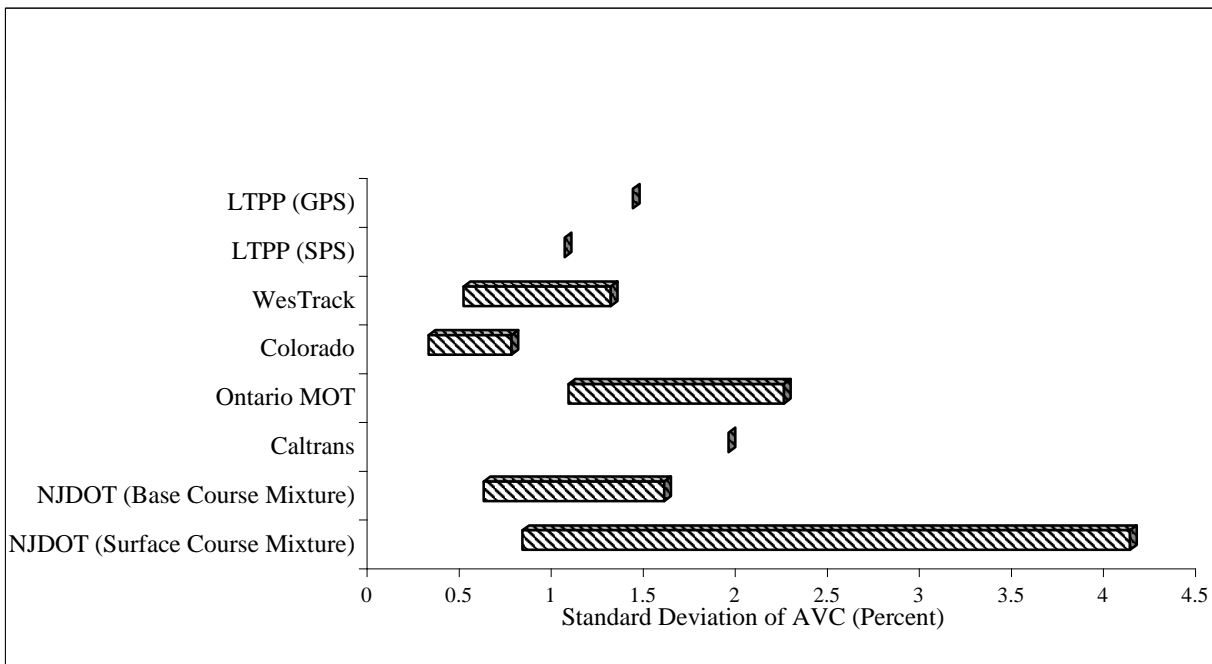
Figure 17. Graphical summary of AVC standard deviations from LTPP and other studies.

Based upon an examination of the individual and overall findings, the following two observations can be made:

1. There appears to be no meaningful differences between the variability in AVCs in the

    GPS and SPS sections (although the analyses indicated that the SPS sections had, in

    general, higher variability).

Excluding the data from NJDOT (surface course mixtures), the general range in standard deviation of AVC is between 0.5 and 2.0 percent.

Chapter 5

Interpretation, Appraisal and Application

5.1 OVERVIEW

This chapter provides basic guidelines for compaction of HMA. The guidelines are based on the results of the sensitivity analyses of HMA performance and stiffness to AVC and include the following:

1. Optimum range of AVC based on pavement performance (i.e., fatigue cracking and

   rutting).

2. Acceptable values of variability for AVC.

3. Desirable levels of compaction.

5.2 OPTIMUM RANGE OF AVC BASED ON PAVEMENT

PERFORMANCE

One of the primary goals of this study was to use the HMA pavement materials and performance information in the LTPP database to determine if optimum AVC values existed that, when used, would help maximize pavement performance in terms of fatigue cracking and rutting. Unfortunately, because of apparent weaknesses in the LTPP data, including a shortage of actual as-constructed AVC data, optimum values that satisfied the test of reasonableness could not be identified. Accordingly, guidelines were developed based on our analysis of the sensitivity of pavement performance to AVC. Pavement performance, in this instance, was characterized in terms of fatigue and rutting.

5.2.1 Fatigue Cracking

Section 3.3 of this report addressed the issue of the sensitivity of fatigue cracking to AVC.   Analysis of data and models available in the literature indicated that deviations in AVC of 1 percent from its target could reduce the pavement fatigue life by an amount in the range of 8 to 44 percent.   Twenty percent was recommended as a "rule of thumb."   This value is twice as high as the 10 percent reduction guideline suggested by researchers in the State of Washington (Linden et al. 1988).   However, considering the variability and the inherent risk, a value of 20 percent for every 1 percent increase in AVC is reasonable.

The fact that the sensitivity statistic, S_{PAV}, is negative, implies that the optimum fatigue life is achieved with the lowest possible AVC without causing rutting, say, 3 to 4 percent. However, since AVC is evaluated during or shortly after construction, and traffic can further densify the HMA, a better target AVC for construction would be 5 to 6 percent.

5.2.2 Rutting

The original hypothesis for optimal AVC related to rutting performance was based on prior work by several researchers (Powell et al. 1975, Linden et al. 1988, Brown 1992).   The optimal AVC to preclude rutting ranged from 3 to 5 percent.   This is based on the observation that values of AVC lower than 3 percent are more likely to close under trafficking and create a situation where shoving and shear flow would lead to severe rutting.   On the other hand, AVC values higher than 5 percent are more likely to experience a minor increase in rutting as a result of further densification under trafficking.

In the sensitivity analysis of rutting performance to AVC, the WesTrack project (Epps et al. 2002) provided the only viable results. Based on these findings (see section 3.4), the value for the effect of AVC on rutting was a 10 percent reduction in rutting life for a 1 percent increase in AVC. Although this value is half the effect of AVC on fatigue performance, it is consistent and, applying the same AVC controls to guard against shoving and shear flow, the recommended target AVC range for original construction is 5 to 6 percent.

5.3 VARIABILITY IN AVC

The variability in AVC was examined using a number of data sources, including LTPP, WesTrack and several state highway agencies as reported in Chapter 4. Figure 17 summarizes the standard deviation of AVCs for the studies investigated. Excluding some data on surface mixes in New Jersey, the general range in AVC standard deviation was from 0.5 to 2.0 percent. Based on the available information for standard deviation and the better understanding of the effect of AVC on pavement performance, the recommended target AVC standard deviation is 1 percent. This value is on the low end of the range; however, based on the data from the Colorado, WesTrack, and LTPP SPS sections, it would serve as both a reasonable and achievable standard for compaction variability on highway construction projects.

5.4 DESIRABLE LEVEL OF COMPACTION

Most agencies currently use 92 percent of maximum density for compaction of state and interstate highways. The overall findings of this study suggest this value is still a good target for fatigue and rutting. However, better performance and longer lasting roadways would likely be achieved at the 94 to 95 percent level, so long as the 97 percent maximum density criterion is not exceeded.

Chapter 6

CONCLUSIONS AND RECOMMENDATIONS

6.1 CONCLUSIONS

Following are the basic conclusions that were drawn from the results of this study.   They

are presented in terms of how well the study satisfied the project objectives.

OBJECTIVE 1 – EVALUATE THE USE OF LTPP DATA FOR DETERMINING THE EFFECT OF IN-

PLACE AVC AND OTHER MIX VOLUMETRICS ON THE PERFORMANCE OF HMA PAVEMENTS.

1. Fatigue cracking – It was not possible to develop a fatigue cracking model based on
   LTPP data that characterize the effect of as-constructed AVC.   Because of a lack of
   data from which to calculate as-constructed AVC and the fact that many sections do
   not exhibit significant cracking, there was simply not enough data.

2. Permanent deformation – Data from three different LTPP experiments were analyzed
   in an attempt to develop one or more models that characterize the effect of as-
   constructed AVC on rutting.   For the model based on data from newly constructed
   HMA pavements, the limited amount of data suggested an optimum AVC of about 10
   percent, well outside the range of reasonableness.   For the model based on data from
   HMA overlays on pre-existing HMA pavements, the limited data indicated that AVC
   had no effect on rutting performance.   For the model based on data from HMA
   overlays on PCC pavements, there were not enough data to make any observations.
   Thus, it was concluded that the available LTPP data did not support the development
   of a valid prediction model.

3. HMA stiffness – Processing of the LTPP data for HMA stiffness yielded 50 pavement
   sections that could potentially be used to develop a prediction model for HMA
   stiffness as a function of AVC.   Analysis of the data, however, indicated that no
   relationship existed.   Because of the apparent validity of the approach and the
   quantity of data, it was concluded that the inherent variability of the results was too
   large to detect what are likely minor trends.

OBJECTIVE 2 – DEVELOP NEW OR MODIFIED AVC GUIDELINES FOR OPTIMUM PAVEMENT

PERFORMANCE.

Although no LTPP models could be developed and included in the analysis, there was a significant amount of data available from the literature that could be used to develop compaction guidelines that could be used in future construction specifications.

1. Fatigue Cracking – The target range for AVC is 5 to 6 percent. This guideline was based on an examination of data from four different sources and the observation that a 1 percent increase in AVC produces an approximate 20 percent reduction in fatigue life (see section 3.3.5). It also takes into consideration the fact that values of AVC below 3 percent can lead to closure of the voids under trafficking, shoving and severe rutting.

2. Rutting – The target range for AVC is 5 to 6 percent. This guideline was based on an examination of data from one data source and the observation that a 1 percent increase in AVC produces an approximate 10 percent reduction in rutting life (see section 3.4.3). It also takes into consideration the fact that values of AVC below 3 percent can lead to closure of the voids under trafficking, shoving, and severe rutting. (Note: Because the apparent sensitivity of rutting to AVC is half that of fatigue cracking and the fact that the only data source used to make the assessment was an accelerated load experiment that experienced little age-hardening of the HMA, this guideline does not carry the same "weight" as the guideline for fatigue cracking performance).

3. Compaction – The compaction guideline is tied to directly to the guidelines for AVC for both fatigue cracking and rutting. Thus, the recommended target compaction level is 94 to 95 percent of maximum density. To avoid the potential for severe rutting, however, care should be taken to avoid over-compaction, i.e., compaction levels of 97 percent of maximum density.

OBJECTIVE 3 – EXAMINE THE EFFECT OF THE LEVEL OF CONSTRUCTION CONTROL BETWEEN THE LTPP GPS AND SPS SECTIONS ON THE VARIABILITY OF AS-CONSTRUCTED AVC AND OTHER VOLUMETRIC PROPERTIES.

Based on a multi-faceted analysis of the variability of AVC in the LTPP database, no meaningful difference exists between the GPS and SPS sections. The overall conclusion from this is that better quality control (if it did indeed exist in the SPS sections) had no effect on the variability of AVC. This was based on the following observations.

1. For the GPS versus SPS overall comparison, the standard deviations of AVC were 1.42 and 1.05 percent, respectively.

2. For comparisons between "like" experiments in the GPS and SPS sections, the standard deviation of the SPS sections was greater in 11 out of the 14 cases than the

standard deviation of the corresponding GPS sections. In 6 of these instances, the standard deviations were statistically significant.

3. For comparisons between GPS and SPS sections grouped by HMA thickness, the standard deviation of the SPS sections was greater in 11 out of the 14 cases than the standard deviation of the corresponding GPS sections. In 9 of these 14 cases, the standard deviations were statistically significant.

6.2 RECOMMENDATIONS

1. The primary recommendations from this study are in the form of the improved guidelines for as-constructed AVC and compaction, as presented in Chapter 4 of the report and summarized under the second objective above.

   - Target as-constructed AVCs in the range of 5 to 6 percent (or compaction levels on the order of 94 to 95 percent of maximum theoretical density) are likely to result in improved pavement performance in terms of fatigue cracking. This target range is also likely to result in improved rutting performance, although the supporting data is not as definitive as for fatigue cracking.

   - The use of the suggested pavement life reduction factors (e.g., 20 percent reduction in life for every 1 percent increase in AVC above the target) as the basis for a life-cycle cost based pay adjustment in the specification can help provide the needed emphasis to the contractor to achieve better compaction levels.

2. Given the nature of the LTPP database and the limited amount of information that can be used to calculate as-constructed AVC on a true section-by-section basis, it is recommended that any future analyses involving the consideration of as-constructed AVC be postponed until such time that more data becomes available. It is recommended that be achieved by developing a valid statistical experiment design, identifying target LTPP sections, and then returning to them to obtain cores for the purpose of determining their in-situ AVC. To obtain the best estimate of the "as-constructed" AVC, the cores would be obtained areas outside the wheel path that have received the least trafficking and densification.

3. In the process of evaluating the relationship between HMA stiffness and AVC in the LTPP database, a relatively simple approach was used to derive a relationship to account for the effect of pavement temperature. Despite the simplicity of the approach and the use of an approximate method of HMA stiffness backcalculation, the model showed a good correlation between stiffness and pavement temperature. Accordingly, it is recommended that a more rigorous analysis of the LTPP database

be carried out to develop a model to predict HMA stiffness as a function of pavement temperature, age of the HMA, and other mix characteristics.

REFERENCES

AASHTO. 1993. "Guide for Design of Pavement Structures", American Association of State Highway and Transportation Officials, Washington, D.C.

Andrei, D., M.W. Witczak, and M.W. Mizra. 1999. "Development of a Revised Predictive Model for the Dynamic (Complex) Modulus of Asphalt Mixtures." NCHRP Project 1-37A Inter Team Report, University of Maryland.

Aschenbrener, T. 1992. "Investigation of the Rutting Performance of Pavements in Colorado," *CDOT-DTD-R-92-12*, Colorado Department of Transportation, Denver, CO.

Aschenbrener, T. 1994a. "Demonstration of a Volumetric Acceptance Program for Hot Mix Asphalt in Colorado, FHWA Demonstration Project No. 74," *CDOT-DTD-R-94-2*, Colorado Department of Transportation, Denver, CO.

Aschenbrener, T. 1994b. "A Documentation of Hot Mix Asphalt Overlays on I-25 in 1994," *CDOT-DTD-R-95-14*, Colorado Department of Transportation, Denver, CO.

The Asphalt Institute. 1982. "Research and Development of The Asphalt Institute's Thickness Design Manual (MS-1) Ninth Edition," Research Report No. 82-2, The Asphalt Institute, College Park, MD.

Aurilio, V. and C. Raymond. 1995. "Development of End Result Specification for Pavement Compaction," *TRR 1491*, pp. 11-17, Transportation Research Board, Washington, D.C.

Bell, C.A., R.G. Hicks, and J.E. Wilson. 1984. "Effect of Percent Compaction on Asphalt Mixture Life," *ASTM STP 829*, American Society for Testing and Materials, Philadelphia, PA.

Benson, P.E. 1995. "Comparison of End-Result and Method Specifications for Managing Quality," *TRR 1491*, pp. 3-10, Transportation Research Board, Washington, D.C.

Brakey, B.A. 1997. "HBP Pilot Void Acceptance Projects Completed in 1993-1996," *CDOT-DTD-R-97-8*, Colorado Department of Transportation, Denver, CO.

Brown, S.F. 1980. "Implementation of Analytical Pavement Design: A Case Study," The Journal of the Institute of Highway Engineers.

Brown, E.R. and S.A. Cross. 1992. "A National Study of Rutting in Asphalt Pavements," *Journal*, Association of Asphalt Paving Technologists, Vol. 61 pp. 535-582.

D'Angelo, J.A. and Ferragut, T. 1991. "Summary of Simulation Studies from Demonstration Project No. 74 Field Management of Asphalt Mixes," *Journal of the Association of Asphalt Paving Technologists*, Volume 60, pp 287-309.

Epps, J.A. and C.L. Monismith. 1969. "Influence of Mixture Variables on the Flexural Fatigue Properties of Asphalt Concrete," *Proceedings*, Association of Asphalt Paving Technologists, Vol. 38, pp. 423-464.

Epps, J.A., A.J. Hand, and P.E. Sebaaly. 2000a. "In-Place Air Void Content and Thickness: Original Construction," WesTrack Technical Report UNR-12.

Epps, J.A., A.J. Hand, and P.E. Sebaaly. 2000b. "In-Place Air Void Content and Thickness: Replacement Sections," WesTrack Technical Report UNR-13.

Epps, J.A., S.B. Seeds, C.L. Monismith, J.T. Harvey, S.H. Alavi, T.V. Scholz, R.B. Leahy, and S.C. Ashmore. 2002. "Recommended Performance-Related Specifications for Hot-Mix Asphalt Construction: Results of the WestTrack Project," NCHRP Report 455, National Cooperative Highway Research Program, Transportation Research Board, Washington, D.C.

Epps, J.A. 1968. *"Influence of Mixture Variables on the Flexural Fatigue and Tensile Properties of Asphalt Concrete"*, Ph.D. Dissertation, University of California, Berkeley.

Harvey, J.T. and B.W. Tsai. 1996. "Effects of Asphalt Content and Air Void Content on Mix Fatigue and Stiffness," *TRR 1543*, Transportation Research Board, Washington, D.C.

Kandhal, P.S. and W.C. Koehler. 1984. "Pennsylvania Experience in the Compaction of Asphalt Pavements," *ASTM STP 829*, pp 93-106.

Linden, R.N., J.P. Mahoney, and N.C. Jackson. 1988. "Effect of Compaction on Asphalt Concrete Performance," *TRR 1217*, pp. 20-28, Transportation Research Board, Washington, D.C.

E.O. Lukanen, R. Stubstad, and R. Briggs. 2000. "Temperature Predictions and Adjustment Factors for Asphalt Pavement," Final Report, FHWA-RD-98-085, Federal Highway Administration, Washington, D.C.

McGennis, R.B., R.M. Anderson, T.W. Kennedy, M. Solaimanian. 1995. "Background of SUPERPAVE Asphalt Mixture Design and Analysis," Final Report, FHWA-SA-95-003, Federal Highway Administration, Washington, D.C.

Oliver, J.W.H. 2000. "The Effect of Binder Film Thickness on Asphalt Cracking and Raveling," Australian Roads Research Board, Victoria, Australia.

Oliver, J.W.H. and A.J. Alderson. 2000. "The Effect of Air Void Content on Resilient Modulus, Dynamic Creep and Wheel Tracking Results," Australian Road Research Board, Victoria, Australia.

Pell, P.S. and K.E. Cooper. 1975. "The Effect of Testing and Mix Variables on the Fatigue Performance of Bituminous Materials," *Proceedings*, The Association of Asphalt Paving Technologists, Vol. 44, pp.1-37.

Powell, W.D. and N.W. Lister. 1975. "Compaction of bituminous Materials." Chapter 4 of a reprint from <u>Developments in Highway Pavement Engineering-1</u>, published by Applied Science Publishers, Ltd., Essex, England.

Simpson, A.L., J.B. Rauhut, P.R. Jordahl, E. Owusu-Antwi, M.I. Darter, R. Ahmad, O. Pendleton, and Y. Lee. 1994. "Sensitivity Analysis for Selected Pavement Distresses," *SHRP-P-393*, Strategic Highway Research Program, National Research Council, Washington, D.C.

Weed, R.M. 1995. "Development of Air Voids Specification for Bituminous Concrete," *TRR 1491*, pp. 33-39, Transportation Research Board, Washington, D.C.

Zhou, H., R.G. Hicks and C.A. Bell. 1990. "BOUSDEF: A Backcalculator Program for Determining Moduli of a Pavement Structure," Transportation Research Record 1260, Transportation 'research Board, Washington, D.C.

PROJECT DATABASE FOR LTPP DATA

Legend:

SC		State Code
CN		Construction No
Exp Type		LTPP Experiment Type
Climate	C_W	Cold Wet
	C_D	Cold Dry
	H_W	Hot Wet
	H_D	Hot Dry
Const_Date		Pavement Construction Completion Date
Test Age	A	Air voids tested less than 3 months
	B	Air voids tested between 3 and 6 months
	C	Air voids tested between 6 and 12 months
	D	Air voids tested between 12 and 18 months
Family	AC New	New asphalt concrete pavement
	AC OL	Asphalt concrete overlay
	AC/PCC	AC/PCC pavement rehab.
T_HMA		Total HMA thickness in the pavement structure, inch
AV		Average air voids (%) for associated HMA layer. If data exist for multiple layers, value for the top layer is listed
AVA		Air voids used for analysis, determined from test data obtained from the same HMA layer at adjacent SPS sections
AC		Average asphalt content for associated HMA layer. If data exist for multiple layers, value for the top layer is listed
A_Lyr		Associated pavement layer that was listed in the Air_Voids and/or Asph_Content columns
HMA_MR		Average of backcalculated modulus, ksi
Base_Type		See note in sheet Section_Data for explaination
Subg_MR		Backcalculated subgrade modulus, ksi
F_Cls	1	Rural Principal Arterial - Interstate
	2	Rural Principal Arterial - Other
	6	Rural Minor Arterial
	7	Rural Major Collector
	8	Rural Minor Collector
	9	Rural Local Collector
	11	Urban Principal Arterial - Interstate
	12	Urban Principal Arterial - Other Freeways or Expressways
	14	Urban Other Principal Arterial
	16	Urban Minor Arterial

17	Urban Collector
19	Urban Local

Table A-1. Section Fundamental Data

SC	SHRP_ID	CN	Exp	Type	Climate	Const_Date	Test Age	Family	T_HMA	AV	AVA	AC	A_Lyr	HMA Density	HMA MR	Base_Type	Subg_Type	Subg MR	F_Cls	For
2	1004	2	G	6B	C_D	02-Jun-91	D	AC OL	5.4	3.97	3.97	5.85	5			GB	Coarse		14	R
4	0113	1	S	1	H_D	05-Aug-93		AC New	4.5		10.52			2275	1110.2	GB	Coarse	31.0	2	F
4	0114	1	S	1	H_D	30-Jul-93		AC New	6.8		9.75			2246	891.2	GB	Coarse	58.0	2	F
4	0115	1	S	1	H_D	30-Jul-93	B	AC New	6.6	9.75	9.75	4.3	3	2252	2050.9	TB	Coarse	47.6	2	R
4	0116	1	S	1	H_D	05-Aug-93	B	AC New	4.1	8.32	9.75	4.7	2		2072.4	TB	Coarse	75.3	2	R
4	0117	1	S	1	H_D	30-Jul-93		AC New	7.6		9.75			2252	2111.4	TB/GB	Coarse	47.3	2	R
4	0118	1	S	1	H_D	05-Aug-93		AC New	4		9.75			2223	2642.7	TB/GB	Coarse	63.0	2	R
4	0119	1	S	1	H_D	30-Jul-93		AC New	6.3		9.75				2051.9	TB/GB	Coarse	40.3	2	R
4	0120	1	S	1	H_D	05-Aug-93		AC New	4		10.52			2289	1510.7	TB/GB	Coarse	55.0	2	R
4	0121	1	S	1	H_D	05-Aug-93		AC New	4.1		10.52			2273	1441.1	TB/GB	Coarse	58.0	2	R
4	0122	1	S	1	H_D	23-Jul-93	B	AC New	4.2	10.52	10.52	3.9	5	2318	2095.2	TB	Coarse	81.1	2	R
4	0123	1	S	1	H_D	30-Jul-93		AC New	6.8		9.75				1684.8	TB	Coarse	46.6	2	R
4	0124	1	S	1	H_D	30-Jul-93	B	AC New	6.7	7.24	9.75	4.5	3		1686.2	TB	Coarse	71.8	2	R
4	0161	1	S	1	H_D	05-Aug-93	B	AC New	5.7	8.71	8.71	4.3	3			GB	Coarse		2	F
4	0162	1	S	1	H_D	05-Aug-93		AC New	8.2		8.71						Coarse		2	F
5	3058	1	G	2	H_W	01-Feb-90	C	AC New	6	7.63	7.63	4.7	4	2360	672.6	TB	Coarse	23.2	12	R
6	8534	2	G	6B	H_W	08-Jul-91	C	AC OL	8.2	6.65	6.65	5.25	7			GB	Coarse		1	R
6	8535	2	G	6B	H_W	29-Jul-91	C	AC OL	10.4	7.65	7.65	5.3	8			GB	Fine		1	R
8	6002	2	G	6C	C_D	10-May-96	C	AC OL	10.5	5.96	5.96	5.3	5		320.9	GB	Fine	16.5	1	R
9	4020	2	G	7B	C_W	13-Sep-90	B	AC/PCC	3.4	6.97	6.97	5	4			GB	Coarse		12	R
12	0101	1	S	1	H_W	08-Mar-95	D	AC New	6.8	4.98	4.98	5.2	3			GB	Coarse		2	F
12	0102	1	S	1	H_W	07-Mar-95		AC New	3.9		4.98					GB	Coarse		2	F
17	5151	2	G	7B	C_W	02-Oct-90	B	AC/PCC	3.3	4.29	4.29	5.1	5			TB	Coarse		1	R
24	1634	2	G	6C	C_W	03-Jun-98	D	AC OL	6.8	7.71	7.71	4.98	6			TB	Fine		2	R
26	0603	2	S	6	C_W	30-May-90	C	AC/PCC	5.1	1.79	1.79		5			GB	Fine			R
26	0604	2	S	6	C_W	30-May-90		AC/PCC	5.4		1.79					GB	Fine			R
26	0606	2	S	6	C_W	30-May-90		AC/PCC	5		1.79					GB	Fine			R
26	0607	2	S	6	C_W	30-May-90		AC/PCC	4.6		1.79					GB	Fine			R
26	0608	2	S	6	C_W	30-May-90		AC/PCC	6.8		1.79					GB	Fine			R
29	5403	2	G	6B	C_W	16-Sep-89	C	AC OL	6.2	8.89	8.89	3.8	5			TB	Coarse		6	R

Table A-1. Section Fundamental Data

SC	SHRP_ID	CN	Exp	Type	Climate	Const_Date	Test Age	Family	T_HMA	AV	AVA	AC	A_Lyr	HMA Density	HMA MR	Base_Type	Subg_Type	Subg MR	F_Cls	For
29	5413	2	G	6B	C_W	16-Sep-89	B	AC OL	6.9	6.97	6.97	3.85	6			TB	Fine		6	R
30	0502	2	S	5	C_D	12-Sep-91	D	AC OL	6.9	5.62	5.62	4.77	6			GB	Coarse		1	R
30	0503	2	S	5	C_D	12-Sep-91		AC OL	8.8		3.19					GB	Coarse		1	R
30	0504	2	S	5	C_D	12-Sep-91		AC OL	10		3.19					GB	Coarse		1	R
30	0505	2	S	5	C_D	11-Sep-91	D	AC OL	6.8	3.19	3.19	5.13	6			GB	Coarse		1	R
30	0506	2	S	5	C_D	11-Sep-91		AC OL	6.8		3.19					GB	Coarse		1	R
30	0507	2	S	5	C_D	11-Sep-91		AC OL	9.5		3.19					GB	Coarse		1	R
30	0508	2	S	5	C_D	11-Sep-91		AC OL	9.3		3.19					GB	Coarse		1	R
30	0509	2	S	5	C_D	11-Sep-91		AC OL	7.2		5.62					GB	Coarse		1	R
30	7066	2	G	6B	C_D	13-Sep-91	D	AC OL	7.1	5.61	5.61	5.55	6			GB	Fine		1	R
30	7076	2	G	6B	C_D	07-Jun-91	D	AC OL	7.6	0.93	0.93		7			TB	Fine		1	R
30	7088	2	G	6B	C_D	04-Sep-91	D	AC OL	6.6	6.68	6.68	4.75	6			GB	Coarse		1	R
31	0113	1	S	1	C_D	21-Jul-95		AC New	5.1		5.8					GB	Fine		2	F
31	0114	1	S	1	C_D	21-Jul-95		AC New	6.7		5.8					GB	Fine		2	F
31	0115	1	S	1	C_D	21-Jul-95		AC New	4.4		5.8					TB	Fine		2	R
31	0116	1	S	1	C_D	21-Jul-95		AC New	4.4		5.8					TB	Fine		2	R
31	0117	1	S	1	C_D	21-Jul-95		AC New	7.9		5.8					TB/GB	Fine		2	R
31	0118	1	S	1	C_D	21-Jul-95		AC New	4.3		5.8					TB/GB	Fine		2	R
31	0119	1	S	1	C_D	21-Jul-95		AC New	7.9		5.8					TB/GB	Fine		2	R
31	0120	1	S	1	C_D	21-Jul-95	B	AC New	4.7	5.8	5.8		5	2291	469.4	TB	Fine	14.5	2	R
31	0121	1	S	1	C_D	24-Jul-95	B	AC New	5.3	6.22	5.8	5.3	4		379.6	TB	Fine	15.1	2	R
31	0122	1	S	1	C_D	21-Jul-95		AC New	3.8		5.8					TB	Fine		2	R
31	0123	1	S	1	C_D	21-Jul-95		AC New	7.5		5.8					TB	Fine		2	R
31	0124	1	S	1	C_D	21-Jul-95		AC New	7.5		5.8					TB	Fine		2	R
34	0502	2	S	5	C_W	13-Aug-92		AC OL	10.8		3.86					GB	Coarse			R
34	0503	2	S	5	C_W	13-Aug-92	A	AC OL	13.7	3.8	3.8	4.3	8			GB	Coarse			R
34	0504	2	S	5	C_W	21-Aug-92	A	AC OL	13.2	2.34	3.86	4.77	7			GB	Coarse			R
34	0505	2	S	5	C_W	13-Aug-92		AC OL	10.8		3.86					GB	Coarse			R
34	0506	2	S	5	C_W	13-Aug-92		AC OL	11.7		3.86					GB	Coarse			R
34	0507	2	S	5	C_W	13-Aug-92	A	AC OL	14.2	3.75	3.75	4.9	8			GB	Coarse			R
34	0508	2	S	5	C_W	13-Aug-92	A	AC OL	14.9	3.86	3.86	4.28	8			GB	Coarse			R

Table A-1. Section Fundamental Data

SC	SHRP_ID	CN	Exp	Type	Climate	Const_Date	Test Age	Family	T_HMA	AV	AVA	AC	A_Lyr	HMA Density	HMA MR	Base_Type	Subg_Type	Subg MR	F_Cls	For
34	0509	2	S	5	C_W	13-Aug-92		AC OL	11.8		3.86					GB	Coarse			R
34	0559	2	S	5	C_W	21-Aug-92	A	AC OL	11	3.42	3.42	4.53	7			GB	Coarse			R
35	0101	1	S	1	H_D	13-Nov-95	B	AC New	7.2	6.82	6.82	4.8	3			GB	Fine		1	F
35	0102	1	S	1	H_D	13-Nov-95	B	AC New	4.8	6.39	6.39		3			GB	Fine		1	F
35	0103	1	S	1	H_D	13-Nov-95		AC New	5.3		7.23					TB	Fine		1	R
35	0104	1	S	1	H_D	13-Nov-95		AC New	8.1		7.23					TB	Fine		1	R
35	0105	1	S	1	H_D	13-Nov-95	B	AC New	5.9	7.23	7.23	4.8	4			TB/GB	Fine		1	R
35	0106	1	S	1	H_D	13-Nov-95		AC New	7.6		7.23					TB/GB	Fine		1	R
35	0107	1	S	1	H_D	13-Nov-95		AC New	5.9		7.23					TB/GB	Fine		1	R
35	0108	1	S	1	H_D	13-Nov-95		AC New	7.8		7.23					TB/GB	Fine		1	R
35	0109	1	S	1	H_D	13-Nov-95	B	AC New	8	7.5	7.5		4			TB/GB	Fine		1	R
35	0110	1	S	1	H_D	13-Nov-95		AC New	8		7.5					TB	Fine		1	R
35	0111	1	S	1	H_D	13-Nov-95	B	AC New	5	7.51	7.5	4.2	4			TB	Coarse		1	R
35	0112	1	S	1	H_D	13-Nov-95	B	AC New	5.1	6.23	7.5	4.1	4			TB	Fine		1	R
37	1992	1	G	1	C_W	01-Feb-90	D	AC New	2.4	5.27	5.27	6	4		3813.5	GB	Coarse	29.3	2	F
39	0101	1	S	1	C_W	26-Oct-95	B	AC New	6.9	10.85	10.85	6.7	4			GB	Fine		2	F
39	0102	1	S	1	C_W	26-Oct-95		AC New	3.9		10.85					GB	Fine		2	F
39	0103	1	S	1	C_W	26-Oct-95	B	AC New	3.9	11.17	11.17	6.4	4			TB	Fine		2	R
39	0104	1	S	1	C_W	09-Oct-95		AC New	7		11.17					TB	Fine		2	R
39	0105	1	S	1	C_W	26-Oct-95	B	AC New	4	11.8	11.8	5.3	4			TB	Fine		2	R
39	0106	1	S	1	C_W	26-Oct-95		AC New	6.8		10.85					TB/GB	Fine		2	R
39	0107	1	S	1	C_W	26-Oct-95		AC New	3.8		10.85					TB/GB	Fine		2	R
39	0108	1	S	1	C_W	26-Oct-95		AC New	6.6		11.8					TB/GB	Fine		2	R
39	0109	1	S	1	C_W	26-Oct-95		AC New	7		11.8					TB/GB	Fine		2	R
39	0110	1	S	1	C_W	26-Oct-95		AC New	7.3		11.8					TB	Fine		2	R
39	0111	1	S	1	C_W	09-Oct-95	B	AC New	4	9.76	9.76	6.4	4			TB	Fine		2	R
39	0112	1	S	1	C_W	09-Oct-95		AC New	4		9.76					TB	Fine		2	R
39	0160	1	S	1	C_W	26-Nov-95		AC New	4.1		9.76					TB	Fine		2	R
39	5010	2	G	7B	C_W	01-Jun-90	C	AC/PCC	2.8	3.16	3.16	4.95	4			TB	Coarse		1	R
40	4086	2	G	6B	H_D	04-Aug-89	D	AC OL	5.5	1.56	1.56	5.2	4			TB	Fine		6	R
40	4161	2	G	2	H_D	14-Jul-89	D	AC New	2.8	1.36	1.36	6.15	3			TB	Coarse		2	R

SC	SHRP_ID	CN	Exp	Type	Climate	Const_Date	Test Age	Family	T_HMA	AV	AVA	AC	A_Lyr	HMA Density	HMA MR	Base_Type	Subg_Type	Subg MR	F_Cls	For
42	1617	2	G	7B	C_W	15-Aug-90	D	AC/PCC	4.7	6.8	6.8	5.9	5			GB	Coarse		11	R
42	1618	1	G	1	C_W	01-Aug-89	D	AC New	2	5.72	5.72	4.65	3		10693.6	GB	Fine	37.9	7	F
42	1618	2	G	6B	C_W	28-Aug-89	D	AC OL	7.9	4.08	4.08	6	5			GB	Fine	37.9	7	R
42	1691	2	G	7B	C_W	15-Sep-90	D	AC/PCC	4	2.09	2.09	6.25	6			GB	Coarse		14	R
48	1119	2	G	6B	H_W	03-Aug-89	C	AC OL	6.9	8.46	8.46	3.8	8			GB	Fine		2	R
48	3835	1	G	1	H_W	01-Oct-91	D	AC New	8.7	4.8	4.8	4.9	4	2287	1268.6	GB	Coarse	24.4	2	F
48	A502	2	S	5	H_W	26-Sep-91		AC OL	11.4		4.49					TB	Fine		2	R
48	A503	2	S	5	H_W	26-Sep-91		AC OL	14.7		4.49					TB	Fine		2	R
48	A504	2	S	5	H_W	26-Sep-91		AC OL	14		4.49					TB	Fine		2	R
48	A505	2	S	5	H_W	26-Sep-91		AC OL	11.4		4.49					TB	Fine		2	R
48	A506	2	S	5	H_W	26-Sep-91		AC OL	11.6		4.49					TB	Fine		2	R
48	A507	2	S	5	H_W	26-Sep-91		AC OL	14.8		4.49					TB	Fine		2	R
48	A508	2	S	5	H_W	26-Sep-91		AC OL	15.6		4.49					TB	Fine		2	R
48	A509	2	S	5	H_W	26-Sep-91	C	AC OL	12.1	4.49	4.49	4.1	6			TB	Fine		2	R
51	1419	2	G	6B	C_W	20-Sep-89	C	AC OL	9.5	4.88	4.88	6.05	4			TB	Fine		2	R
51	1419	3	G	6D	C_W	30-Aug-97	C	AC OL	11.1	4.23	4.23	6.1	5			TB	Fine		2	R
53	1008	2	G	6B	C_D	26-Jul-94	C	AC OL	5.6	8.33	8.33	5	5		909.5	GB	Coarse	30.5	2	R
81	1805	2	G	6B	C_D	18-Jul-95	B	AC OL	16.3	9.1	9.1	5.15	7	2308	309.0	GB	Fine	42.2	2	R
83	6450	2	G	6B	C_D	13-Sep-89	C	AC OL	10.3	4.24	4.24	4.8	7			GB	Coarse		1	R
83	6451	2	G	6B	C_D	13-Sep-89	C	AC OL	6.7	5.33	5.33	5.2	7			GB	Coarse		1	R
89	1125	2	G	6B	C_W	28-Jun-96	D	AC OL	7.1	7.25	7.25	4.55	6			GB	Coarse		1	R
90	6410	2	G	6B	C_D	28-May-90	D	AC OL	13.6	3.03	3.03	4.55	6			GB	Fine		2	R
90	6412	2	G	6B	C_D	28-May-90	D	AC OL	16.8	2.96	2.96	4.75	6			GB	Coarse		2	R

Table A-1. Section Fundamental Data

Table A-2. Traffic Data

					Estimated Traffic (KESAL)										Monitored Traffic (ESAL)									
SC	SHRP_ID	CN	Exp	Type	1989	1990	1991	1992	1993	1994	1995	1996	1997	1998	1990	1991	1992	1993	1994	1995	1996	1997	1998	1999
2	1004	2	G	6B			100	112	108	111	70		74								54962	53460		
4	0113	1	S	1					230	300	300								225726	234566		418143	281183	
4	0114	1	S	1															211991	219696	236280	222528	260585	
4	0115	1	S	1															212677	220415	237062	223376	261566	
4	0116	1	S	1															216340	224732	241751	228176	267451	
4	0117	1	S	1															211075	218736	235238	221399	259277	
4	0118	1	S	1															220232	228810	246440	232977	273336	
4	0119	1	S	1															210159	217777	233936	219987	257642	
4	0120	1	S	1															215653	223773	240969	227329	266470	
4	0121	1	S	1															210159	217777	233936	219987	257969	
4	0122	1	S	1															210388	217777	234196	220269	257969	
4	0123	1	S	1															204665	211301	226641	212644	249141	
4	0124	1	S	1															202375	208663	223515	209256	245218	
4	0161	1	S	1																				
4	0162	1	S	1															222750	231448	249566	236083	276933	
5	3058	1	G	2		87	91	112				564		774		0	77937	146373	128764	210481	204240			
6	8534	2	G	6B					504			504				102937	100097	0	101757	84676		130568	237592	
6	8535	2	G	6B			982										126914	138847	131254	187006	218926	233605	193725	
8	6002	2	G	6C																	93149	155801		
9	4020	2	G	7B		78	167	168				191	196			0	0	148854	189235	184581			
12	0101	1	S	1																	31524	507112	426736	
12	0102	1	S	1																	33835	526072	448419	
17	5151	2	G	7B		1182	1140										1236546	1313989	1516463	1411572	1342208	789715	1990858	
24	1634	2	G	6C										41										
26	0603	2	S	6												619513	194658	379469	297051	373417	485800	247330	198373	
26	0604	2	S	6												622212	194912	379922	297793	374867	487829	247771	198661	
26	0606	2	S	6												623930	195040	380148	298388	375995	489351	248211	198805	
26	0607	2	S	6												618367	194530	379243	296754	372772	484954	247037	198229	
26	0608	2	S	6												626302	195295	380600	299130	377285	491211	248651	199094	
29	5403	2	G	6B	115				239						0	0	171576	163366	0	0	327932	0		
29	5413	2	G	6B	137										148622	0	169846	90900	0	0	319591	0		0
30	0502	2	S	5				178	183	192	197	209					0	0	0	0	0			
30	0503	2	S	5													0	0	0	0	0			
30	0504	2	S	5													0	0	0	0	0			
30	0505	2	S	5													0	0	0	0	0			
30	0506	2	S	5													0	0	0	0	0			

Table A-2. Traffic Data

SC	SHRP_ID	CN	Exp	Type	Estimated Traffic (KESAL)										Monitored Traffic (ESAL)									
					1989	1990	1991	1992	1993	1994	1995	1996	1997	1998	1990	1991	1992	1993	1994	1995	1996	1997	1998	1999
30	0507	2	S	5													0	0	0	0		0		
30	0508	2	S	5													0	0	0	0		0		
30	0509	2	S	5													0	0	0	0		0		
30	7066	2	G	6B				178	182	192	196	208					0	0	0	0		0		0
30	7076	2	G	6B				81	80	71	85	95					0	0	0	0		0	0	
30	7088	2	G	6B				204	178	169	206	205					0	0	0	0		0	0	
31	0113	1	S	1																	147405	77347		
31	0114	1	S	1																	144911	75490		
31	0115	1	S	1																	146505	76625		
31	0116	1	S	1																	145881	76109		
31	0117	1	S	1																	145396	75851		
31	0118	1	S	1																	146435	76624		
31	0119	1	S	1																	145951	76264		
31	0120	1	S	1																	145882	76161		
31	0121	1	S	1																	144912	75439		
31	0122	1	S	1																	147821	77656		
31	0123	1	S	1																	145188	75593		
31	0124	1	S	1																	144011	74768		
34	0502	2	S	5														389194	324447	316348	295173	407502	267922	589484
34	0503	2	S	5														387078	322945	314674	294213	405690	267411	584657
34	0504	2	S	5														385809	321818	313837	293253	404332	266964	581439
34	0505	2	S	5														375656	315058	307142	287494	394371	264923	556229
34	0506	2	S	5														364234	307924	299191	281734	383051	263902	524046
34	0507	2	S	5														398500	330830	322624	300933	417010	270027	613085
34	0508	2	S	5														390886	325573	317603	296133	409313	267985	593775
34	0509	2	S	5														382425	319941	311745	291333	401163	265943	572857
34	0559	2	S	5														384963	321443	313419	292773	403426	266454	579293
35	0101	1	S	1																			147378	
35	0102	1	S	1																			150728	
35	0103	1	S	1																			145982	
35	0104	1	S	1																			145843	
35	0105	1	S	1																			148774	
35	0106	1	S	1																			145285	
35	0107	1	S	1																			148774	
35	0108	1	S	1																			145145	
35	0109	1	S	1																			145145	
35	0110	1	S	1																			145145	
35	0111	1	S	1																			145145	

Table A-2. Traffic Data

SC	SHRP_ID	CN	Exp	Type	Estimated Traffic (KESAL)										Monitored Traffic (ESAL)									
					1989	1990	1991	1992	1993	1994	1995	1996	1997	1998	1990	1991	1992	1993	1994	1995	1996	1997	1998	1999
35	0112	1	S	1																			145703	
37	1992	1	G	1		94	92	124	138	154	172	192		140								0	162497	
39	0101	1	S	1																			71403	
39	0102	1	S	1																			74079	
39	0103	1	S	1																			74231	
39	0104	1	S	1																			68574	
39	0105	1	S	1																			73696	
39	0106	1	S	1																			69186	
39	0107	1	S	1																			73773	
39	0108	1	S	1																			68880	
39	0109	1	S	1																			68192	
39	0110	1	S	1																			69109	
39	0111	1	S	1																			69109	
39	0112	1	S	1																			67810	
39	0160	1	S	1																			70485	
39	5010	2	G	7B		173	227	317											125454	119342	121025	72756		
40	4086	2	G	6B	195	248	248	248										79071		38495	35544			
40	4161	2	G	2	107	93	93	93										41904		61780				
42	1617	2	G	7B		0	0	837	1171	2133	2240	1160	1160											
42	1618	1	G	1	16	18		18						23	31686	12401		27445	10599	20518	25995			
42	1618	2	G	6B	16	18		18						23	31686	12401		27445	10599	20518	25995			
42	1691	2	G	7B		75		77	87					143		69706		0	99473	135051	85912			0
48	1119	2	G	6B	90	31	37	40	39	130	141	141			0	0	0	0	0	0	0	0	0	0
48	3835	1	G	1						248	221	300					0	36704	0	0	133183	0	205543	
48	A502	2	S	5												0	0	0	0	0	93823	0	135390	
48	A503	2	S	5												0	0	0	0	0	90737	0	133620	
48	A504	2	S	5												0	0	0	0	0	90943	0	133841	
48	A505	2	S	5												0	0	0	0	0	93412	0	135169	
48	A506	2	S	5												0	0	0	0	0	93412	0	135169	
48	A507	2	S	5												0	0	0	0	0	90531	0	133620	
48	A508	2	S	5												0	0	0	0	0	90326	0	133620	
48	A509	2	S	5												0	0	0	0	0	92795	0	134726	
51	1419	2	G	6B	85	85	82									66664	73267	75917	72170		56117	64652	87869.5	
51	1419	3	G	6D																		64652	87869.5	
53	1008	2	G	6B						85									123148		52949	95312	63322	
81	1805	2	G	6B						161	180	200	230											
83	6450	2	G	6B	160	205	193								0	0	0	186620						
83	6451	2	G	6B	160	205	193								0	0	0							

Table A-2. Traffic Data

SC	SHRP_ID	CN	Exp	Type	Estimated Traffic (KESAL)											Monitored Traffic (ESAL)									
					1989	1990	1991	1992	1993	1994	1995	1996	1997	1998		1990	1991	1992	1993	1994	1995	1996	1997	1998	1999
89	1125	2	G	6B								357	574										277096	279076	
90	6410	2	G	6B		315											0		167499	183082	178947	271327	294618	274319	
90	6412	2	G	6B		315											0		165255	166330	174715	268295	290886	270880	

Table A-3. Performance Data

					Fatigue Data											Rut Data											
SC	SHRP_ID	CN	Exp	Type	1989	1991	1992	1993	1994	1995	1996	1997	1998	1999	2000	1989	1990	1991	1992	1993	1994	1995	1996	1997	1998	1999	2000
2	1004	2	G	6B		0		0		0.93		0		0.65				3		6		8		10		12	
4	0113	1	S	1						0	0		4.983	12.48	15.3							4	3.25		3	3	3
4	0114	1	S	1						0	0.68		7.704	24.4	25.7							7	7		8	8	10
4	0115	1	S	1						0			0	2.175	5.6							4			2	3	4
4	0116	1	S	1						0			0	1.715	4.5							6			6	5	6
4	0117	1	S	1						0			0	0.225	1.46							6			5	5	7
4	0118	1	S	1						0			0	6.665	13.5							7			6	6	8
4	0119	1	S	1						0			7.5	12.39	12.8							11.5			11	12	14
4	0120	1	S	1						0			3.045	8.98	13.6							6			5	5	8
4	0121	1	S	1						0			9.39	17.97	37.8							6			5	5	7
4	0122	1	S	1						0			0	5.46	6.35							6			5	6	8
4	0123	1	S	1						0			1.395	3.825	10.3							6			5	5	7
4	0124	1	S	1						0			0	1.065	8.31							6			5	5	6
4	0161	1	S	1						0			0.3	33.5	10.5							6			6	5	6
4	0162	1	S	1						0			0	0	0							6			4	4	4
5	3058	1	G	2		0			18.1	84		2.445						4		4							3	
6	8534	2	G	6B			0					0		0				1		3			1		1	
6	8535	2	G	6B								0		0	0			2		4						2	3
8	6002	2	G	6C								0	113.5										9		6		
9	4020	2	G	7B								0						3	4			4		3			
12	0101	1	S	1					0																		4
12	0102	1	S	1					0						0												2.5
17	5151	2	G	7B									0						6		4			5		7	
24	1634	2	G	6C									0													3.5	
26	0603	2	S	6			0	0		0.24	0.24		0						5	6		6.5	5		8	
26	0604	2	S	6			0	0		1.04			0						5	5.5		7	5		8	
26	0606	2	S	6			0	0		0			1.44							6.5		7	5		9	
26	0607	2	S	6			0	0		0			0						4	6		6	4		7	
26	0608	2	S	6			0	0		0.45			0.3						6	8		9	6		10	
29	5403	2	G	6B			0		0					4.705				4		3	2	4				3
29	5413	2	G	6B			0		0					3				4	5			6				5
30	0502	2	S	5									274.5	276.4	304								9		11	11	
30	0503	2	S	5							180		172	266.7	278								5.5		7	7	
30	0504	2	S	5							0		0	0	0								6		8	8	
30	0505	2	S	5						0.32			10.24	1.845	0.18								4.5		6		
30	0506	2	S	5						0			0	0.7	0.6								8.5		9	11	
30	0507	2	S	5						0			0	0	0								8		8	9	

Table A-3. Performance Data

SC	SHRP_ID	CN	Exp	Type	Fatigue Data											Rut Data											
					1989	1991	1992	1993	1994	1995	1996	1997	1998	1999	2000	1989	1990	1991	1992	1993	1994	1995	1996	1997	1998	1999	2000
30	0508	2	S	5							82.9		151.9	151.9	254								4		4	5	
30	0509	2	S	5							0		580	351	305								9		11	11	
30	7066	2	G	6B							0		0	0	0								7		8	10	
30	7076	2	G	6B		0							0							6.5			12		13		
30	7088	2	G	6B		0					0		0		0.6					1			7		8		
31	0113	1	S	1						0				28.92									8			27	
31	0114	1	S	1						0	0	0		0								1	5.75			20	
31	0115	1	S	1						0				0								1	5.5			21	
31	0116	1	S	1						0				0									6			15	
31	0117	1	S	1						0				0								1	4.5			17	
31	0118	1	S	1						0				0									7			15	
31	0119	1	S	1						0				0								1	4			13	
31	0120	1	S	1						0				0									7			11	
31	0121	1	S	1						0				0								1	3.5			11	
31	0122	1	S	1						0				0									5			14	
31	0123	1	S	1						0				0								1	6			22	
31	0124	1	S	1						0				0								1	5.5			19	
34	0502	2	S	5							0		7	12.73						3		5	1		4	4.5	
34	0503	2	S	5						0	0.12		1	2.055							4	3.5	3		3	3.5	
34	0504	2	S	5							0		0	0							5	4	1		3	3.5	
34	0505	2	S	5							0.23		1.6	2.7							3	4	1		2	3	
34	0506	2	S	5							0		0	0							3	4	3		3	3.5	
34	0507	2	S	5						0	0		0	0							5	4.5	4		4	4	
34	0508	2	S	5						0	0		0	0.75							4	4	3		3	3.5	
34	0509	2	S	5							0.11		4.7	8.69							5	4	3		3	3.5	
34	0559	2	S	5							0		1.9	19.2							4	3	1		2	3.5	
35	0101	1	S	1									0	0	0.78									5		6.5	5
35	0102	1	S	1									0	0	0.9									5		5.5	6
35	0103	1	S	1									0	0	0									5		6.5	6
35	0104	1	S	1									0	0	0									6		7.5	7
35	0105	1	S	1									0	0	0.45									6		6	6
35	0106	1	S	1									0	0	0								4			5	5
35	0107	1	S	1									0	0	0									5		5.5	7
35	0108	1	S	1									0	0	0									5		5.5	7
35	0109	1	S	1									0	0	0									6		5	7
35	0110	1	S	1									0	0	0									5		6	6
35	0111	1	S	1									0	0	0									5		4.5	6

Table A-3. Performance Data

SC	SHRP_ID	CN	Exp	Type	Fatigue Data											Rut Data											
					1989	1991	1992	1993	1994	1995	1996	1997	1998	1999	2000	1989	1990	1991	1992	1993	1994	1995	1996	1997	1998	1999	2000
35	0112	1	S	1								0		0	0											6.5	6
37	1992	1	G	1					0									5		1			3		6		8
39	0101	1	S	1							0												10				
39	0102	1	S	1							0												12.7				
39	0103	1	S	1							0	0		4.47									2	3		7	
39	0104	1	S	1							0			0									2.5			2	
39	0105	1	S	1							0	0	0									3.5	7	7		
39	0106	1	S	1							0	0		1.425								2	1		2	
39	0107	1	S	1							0											6				
39	0108	1	S	1							0	0		0.24								3	4		9	
39	0109	1	S	1							0	0		0.3								2	2		9	
39	0110	1	S	1							0	0		0.33								2	2		3	
39	0111	1	S	1							0			0.54								2			2	
39	0112	1	S	1							0											3			2	
39	0160	1	S	1							0	0		0								2	1		2	
39	5010	2	G	7B					0								3			6		4					
40	4086	2	G	6B		1.01	0.75		1.05			1.11		1.185			3			3		4		2		3	
40	4161	2	G	2		0	0		5.73			50.00					6	9		9		14		14.5			
42	1617	2	G	7B								1.8								4		6		6			
42	1618	1	G	1	5.91											4											
42	1618	2	G	6B								6.91					4	4	5					4		5	
42	1691	2	G	7B								0					3	6.5					8		7		
48	1119	2	G	6B		0		0		0.51		11.09		19.57			5	4	9	10			11				9
48	3835	1	G	1		0	4.22		10.2			11.68		20.77					4	3		5					4
48	A502	2	S	5				0		0		0		0.24					3	4		6			7	8	7
48	A503	2	S	5				0		0		0		0.35					2	3		6			4	5	5
48	A504	2	S	5				0		0		0			0				2	5		6			7	7	7
48	A505	2	S	5				0		0		0			0				2	4		6			6	6	6
48	A506	2	S	5				0		0		0			0				2	5		6			7	6	8
48	A507	2	S	5				0		0		0		0.05					2	6		8			8	8	9
48	A508	2	S	5				0		0		0		0.47					2	4		5			7	5	5
48	A509	2	S	5				0		0			0.33	2.72					2	3		5			4	5	6
51	1419	2	G	6B								12.08				4		4	4				5		2.5		
51	1419	3	G	6D								0													2.5	3	
53	1008	2	G	6B					0			0		7.375							1	4		4		6	
81	1805	2	G	6B				0	0	0			0										2	2	2		
83	6450	2	G	6B				0				14.1					3			3.5						3	

Table A-3. Performance Data

SC	SHRP_ID	CN	Exp	Type	Fatigue Data											Rut Data											
					1989	1991	1992	1993	1994	1995	1996	1997	1998	1999	2000	1989	1990	1991	1992	1993	1994	1995	1996	1997	1998	1999	2000
83	6451	2	G	6B				0					82.74				3			3					3		
89	1125	2	G	6B							0			7.455									11.5			7	
90	6410	2	G	6B					0					0			7			3						2	
90	6412	2	G	6B					0					0			5			4						5	

Table A-4. Laboratory Air Voids Test Data

SC	SHRP_ID	CN	Experiment Type		LAYER_NO	LOC_NO	Maximum Specific Gravity	Bulk Specific Gravity	Computed Air Voids (%)
2	1004	2	G	6B	5	A1	2.495	2.352	5.73
2	1004	2	G	6B	5	A2	2.484	2.382	4.11
2	1004	2	G	6B	5	C10	2.495	2.389	4.25
2	1004	2	G	6B	5	C19	2.484	2.450	1.37
2	1004	2	G	6B	5	C21	2.484	2.421	2.54
2	1004	2	G	6B	5	C22	2.484	2.423	2.46
2	1004	2	G	6B	5	C7	2.495	2.357	5.53
2	1004	2	G	6B	5	C9	2.495	2.351	5.77
4	0115	1	S	1	3	C1	2.500	2.254	9.84
4	0115	1	S	1	3	C2	2.500	2.269	9.24
4	0115	1	S	1	3	C4	2.500	2.246	10.16
4	0115	1	S	1	2	C1	2.508	2.365	5.70
4	0115	1	S	1	2	C2	2.508	2.393	4.59
4	0115	1	S	1	2	C3	2.508	2.325	7.30
4	0115	1	S	1	2	C4	2.508	2.354	6.14
4	0116	1	S	1	2	C31	2.513	2.365	5.89
4	0116	1	S	1	2	C32	2.513	2.336	7.04
4	0116	1	S	1	2	C33	2.513	2.378	5.37
4	0116	1	S	1	2	C34	2.513	2.137	14.96
4	0122	1	S	1	5	C41	2.534	2.245	11.40
4	0122	1	S	1	5	C42	2.534	2.255	11.01
4	0122	1	S	1	5	C43	2.534	2.302	9.16
4	0122	1	S	1	4	C41	2.525	2.398	5.03
4	0122	1	S	1	4	C42	2.525	2.354	6.77
4	0122	1	S	1	4	C43	2.525	2.311	8.48
4	0122	1	S	1	4	C44	2.525	2.391	5.31
4	0124	1	S	1	3	C11	2.503	2.332	6.83
4	0124	1	S	1	3	C12	2.503	2.301	8.07
4	0124	1	S	1	3	C13	2.503	2.374	5.15
4	0124	1	S	1	3	C14	2.503	2.280	8.91
4	0161	1	S	1	3	C66	2.525	2.305	8.71
5	3058	1	G	2	4	A2	2.490	2.300	7.63
5	3058	1	G	2	3	A1	2.535	2.395	5.52
5	3058	1	G	2	3	A2	2.532	2.427	4.15
6	8534	2	G	6B	7	A1	2.452	2.290	6.61
6	8534	2	G	6B	7	A2	2.466	2.301	6.69
6	8535	2	G	6B	8	A1	2.462	2.281	7.35
6	8535	2	G	6B	8	A2	2.453	2.258	7.95
8	6002	2	G	6C	5	A1	2.466	2.323	5.80
8	6002	2	G	6C	5	A2	2.466	2.315	6.12
9	4020	2	G	7B	4	A2	2.595	2.414	6.97
12	0101	1	S	1	3	C55	2.370	2.252	4.98
12	0104	1	S	1	4	C37	2.354	2.248	4.50
12	0104	1	S	1	4	C38	2.354	2.242	4.76
12	0104	1	S	1	4	C39	2.354	2.284	2.97
12	0104	1	S	1	3	C37	2.372	2.269	4.34
12	0104	1	S	1	3	C38	2.372	2.273	4.17
12	0104	1	S	1	3	C39	2.372	2.242	5.48
12	0110	1	S	1	5	C17	2.378	2.191	7.86

Table A-4. Laboratory Air Voids Test Data

SC	SHRP_ID	CN	Experiment Type	LAYER_NO	LOC_NO	Maximum Specific Gravity	Bulk Specific Gravity	Computed Air Voids (%)
12	0110	1	S	1	5	C18	2.378	2.178	8.41
12	0110	1	S	1	5	C19	2.378	2.179	8.37
12	0110	1	S	1	5	C20	2.378	2.214	6.90
12	0111	1	S	1	4	C21	2.360	2.245	4.87
12	0111	1	S	1	4	C22	2.360	2.240	5.08
12	0111	1	S	1	4	C24	2.360	2.260	4.24
12	0505	2	S	5	6	C93	2.346	2.056	12.36
12	0505	2	S	5	6	C94	2.346	2.131	9.16
12	0505	2	S	5	6	C95	2.346	2.074	11.59
12	0505	2	S	5	6	C96	2.346	2.142	8.70
12	0509	2	S	5	6	C65	2.322	2.116	8.87
12	0509	2	S	5	6	C66	2.322	2.159	7.02
12	0509	2	S	5	6	C67	2.322	2.124	8.53
12	0509	2	S	5	6	C68	2.322	2.144	7.67
12	0509	2	S	5	5	C65	2.326	2.187	5.98
12	0509	2	S	5	5	C66	2.326	2.206	5.16
12	0509	2	S	5	5	C67	2.326	2.210	4.99
12	0509	2	S	5	5	C68	2.326	2.246	3.44
12	0561	2	S	5	5	C45	2.371	2.207	6.92
12	0561	2	S	5	5	C46	2.371	2.232	5.86
12	0561	2	S	5	5	C47	2.371	2.188	7.72
12	0561	2	S	5	5	C48	2.371	2.234	5.78
12	0562	2	S	5	5	C89	2.374	2.163	8.89
12	0562	2	S	5	5	C90	2.374	2.174	8.42
12	0562	2	S	5	5	C91	2.374	2.150	9.44
12	0562	2	S	5	5	C92	2.374	2.171	8.55
12	0565	2	S	5	7	C61	2.329	2.081	10.65
12	0565	2	S	5	7	C62	2.329	2.138	8.20
12	0565	2	S	5	7	C63	2.329	2.147	7.81
12	0565	2	S	5	7	C64	2.329	2.188	6.05
12	0565	2	S	5	5	C61	2.338	2.259	3.38
12	0565	2	S	5	5	C62	2.338	2.253	3.64
12	0565	2	S	5	5	C63	2.338	2.236	4.36
12	0565	2	S	5	5	C64	2.338	2.266	3.08
12	0566	2	S	5	5	C73	2.350	2.255	4.04
12	0566	2	S	5	5	C74	2.350	2.238	4.77
12	0566	2	S	5	5	C75	2.350	2.204	6.21
12	0566	2	S	5	5	C76	2.350	2.252	4.17
17	5151	2	G	7B	5	A1	2.539	2.430	4.29
17	5151	2	G	7B	5	A2	2.546	2.437	4.28
17	5151	2	G	7B	4	A1	2.589	2.470	4.60
17	5151	2	G	7B	4	A2	2.588	2.467	4.68
24	1634	2	G	6C	6	A1	2.563	2.356	8.08
24	1634	2	G	6C	6	A2	2.560	2.372	7.34
24	1634	2	G	6C	5	A1	2.585	2.448	5.30
24	1634	2	G	6C	5	A2	2.614	2.454	6.12
26	0603	2	S	6	5	C13	2.460	2.439	0.85
26	0603	2	S	6	5	C13	2.453	2.415	1.55
26	0603	2	S	6	5	C13	2.453	2.412	1.67

Table A-4. Laboratory Air Voids Test Data

SC	SHRP_ID	CN	Experiment Type		LAYER_NO	LOC_NO	Maximum Specific Gravity	Bulk Specific Gravity	Computed Air Voids (%)
26	0603	2	S	6	5	C14	2.460	2.433	1.10
26	0603	2	S	6	5	C14	2.453	2.417	1.47
26	0603	2	S	6	5	C14	2.453	2.387	2.69
26	0603	2	S	6	5	C15	2.453	2.426	1.10
26	0603	2	S	6	5	C15	2.453	2.406	1.92
26	0603	2	S	6	5	C15	2.460	2.396	2.60
26	0603	2	S	6	5	C16	2.453	2.419	1.39
26	0603	2	S	6	5	C16	2.460	2.419	1.67
26	0603	2	S	6	5	C16	2.453	2.368	3.47
29	5403	2	G	6B	5	A1	2.529	2.295	9.25
29	5403	2	G	6B	5	A2	2.521	2.306	8.53
29	5403	2	G	6B	4	A1	2.546	2.515	1.22
29	5403	2	G	6B	4	A2	2.547	2.508	1.53
29	5413	2	G	6B	6	A1	2.506	2.328	7.10
29	5413	2	G	6B	6	A2	2.498	2.327	6.85
29	5413	2	G	6B	3	A1	2.534	2.466	2.68
29	5413	2	G	6B	3	A2	2.527	2.493	1.35
30	0502	2	S	5	6	C65	2.517	2.381	5.40
30	0502	2	S	5	6	C66	2.517	2.356	6.40
30	0502	2	S	5	6	C67	2.517	2.388	5.13
30	0502	2	S	5	6	C68	2.517	2.377	5.56
30	0505	2	S	5	6	C27	2.513	2.426	3.46
30	0505	2	S	5	6	C28	2.513	2.422	3.62
30	0505	2	S	5	6	C29	2.513	2.447	2.63
30	0505	2	S	5	6	C30	2.513	2.436	3.06
30	7066	2	G	6B	6	A1	2.506	2.391	4.59
30	7066	2	G	6B	6	A2	2.504	2.361	5.71
30	7066	2	G	6B	6	C10	2.506	2.391	4.59
30	7066	2	G	6B	6	C19	2.504	2.343	6.43
30	7066	2	G	6B	6	C21	2.504	2.357	5.87
30	7066	2	G	6B	6	C22	2.504	2.388	4.63
30	7066	2	G	6B	6	C7	2.506	2.343	6.50
30	7066	2	G	6B	6	C9	2.506	2.342	6.54
30	7076	2	G	6B	7	A1	2.426	2.418	0.33
30	7076	2	G	6B	7	A2	2.431	2.394	1.52
30	7088	2	G	6B	6	A1	2.525	2.367	6.26
30	7088	2	G	6B	6	A2	2.512	2.358	6.13
30	7088	2	G	6B	6	C10	2.525	2.361	6.50
30	7088	2	G	6B	6	C12	2.525	2.361	6.50
30	7088	2	G	6B	6	C19	2.512	2.351	6.41
30	7088	2	G	6B	6	C21	2.512	2.335	7.05
30	7088	2	G	6B	6	C22	2.512	2.320	7.64
30	7088	2	G	6B	6	C9	2.525	2.349	6.97
31	0120	1	S	1	5	C39	2.432	2.286	6.00
31	0120	1	S	1	5	C40	2.432	2.296	5.59
31	0121	1	S	1	4	B53	2.438	2.354	3.45
31	0121	1	S	1	4	C31	2.426	2.241	7.63
31	0121	1	S	1	4	C32	2.426	2.272	6.35
31	0121	1	S	1	4	C33	2.438	2.296	5.82

Table A-4. Laboratory Air Voids Test Data

SC	SHRP_ID	CN	Experiment Type	LAYER_NO	LOC_NO	Maximum Specific Gravity	Bulk Specific Gravity	Computed Air Voids (%)
31	0121	1	S	1	4	C34	2.438	2.247	7.83
34	0503	2	S	5	8	C101	2.639	2.549	3.41
34	0503	2	S	5	8	C102	2.639	2.526	4.28
34	0503	2	S	5	8	C103	2.639	2.552	3.30
34	0503	2	S	5	8	C104	2.639	2.535	3.94
34	0503	2	S	5	8	C105	2.639	2.538	3.83
34	0503	2	S	5	8	C106	2.639	2.533	4.02
34	0504	2	S	5	7	C39	2.685	2.612	2.72
34	0504	2	S	5	7	C40	2.685	2.596	3.31
34	0504	2	S	5	7	C42	2.685	2.609	2.83
34	0504	2	S	5	7	C43	2.685	2.605	2.98
34	0504	2	S	5	7	C44	2.685	2.637	1.79
34	0504	2	S	5	7	C45	2.685	2.644	1.53
34	0504	2	S	5	7	C46	2.685	2.631	2.01
34	0504	2	S	5	7	C47	2.685	2.640	1.68
34	0504	2	S	5	7	C48	2.685	2.625	2.23
34	0507	2	S	5	8	C107	2.638	2.539	3.75
34	0507	2	S	5	8	C108	2.638	2.545	3.53
34	0507	2	S	5	8	C109	2.638	2.537	3.83
34	0507	2	S	5	8	C110	2.638	2.537	3.83
34	0507	2	S	5	8	C111	2.638	2.556	3.11
34	0507	2	S	5	8	C112	2.638	2.521	4.44
34	0508	2	S	5	8	C100	2.673	2.569	3.89
34	0508	2	S	5	8	C91	2.673	2.564	4.08
34	0508	2	S	5	8	C92	2.673	2.563	4.12
34	0508	2	S	5	8	C93	2.673	2.568	3.93
34	0508	2	S	5	8	C94	2.673	2.571	3.82
34	0508	2	S	5	8	C95	2.673	2.561	4.19
34	0508	2	S	5	8	C96	2.673	2.587	3.22
34	0508	2	S	5	8	C97	2.673	2.561	4.19
34	0508	2	S	5	8	C98	2.673	2.579	3.52
34	0508	2	S	5	8	C99	2.673	2.575	3.67
34	0559	2	S	5	7	C49	2.645	2.562	3.14
34	0559	2	S	5	7	C50	2.645	2.564	3.06
34	0559	2	S	5	7	C51	2.645	2.566	2.99
34	0559	2	S	5	7	C52	2.645	2.562	3.14
34	0559	2	S	5	7	C53	2.645	2.572	2.76
34	0559	2	S	5	7	C54	2.645	2.540	3.97
34	0559	2	S	5	7	C55	2.645	2.558	3.29
34	0559	2	S	5	7	C56	2.645	2.549	3.63
34	0559	2	S	5	7	C57	2.645	2.544	3.82
34	0559	2	S	5	7	C58	2.645	2.556	3.36
34	0559	2	S	5	7	C59	2.645	2.548	3.67
34	0559	2	S	5	7	C60	2.645	2.546	3.74
34	0559	2	S	5	7	C61	2.645	2.553	3.48
34	0559	2	S	5	7	C62	2.645	2.551	3.55
34	0559	2	S	5	7	C63	2.645	2.546	3.74
34	0802	1	S	8	3	C25	2.628	2.535	3.54
34	0802	1	S	8	3	C26	2.628	2.535	3.54

Table A-4. Laboratory Air Voids Test Data

SC	SHRP_ID	CN	Experiment Type	LAYER_ NO	LOC_NO	Maximum Specific Gravity	Bulk Specific Gravity	Computed Air Voids (%)
34	0802	1	S	8	3	C27	2.628	2.544	3.20
34	0802	1	S	8	3	C28	2.628	2.536	3.50
34	0802	1	S	8	3	C29	2.628	2.566	2.36
34	0802	1	S	8	3	C30	2.628	2.581	1.79
34	0802	1	S	8	3	C31	2.628	2.581	1.79
34	0802	1	S	8	3	C32	2.628	2.575	2.02
34	0860	1	S	8	4	C17	2.660	2.566	3.53
34	0860	1	S	8	4	C18	2.660	2.585	2.82
34	0860	1	S	8	4	C19	2.660	2.591	2.59
34	0860	1	S	8	4	C20	2.660	2.540	4.51
34	0860	1	S	8	4	C21	2.660	2.504	5.86
34	0860	1	S	8	4	C22	2.660	2.554	3.98
34	0860	1	S	8	4	C23	2.660	2.540	4.51
34	0860	1	S	8	4	C24	2.660	2.508	5.71
35	0101	1	S	1	3	C5	2.390	2.237	6.40
35	0101	1	S	1	3	C6	2.390	2.217	7.24
35	0102	1	S	1	3	C7	2.390	2.243	6.15
35	0102	1	S	1	3	C8	2.390	2.236	6.44
35	0102	1	S	1	3	C9	2.390	2.233	6.57
35	0105	1	S	1	4	C23	2.394	2.239	6.47
35	0105	1	S	1	4	C24	2.394	2.203	7.98
35	0109	1	S	1	4	C43	2.402	2.233	7.04
35	0109	1	S	1	4	C44	2.402	2.201	8.37
35	0109	1	S	1	4	C45	2.402	2.236	6.91
35	0109	1	S	1	4	C46	2.402	2.217	7.70
35	0111	1	S	1	4	C51	2.428	2.247	7.45
35	0111	1	S	1	4	C52	2.428	2.255	7.13
35	0111	1	S	1	4	C53	2.428	2.229	8.20
35	0111	1	S	1	4	C54	2.428	2.252	7.25
35	0112	1	S	1	4	C59	2.423	2.280	5.90
35	0112	1	S	1	4	C60	2.423	2.264	6.56
37	1992	1	G	1	4	A1	2.498	2.353	5.80
37	1992	1	G	1	4	A2	2.510	2.391	4.74
39	0101	1	S	1	4	C21	2.444	2.186	10.56
39	0101	1	S	1	4	C22	2.444	2.196	10.15
39	0101	1	S	1	4	C23	2.444	2.165	11.42
39	0101	1	S	1	4	C24	2.444	2.171	11.17
39	0101	1	S	1	4	C25	2.444	2.176	10.97
39	0101	1	S	1	4	C26	2.444	2.179	10.84
39	0103	1	S	1	4	C63	2.460	2.176	11.54
39	0103	1	S	1	4	C64	2.460	2.170	11.79
39	0103	1	S	1	4	C65	2.460	2.205	10.37
39	0103	1	S	1	4	C66	2.460	2.190	10.98
39	0105	1	S	1	4	C47	2.487	2.200	11.54
39	0105	1	S	1	4	C48	2.487	2.187	12.06
39	0111	1	S	1	4	C10	2.458	2.241	8.83
39	0111	1	S	1	4	C7	2.458	2.230	9.28
39	0111	1	S	1	4	C8	2.458	2.203	10.37
39	0111	1	S	1	4	C9	2.458	2.198	10.58

Table A-4. Laboratory Air Voids Test Data

SC	SHRP_ID	CN	Experiment Type		LAYER_NO	LOC_NO	Maximum Specific Gravity	Bulk Specific Gravity	Computed Air Voids (%)
39	5010	2	G	7B	4	A1	2.382	2.353	1.22
39	5010	2	G	7B	4	A2	2.485	2.358	5.11
40	4086	2	G	6B	4	A1	2.442	2.404	1.56
40	4086	2	G	6B	3	A1	2.457	2.447	0.41
40	4161	2	G	2	3	A1	2.420	2.394	1.07
40	4161	2	G	2	3	A2	2.432	2.392	1.64
42	1617	2	G	7B	5	A1	2.513	2.359	6.13
42	1617	2	G	7B	5	A2	2.514	2.326	7.48
42	1617	2	G	7B	4	A1	2.618	2.538	3.06
42	1617	2	G	7B	4	A2	2.620	2.548	2.75
42	1618	1	G	1	3	A1	2.545	2.400	5.70
42	1618	1	G	1	3	A2	2.545	2.399	5.74
42	1618	2	G	6B	5	A1	2.481	2.395	3.47
42	1618	2	G	6B	5	A2	2.510	2.392	4.70
42	1618	2	G	6B	4	A2	2.461	2.212	10.12
42	1691	2	G	7B	6	A1	2.421	2.373	1.98
42	1691	2	G	7B	6	A3	2.406	2.353	2.20
42	1691	2	G	7B	5	A1	2.516	2.417	3.93
42	1691	2	G	7B	5	A3	2.514	2.415	3.94
47	0603	2	S	6	6	C26	2.327	2.170	6.75
47	0603	2	S	6	6	C27	2.327	2.240	3.74
47	0603	2	S	6	6	C28	2.327	2.240	3.74
47	0606	2	S	6	4	C29	2.536	2.363	6.82
47	0606	2	S	6	4	C30	2.536	2.389	5.80
47	0606	2	S	6	4	C31	2.536	2.363	6.82
47	0606	2	S	6	4	C32	2.536	2.373	6.43
47	0608	2	S	6	6	C41	2.312	2.250	2.68
47	0608	2	S	6	6	C42	2.312	2.240	3.11
47	0608	2	S	6	6	C43	2.312	2.240	3.11
47	0608	2	S	6	6	C44	2.312	2.230	3.55
47	0661	2	S	6	6	C49	2.344	2.175	7.21
47	0661	2	S	6	6	C50	2.344	2.226	5.03
47	0661	2	S	6	6	C52	2.344	2.238	4.52
47	0662	2	S	6	6	C46	2.324	2.200	5.34
47	0662	2	S	6	6	C47	2.324	2.195	5.55
48	0114	1	S	1	5	C45	2.434	2.308	5.18
48	0114	1	S	1	5	C46	2.434	2.402	1.31
48	0116	1	S	1	4	C89	2.428	2.324	4.28
48	0116	1	S	1	4	C90	2.428	2.370	2.39
48	0116	1	S	1	4	C91	2.428	2.335	3.83
48	0116	1	S	1	4	C92	2.428	2.333	3.91
48	0117	1	S	1	5	C69	2.467	2.333	5.43
48	0117	1	S	1	5	C70	2.467	2.374	3.77
48	0117	1	S	1	5	C71	2.467	2.360	4.34
48	0117	1	S	1	5	C72	2.467	2.380	3.53
48	0117	1	S	1	4	C69	2.412	2.292	4.98
48	0117	1	S	1	4	C70	2.412	2.288	5.14
48	0117	1	S	1	4	C71	2.412	2.328	3.48
48	0117	1	S	1	4	C72	2.412	2.336	3.15

Table A-4. Laboratory Air Voids Test Data

SC	SHRP_ID	CN		Experiment Type	LAYER_NO	LOC_NO	Maximum Specific Gravity	Bulk Specific Gravity	Computed Air Voids (%)
48	0120	1	S	1	6	C33	2.433	2.333	4.11
48	0120	1	S	1	6	C34	2.433	2.387	1.89
48	0121	1	S	1	6	C39	2.430	2.371	2.43
48	0121	1	S	1	6	C40	2.430	2.378	2.14
48	0123	1	S	1	5	C79	2.423	2.395	1.16
48	0123	1	S	1	5	C80	2.423	2.395	1.16
48	0123	1	S	1	5	C81	2.423	2.321	4.21
48	0123	1	S	1	5	C82	2.423	2.395	1.16
48	1119	2	G	6B	8	A1	2.483	2.273	8.46
48	1119	2	G	6B	3	A1	2.450	2.358	3.76
48	3835	1	G	1	4	C11	2.408	2.276	5.48
48	3835	1	G	1	4	C12	2.408	2.265	5.94
48	3835	1	G	1	4	C23	2.386	2.297	3.73
48	3835	1	G	1	4	C24	2.386	2.289	4.07
48	A509	2	S	5	6	C34	2.537	2.423	4.49
48	A509	2	S	5	6	C35	2.537	2.423	4.49
49	0804	1	S	8	4	C10	2.307	2.159	6.42
49	0804	1	S	8	4	C11	2.307	2.153	6.68
49	0804	1	S	8	4	C12	2.307	2.149	6.85
51	1417	2	G	6B	6	A1	2.667	2.502	6.19
51	1417	2	G	6B	6	A2	2.664	2.433	8.67
51	1419	2	G	6B	4	A1	2.477	2.359	4.76
51	1419	2	G	6B	4	A2	2.500	2.375	5.00
51	1419	2	G	6B	3	A1	2.519	2.423	3.81
51	1419	2	G	6B	3	A2	2.530	2.421	4.31
51	1419	3	G	6D	5	A2	2.461	2.357	4.23
53	1008	2	G	6B	5	A1	2.485	2.283	8.13
53	1008	2	G	6B	5	A2	2.499	2.286	8.52
53	6020	2	G	6D	6	A1	2.506	2.332	6.94
53	6020	2	G	6D	6	A2	2.524	2.320	8.08
53	6020	2	G	6D	6	C10	2.506	2.365	5.63
53	6020	2	G	6D	6	C19	2.524	2.322	8.00
53	6020	2	G	6D	6	C20	2.524	2.326	7.84
53	6020	2	G	6D	6	C21	2.524	2.330	7.69
53	6020	2	G	6D	6	C22	2.524	2.369	6.14
53	6020	2	G	6D	6	C7	2.506	2.300	8.22
53	6020	2	G	6D	6	C8	2.506	2.291	8.58
53	6020	2	G	6D	6	C9	2.506	2.296	8.38
53	7322	2	G	6D	6	A1	2.564	2.436	4.99
53	7322	2	G	6D	6	A2	2.571	2.398	6.73
53	7322	2	G	6D	6	C10B	2.564	2.415	5.81
53	7322	2	G	6D	6	C19	2.571	2.414	6.11
53	7322	2	G	6D	6	C20	2.571	2.420	5.87
53	7322	2	G	6D	6	C21	2.571	2.430	5.48
53	7322	2	G	6D	6	C22	2.571	2.454	4.55
53	7322	2	G	6D	6	C7	2.564	2.395	6.59
53	7322	2	G	6D	6	C8	2.564	2.402	6.32
53	7322	2	G	6D	6	C9	2.564	2.410	6.01
55	0115	1	S	1	5	C47	2.449	2.267	7.43

Table A-4. Laboratory Air Voids Test Data

SC	SHRP_ID	CN	Experiment Type	LAYER_ NO	LOC_NO	Maximum Specific Gravity	Bulk Specific Gravity	Computed Air Voids (%)
55	0115	1	S	1	5 C48	2.449	2.325	5.06
55	0115	1	S	1	5 C49	2.449	2.284	6.74
55	0115	1	S	1	5 C50	2.449	2.303	5.96
55	0116	1	S	1	5 C10	2.463	2.300	6.62
55	0116	1	S	1	5 C7	2.463	2.318	5.89
55	0116	1	S	1	5 C8	2.463	2.367	3.90
55	0116	1	S	1	5 C9	2.463	2.260	8.24
55	0116	1	S	1	3 C10	2.448	2.318	5.31
55	0116	1	S	1	3 C7	2.448	2.310	5.64
55	0116	1	S	1	3 C8	2.448	2.319	5.27
55	0116	1	S	1	3 C9	2.448	2.350	4.00
55	0118	1	S	1	5 C11	2.489	2.277	8.52
55	0118	1	S	1	5 C12	2.489	2.290	8.00
55	0118	1	S	1	5 C13	2.489	2.286	8.16
55	0118	1	S	1	5 C14	2.489	2.284	8.24
55	0118	1	S	1	5 C15	2.489	2.283	8.28
55	0118	1	S	1	5 C16	2.489	2.308	7.27
55	0121	1	S	1	5 C27	2.457	2.279	7.24
55	0121	1	S	1	5 C28	2.457	1.546	37.08
55	0121	1	S	1	5 C29	2.457	2.320	5.58
55	0121	1	S	1	5 C30	2.457	2.277	7.33
55	0805	1	S	8	4 C1	2.440	2.277	6.68
55	0805	1	S	8	4 C2	2.440	2.266	7.13
55	0805	1	S	8	4 C3	2.440	2.276	6.72
55	0805	1	S	8	4 C4	2.440	2.255	7.58
55	0805	1	S	8	4 C5	2.440	2.242	8.11
55	0805	1	S	8	4 C6	2.440	2.236	8.36
55	0805	1	S	8	4 C7	2.440	2.250	7.79
55	0805	1	S	8	4 C8	2.440	2.262	7.30
55	0806	1	S	8	4 C10	2.443	2.239	8.35
55	0806	1	S	8	4 C11	2.443	2.275	6.88
55	0806	1	S	8	4 C12	2.443	2.272	7.00
55	0806	1	S	8	4 C13	2.443	2.230	8.72
55	0806	1	S	8	4 C14	2.443	2.219	9.17
55	0806	1	S	8	4 C15	2.443	2.275	6.88
55	0806	1	S	8	4 C16	2.443	2.269	7.12
55	0806	1	S	8	4 C9	2.443	2.257	7.61
55	0806	1	S	8	3 C10	2.468	2.344	5.02
55	0806	1	S	8	3 C11	2.468	2.355	4.58
55	0806	1	S	8	3 C12	2.468	2.355	4.58
55	0806	1	S	8	3 C13	2.468	2.348	4.86
55	0806	1	S	8	3 C14	2.468	2.308	6.48
55	0806	1	S	8	3 C15	2.468	2.326	5.75
55	0806	1	S	8	3 C16	2.468	2.301	6.77
55	0806	1	S	8	3 C9	2.468	2.336	5.35
81	1805	2	G	6B	7 A1	2.463	2.259	8.28
81	1805	2	G	6B	7 A2	2.478	2.232	9.93
81	1805	2	G	6B	6 A1	2.473	2.306	6.75
81	1805	2	G	6B	6 A2	2.480	2.294	7.50

Table A-4. Laboratory Air Voids Test Data

SC	SHRP_ID	CN	Experiment Type		LAYER_NO	LOC_NO	Maximum Specific Gravity	Bulk Specific Gravity	Computed Air Voids (%)
83	6450	2	G	6B	7	A1	2.451	2.348	4.20
83	6450	2	G	6B	7	A2	2.450	2.345	4.29
83	6450	2	G	6B	5	A1	2.531	2.333	7.82
83	6450	2	G	6B	5	A2	2.536	2.338	7.81
83	6450	2	G	6B	4	A1	2.523	2.302	8.76
83	6450	2	G	6B	4	A2	2.557	2.317	9.39
83	6451	2	G	6B	7	A2	2.456	2.325	5.33
83	6451	2	G	6B	5	C24	2.535	2.336	7.85
83	6451	2	G	6B	4	A2	2.516	2.307	8.31
89	1125	2	G	6B	6	A1	2.449	2.247	8.25
89	1125	2	G	6B	6	A2	2.423	2.276	6.07
89	1125	2	G	6B	6	C10	2.449	2.234	8.78
89	1125	2	G	6B	6	C19	2.423	2.293	5.37
89	1125	2	G	6B	6	C20	2.423	2.293	5.37
89	1125	2	G	6B	6	C21	2.423	2.290	5.49
89	1125	2	G	6B	6	C22	2.423	2.294	5.32
89	1125	2	G	6B	6	C7	2.449	2.215	9.55
89	1125	2	G	6B	6	C8	2.449	2.231	8.90
89	1125	2	G	6B	6	C9	2.449	2.219	9.39
90	6410	2	G	6B	6	A1	2.478	2.407	2.87
90	6410	2	G	6B	6	A2	2.467	2.388	3.20
90	6410	2	G	6B	5	A1	2.447	2.363	3.43
90	6410	2	G	6B	5	A2	2.454	2.386	2.77
90	6410	2	G	6B	4	A1	2.446	2.333	4.62
90	6410	2	G	6B	4	A2	2.458	2.317	5.74
90	6412	2	G	6B	6	A1	2.453	2.396	2.32
90	6412	2	G	6B	6	A2	2.473	2.384	3.60
90	6412	2	G	6B	5	A2	2.457	2.390	2.73
90	6412	2	G	6B	4	A2	2.452	2.288	6.69

Table A-5. Pavement structure data

SC	SHRP_ID	CN	Experiment Type		HMA	PCC	Treated Base	Treated Subbase	Granular Base	Granular Subbase	Subgrade
					Pavement Layer Thickness (inch)						
2	1004	2	G	6B	5.4				14	13	
4	0113	1	S	1	4.5				7.5		
4	0114	1	S	1	6.8				12		
4	0115	1	S	1	6.6		8.5				
4	0116	1	S	1	4.1		12.1				132
4	0117	1	S	1	7.6		4.2		4.2		
4	0118	1	S	1	4		7.7		4.1		
4	0119	1	S	1	6.3		4.5		4.2		
4	0120	1	S	1	4		4.3		7.6		
4	0121	1	S	1	4.1		4.2		11.8		
4	0122	1	S	1	4.2		8.6			5.5	
4	0123	1	S	1	6.8		11.7				
4	0124	1	S	1	6.7		15.8				
4	0161	1	S	1	5.7				3.8		
4	0162	1	S	1	8.2						
5	3058	1	G	2	6		7.3				
6	8534	2	G	6B	8.2				6.3	32.3	
6	8535	2	G	6B	10.4				5.9	19.6	
8	6002	2	G	6C	10.5				9.7		
9	4020	2	G	7B	3.4	9			8.8		
12	0101	1	S	1	6.8				8.1		
12	0102	1	S	1	3.9				12.1		
17	5151	2	G	7B	3.3	8.6	3.1				
24	1634	2	G	6C	6.8		4.8			13	
26	0603	2	S	6	5.1	9			4	36	
26	0604	2	S	6	5.4	9.2			4	36	
26	0606	2	S	6	5	9.5			4	36	
26	0607	2	S	6	4.6	9			4	66	
26	0608	2	S	6	6.8	9.3			4	48	
29	5403	2	G	6B	6.2		6.2				
29	5413	2	G	6B	6.9		5				
30	0502	2	S	5	6.9				2.8	14.4	
30	0503	2	S	5	8.8				4.2	14.5	
30	0504	2	S	5	10				3.5	15.6	
30	0505	2	S	5	6.8				2.8	15.3	
30	0506	2	S	5	6.8				2.8	15.3	
30	0507	2	S	5	9.5				3.5	15.6	234
30	0508	2	S	5	9.3				4.2	14.7	
30	0509	2	S	5	7.2				3.8	15	
30	7066	2	G	6B	7.1				3	15.9	
30	7076	2	G	6B	7.6		9.4			27.2	
30	7088	2	G	6B	6.6				1.8	15.8	
31	0113	1	S	1	5.1				8	24	
31	0114	1	S	1	6.7				12	24	
31	0115	1	S	1	4.4		12.7			24	
31	0116	1	S	1	4.4		12.7			24	
31	0117	1	S	1	7.9		3.8		4	24	
31	0118	1	S	1	4.3		8.4		4	24	

Table A-5. Pavement structure data

SC	SHRP_ID	CN	Experiment Type	Pavement Layer Thickness (inch)						
				HMA	PCC	Treated Base	Treated Subbase	Granular Base	Granular Subbase	Subgrade
31	0119	1	S 1	7.9		4		4	12	
31	0120	1	S 1	4.7		4		8	24	
31	0121	1	S 1	5.3		4		12	24	
31	0122	1	S 1	3.8		8.4			24	
31	0123	1	S 1	7.5		12.1			12	
31	0124	1	S 1	7.5		16.3			24	
34	0502	2	S 5	10.8				10.4	41	
34	0503	2	S 5	13.7				11.3	22	
34	0504	2	S 5	13.2				10.7	21	
34	0505	2	S 5	10.8				10	20	
34	0506	2	S 5	11.7				10		
34	0507	2	S 5	14.2				10	54	
34	0508	2	S 5	14.9				11.3	22	
34	0509	2	S 5	11.8				11.3	22	
34	0559	2	S 5	11				10.5	30	
35	0101	1	S 1	7.2				8.6		
35	0102	1	S 1	4.8				12.2		
35	0103	1	S 1	5.3		7.2				
35	0104	1	S 1	8.1		11.1				
35	0105	1	S 1	5.9		4		3.7		
35	0106	1	S 1	7.6		8		2.9		
35	0107	1	S 1	5.9		4		4		
35	0108	1	S 1	7.8		4.2		8		
35	0109	1	S 1	8		4.5		11.9		
35	0110	1	S 1	8		8.3				
35	0111	1	S 1	5		11.3				
35	0112	1	S 1	5.1		14.8				
37	1992	1	G 1	2.4				12	24	
39	0101	1	S 1	6.9				8		
39	0102	1	S 1	3.9				11.8		
39	0103	1	S 1	3.9		8				
39	0104	1	S 1	7		11.8				
39	0105	1	S 1	4		3.7		4		
39	0106	1	S 1	6.8		7.9		3.9		
39	0107	1	S 1	3.8		3.9		4.1		
39	0108	1	S 1	6.6		4		8		
39	0109	1	S 1	7		3.9		12		
39	0110	1	S 1	7.3		7.6				
39	0111	1	S 1	4		12.1				
39	0112	1	S 1	4		15.8				
39	0160	1	S 1	4.1		10.9		4		
39	5010	2	G 7B	2.8	8.8	5				
40	4086	2	G 6B	5.5		7.9				
40	4161	2	G 2	2.8		7.6				
42	1617	2	G 7B	4.7	9.4			9		
42	1618	1	G 1	2				9.6		204
42	1618	2	G 6B	7.9				9.6		204
42	1691	2	G 7B	4	9.7			6		

Table A-5. Pavement structure data

SC	SHRP_ID	CN	Experiment Type		Pavement Layer Thickness (inch)						
					HMA	PCC	Treated Base	Treated Subbase	Granular Base	Granular Subbase	Subgrade
48	1119	2	G	6B	6.9				7.2		
48	3835	1	G	1	8.7			6	14		
48	A502	2	S	5	11.4		14.8	8			
48	A503	2	S	5	14.7		10.6	8			
48	A504	2	S	5	14		10.6	8			
48	A505	2	S	5	11.4		8.8	5.8			
48	A506	2	S	5	11.6		8.8	5.8			
48	A507	2	S	5	14.8		8.8	5.8			
48	A508	2	S	5	15.6		14	8			
48	A509	2	S	5	12.1		14.8	8			
51	1419	2	G	6B	9.5		5.8				144
51	1419	3	G	6D	11.1		5.8				144
53	1008	2	G	6B	5.6				3.1	9.8	
81	1805	2	G	6B	16.3				8.9	4	
83	6450	2	G	6B	10.3				4.5	4.2	
83	6451	2	G	6B	6.7				7.2	3.7	
89	1125	2	G	6B	7.1				14	23.8	
90	6410	2	G	6B	6.8				5.2	4.2	
90	6412	2	G	6B	8.4				5	4.8	

Table A-6. LTPP test section with computed air voids, VMA, and VFA

SC	SHRP_ID	CN	Experiment Type		Layer Number	Layer Type	Average Bulk Specific Gravity	Average Maximum Specific Gravity	Mean Asphalt Content (%)	Aggregate Combined Bulk Specific Gravity	Air Voids (%)	VMA (%)	VFA (%)
1	1001	2	G	6B	7	AC	2.473	2.565	7.20	2.65	3.61	12.96	72.18
1	1019	1	G	2	3	TB	2.280	2.452	3.91	2.59	7.03	15.29	54.03
1	1021	1	G	2	3	TB	2.284	2.450	4.75	2.59	6.79	15.89	57.29
1	4073	1	G	2	5	AC	2.219	2.415	5.20	2.52	8.13	16.21	49.85
1	4126	1	G	1	3	AC	2.345	2.524	3.53	2.67	7.08	15.04	52.91
1	4129	2	G	6B	4	AC	2.331	2.549	4.15	2.75	8.53	18.61	54.15
1	6019	2	G	6D	9	AC	2.308	2.444	5.97	2.60	5.55	16.23	65.80
2	1004	2	G	6B	5	AC	2.391	2.490	5.85	2.70	3.97	16.35	75.71
4	1001	1	G	1	2	AC	2.409	2.429	4.75	2.61	0.84	11.71	92.86
4	1002	1	G	1	2	AC	2.408	2.503	5.50	2.64	3.77	13.60	72.26
4	1006	1	G	1	3	AC	2.276	2.402	4.95	2.63	5.26	17.58	70.06
4	1007	1	G	1	3	AC	2.402	2.404	5.35	2.61	0.09	12.60	99.31
4	1015	1	G	1	3	AC	2.302	2.344	5.45	2.56	1.79	14.70	87.80
4	1016	1	G	1	3	AC	2.333	2.368	5.85	2.56	1.46	13.87	89.46
4	1022	1	G	1	4	AC	2.380	2.431	5.10	2.60	2.08	12.89	83.88
4	1024	1	G	1	3	AC	2.413	2.589	4.20	2.70	6.77	14.35	52.84
4	1034	1	G	1	3	AC	2.340	2.411	4.55	2.62	2.94	14.44	79.61
4	1036	1	G	1	3	AC	2.237	2.356	4.65	2.54	5.07	15.68	67.67
4	1062	1	G	2	4	AC	2.250	2.393	5.40	2.49	6.01	14.32	58.02
4	1065	1	G	2	4	AC	2.255	2.357	5.61	2.49	4.34	14.29	69.59
5	2042	1	G	2	4	AC	2.357	2.386	5.83	2.64	1.20	15.64	92.34
5	2042	1	G	2	3	AC	2.381	2.443	4.46	2.66	2.53	14.34	82.36
5	3048	1	G	2	4	AC	2.346	2.432	5.45	2.63	3.54	15.30	76.88
5	3071	1	G	2	4	AC	2.362	2.452	5.03	2.62	3.67	14.02	73.85
5	3071	1	G	2	3	AC	2.374	2.476	4.36	2.64	4.14	13.81	70.03
6	1253	1	G	1	3	AC	2.384	2.513	5.25	2.72	5.12	16.73	69.39
6	2002	1	G	2	4	AC	2.420	2.453	5.85	2.67	1.34	14.37	90.70
6	2004	1	G	2	4	AC	2.456	2.595	5.05	2.66	5.35	12.04	55.60
6	2038	1	G	2	4	AC	2.331	2.600	5.00	2.78	10.37	20.24	48.76
6	2051	1	G	2	4	AC	2.303	2.509	4.90	2.69	8.17	18.37	55.50
6	2647	1	G	2	4	AC	2.421	2.473	4.95	2.68	2.10	13.80	84.81
6	7452	1	G	2	4	AC	2.243	2.468	4.95	2.66	9.10	19.64	53.66
6	8149	1	G	2	3	AC	2.426	2.475	4.70	2.65	1.99	12.56	84.18
6	8150	1	G	2	4	AC	2.317	2.473	5.10	2.66	6.34	17.13	63.02
6	8156	1	G	1	3	AC	2.292	2.366	6.15	2.57	3.11	15.97	80.52
6	8201	1	G	2	4	AC	2.231	2.429	5.28	2.57	8.12	17.53	53.70
6	8535	1	G	1	5	AC	2.330	2.473	5.35	2.69	5.80	17.79	67.39

Table A-6. LTPP test section with computed air voids, VMA, and VFA

SC	SHRP_ID	CN	Experiment Type	Layer Number	Layer Type	Average Bulk Specific Gravity	Average Maximum Specific Gravity	Mean Asphalt Content (%)	Aggregate Combined Bulk Specific Gravity	Air Voids (%)	VMA (%)	VFA (%)
12	1060	1	G	1	3	AC	2.099	2.349	5.85	2.46	10.65	19.40	45.09
12	3995	1	G	1	4	AC	2.214	2.370	5.60	2.49	6.57	15.76	58.33
12	3997	1	G	1	4	AC	2.247	2.305	6.77	2.44	2.49	13.74	81.88
12	4097	1	G	2	7	AC	2.229	2.316	5.95	2.42	3.78	13.16	71.28
12	4105	1	G	1	4	AC	2.203	2.341	5.55	2.43	5.90	14.13	58.27
12	4106	1	G	1	4	AC	2.179	2.321	6.25	2.41	6.09	14.97	59.31
12	4108	1	G	2	4	AC	2.385	2.443	5.93	2.65	2.36	15.02	84.31
12	4108	1	G	2	3	TB	2.268	2.491	4.85	2.66	8.93	18.68	52.18
12	4135	1	G	1	4	AC	2.285	2.329	6.80	2.46	1.90	12.90	85.24
12	4136	1	G	1	4	AC	2.287	2.353	6.70	2.46	2.80	12.73	77.96
12	4137	1	G	1	4	AC	2.206	2.256	6.10	2.46	2.22	15.34	85.56
13	1004	1	G	1	5	AC	2.325	2.431	6.43	2.48	4.35	12.06	63.94
13	1004	1	G	1	4	AC	2.340	2.486	4.80	2.51	5.89	10.97	46.31
13	1004	1	G	1	3	AC	2.369	2.516	4.24	2.52	5.86	9.80	40.22
13	1005	1	G	1	4	AC	2.316	2.490	4.52	2.54	6.99	12.78	45.30
13	1005	1	G	1	3	AC	2.386	2.469	4.81	2.54	3.37	10.51	67.95
13	1031	1	G	1	4	AC	2.371	2.455	5.40	2.63	3.43	14.59	76.52
13	1031	1	G	1	3	AC	2.429	2.528	4.65	2.65	3.90	12.42	68.57
13	4092	1	G	2	4	AC	2.416	2.491	4.60	2.66	3.04	13.19	76.97
13	4092	1	G	2	3	AC	2.371	2.514	3.45	2.66	5.67	13.84	59.01
13	4093	1	G	2	4	AC	2.425	2.473	5.30	2.67	1.94	13.76	85.88
13	4111	1	G	1	3	AC	2.380	2.519	4.85	2.68	5.52	15.30	63.90
15	1003	1	G	1	5	AC	2.452	2.586	5.55	3.03	5.19	23.32	77.75
15	1003	1	G	1	4	AC	2.461	2.591	5.60	2.94	5.02	20.75	75.81
16	1001	1	G	1	3	AC	2.356	2.433	6.25	2.54	3.15	12.69	75.14
16	1005	1	G	1	3	AC	2.301	2.371	5.65	2.57	2.97	15.21	80.45
16	1007	1	G	1	3	AC	2.447	2.560	7.15	2.76	4.42	17.12	74.15
16	1009	1	G	1	4	AC	2.322	2.338	5.20	2.62	0.68	15.68	95.64
16	1009	1	G	1	3	AC	2.254	2.335	5.05	2.59	3.50	17.20	79.66
16	1010	1	G	1	4	AC	2.306	2.404	5.30	2.63	4.08	16.75	75.62
16	1010	1	G	1	3	AC	2.312	2.399	5.15	2.61	3.63	15.77	76.96
16	1020	1	G	1	4	AC	2.225	2.362	4.85	2.52	5.80	15.62	62.85
16	1021	1	G	1	3	AC	2.292	2.315	5.55	2.61	0.99	16.81	94.11
16	9032	1	G	1	4	AC	2.282	2.462	5.50	2.53	7.35	14.52	49.40
16	9034	1	G	1	4	AC	2.363	2.446	5.80	2.61	3.39	14.44	76.52
17	1002	1	G	1	2	AC	2.453	2.566	4.75	2.71	4.39	13.59	67.73
17	1003	1	G	1	4	AC	2.420	2.478	4.75	2.51	2.36	8.01	70.54

Table A-6. LTPP test section with computed air voids, VMA, and VFA

SC	SHRP_ID	CN	Experiment Type	Layer Number	Layer Type	Average Bulk Specific Gravity	Average Maximum Specific Gravity	Mean Asphalt Content (%)	Aggregate Combined Bulk Specific Gravity	Air Voids (%)	VMA (%)	VFA (%)
18	1028	1	G 1	4	AC	2.363	2.444	4.40	2.68	3.32	15.65	78.81
18	1037	1	G 1	3	AC	2.446	2.465	4.50	2.71	0.79	13.65	94.20
18	2008	2	G 2	5	AC	2.360	2.541	4.45	2.60	7.14	13.22	45.95
18	2008	2	G 2	4	AC	2.365	2.531	4.75	2.59	6.56	12.78	48.67
19	1044	1	G 1	5	AC	2.350	2.496	4.90	2.67	5.83	16.06	63.71
20	1009	1	G 1	3	AC	2.328	2.430	4.55	2.60	4.18	14.36	70.90
20	1009	1	G 1	2	AC	2.298	2.428	4.55	2.60	5.35	15.46	65.37
20	1010	1	G 1	4	AC	2.364	2.436	4.45	2.60	2.96	12.95	77.18
20	1010	1	G 1	3	AC	2.369	2.430	4.65	2.60	2.53	12.95	80.46
23	1001	2	G 6S	6	AC	2.400	2.480	5.65	2.69	3.24	15.57	79.21
23	1009	1	G 1	5	AC	2.307	2.414	7.20	2.69	4.43	20.10	77.95
23	1009	1	G 1	4	AC	2.400	2.475	5.35	2.69	3.03	15.38	80.33
23	1012	1	G 1	5	AC	2.376	2.445	5.10	2.66	2.80	14.85	81.13
23	1012	1	G 1	4	AC	2.419	2.456	4.75	2.66	1.51	13.20	88.52
23	1026	1	G 1	4	AC	2.483	2.530	5.75	2.76	1.89	14.94	87.37
23	1028	2	G 6B	5	AC	2.311	2.488	5.85	2.71	7.10	19.44	63.49
23	1028	1	G 1	4	AC	2.431	2.502	6.15	2.73	2.84	16.11	82.35
24	1632	1	G 2	5	AC	2.344	2.474	6.45	2.83	5.26	22.05	76.15
24	1632	1	G 2	4	AC	2.324	2.415	4.95	2.64	3.77	16.14	76.67
24	2401	1	G 2	6	AC	2.231	2.419	6.15	2.63	7.75	20.09	61.40
24	2401	1	G 2	5	AC	2.265	2.451	6.35	2.64	7.57	19.30	60.77
24	2805	1	G 2	5	AC	2.361	2.437	5.35	2.67	3.13	16.05	80.51
24	2805	1	G 2	4	AC	2.439	2.534	5.35	2.69	3.76	13.95	73.03
26	1012	1	G 1	5	AC	2.336	2.494	4.00	2.42	6.33	7.34	13.77
28	1802	1	G 2	4	AC	2.305	2.438	3.70	2.63	5.44	15.52	64.92
28	1802	1	G 2	3	TB	2.280	2.441	4.05	2.62	6.58	16.23	59.49
28	3082	1	G 2	5	AC	2.300	2.415	4.25	2.64	4.78	16.42	70.87
29	1002	1	G 1	4	AC	2.356	2.474	5.15	2.52	4.75	11.16	57.42
29	1002	1	G 1	3	AC	2.398	2.463	4.75	2.57	2.66	11.05	75.92
29	1005	1	G 1	4	AC	2.527	2.570	4.10	2.71	1.69	10.41	83.74
29	1005	1	G 1	3	AC	2.434	2.546	4.95	2.75	4.40	15.68	71.94
29	1008	1	G 1	4	AC	2.385	2.477	4.15	2.64	3.71	13.11	71.67
29	1010	1	G 1	4	AC	2.347	2.531	5.05	2.61	7.27	14.25	48.99
29	5403	2	G 6B	4	AC	2.512	2.547	4.20	2.68	1.37	10.13	86.43
29	5413	2	G 6B	3	AC	2.480	2.531	3.65	2.67	2.02	10.47	80.75
31	1030	2	G 1	2	AC	2.308	2.405	4.70	2.63	4.06	16.20	74.95
31	6700	2	G 6B	2	AC	2.360	2.412	4.50	2.64	2.18	14.47	84.96

Table A-6. LTPP test section with computed air voids, VMA, and VFA

SC	SHRP_ID	CN	Experiment Type	Layer Number	Layer Type	Average Bulk Specific Gravity	Average Maximum Specific Gravity	Mean Asphalt Content (%)	Aggregate Combined Bulk Specific Gravity	Air Voids (%)	VMA (%)	VFA (%)
32	1020	1	G	1	3	AC	2.380	2.468	4.65	2.64	3.56	13.87	74.30
32	1021	1	G	1	4	AC	2.219	2.414	4.50	2.58	8.09	17.70	54.30
32	2027	1	G	2	4	AC	2.313	2.399	5.50	2.62	3.58	16.31	78.03
33	1001	1	G	1	5	AC	2.406	2.468	5.25	2.70	2.48	15.32	83.82
34	1003	1	G	1	4	AC	2.425	2.544	4.40	2.68	4.68	13.32	64.86
34	1011	1	G	1	4	AC	2.600	2.673	4.00	2.92	2.75	14.45	80.98
34	1030	1	G	1	5	AC	2.381	2.495	6.45	2.71	4.56	17.48	73.91
34	1031	1	G	1	4	AC	2.452	2.568	5.50	2.79	4.52	16.55	72.70
34	1031	1	G	1	3	AC	2.507	2.567	4.15	2.85	2.32	15.59	85.09
34	1033	2	G	6C	5	AC	2.287	2.530	4.75	2.97	9.62	26.55	63.75
34	1033	1	G	2	4	AC	2.583	2.624	6.02	2.96	1.55	17.69	91.21
34	1033	1	G	2	3	TB	2.579	2.713	4.48	2.95	4.95	16.42	69.83
34	1034	1	G	2	3	AC	2.393	2.483	5.26	2.68	3.62	15.08	75.96
34	1034	1	G	2	2	AC	2.426	2.528	4.78	2.67	4.04	13.36	69.76
34	1638	1	G	2	4	AC	2.335	2.490	4.88	2.68	6.23	16.85	63.03
34	1638	1	G	2	3	AC	2.374	2.536	4.20	2.67	6.39	14.73	56.63
35	1022	1	G	1	3	AC	2.349	2.446	5.55	2.65	3.97	16.10	75.35
36	1011	1	G	1	4	AC	2.373	2.486	4.95	2.61	4.55	13.52	66.37
37	1006	1	G	1	4	AC	2.166	2.439	5.75	2.65	11.18	22.77	50.88
37	1024	1	G	1	4	AC	2.360	2.506	6.20	2.79	5.81	20.46	71.62
37	1024	1	G	1	3	AC	2.399	2.515	5.10	2.85	4.60	19.85	76.82
37	1028	1	G	1	3	AC	2.292	2.409	7.20	2.65	4.87	19.32	74.77
37	1028	1	G	1	2	AC	2.339	2.502	4.40	2.65	6.54	15.51	57.82
37	1645	1	G	2	4	AC	2.339	2.451	4.86	2.63	4.58	15.21	69.88
37	1645	1	G	2	3	AC	2.380	2.453	4.30	2.66	2.98	14.05	78.77
37	1802	1	G	1	4	AC	2.252	2.363	6.35	2.66	4.70	20.40	76.97
37	1802	2	G	6B	4	AC	2.415	2.467	5.40	2.66	2.11	13.86	84.79
37	1802	1	G	1	3	AC	2.313	2.467	4.80	2.66	6.23	17.03	63.44
37	1817	1	G	1	4	AC	2.332	2.516	6.20	2.76	7.32	20.31	63.98
37	1817	1	G	1	3	AC	2.395	2.492	4.85	2.75	3.92	17.08	77.05
37	1992	1	G	1	4	AC	2.370	2.503	6.00	2.73	5.32	18.07	70.57
37	2819	1	G	2	4	AC	2.387	2.421	4.50	2.71	1.42	15.73	90.98
37	2824	1	G	2	4	AC	2.292	2.474	5.05	2.65	7.36	17.55	58.07
37	2824	1	G	2	3	AC	2.360	2.506	4.70	2.65	5.82	15.04	61.30
37	2825	1	G	2	4	AC	2.467	2.687	4.90	2.88	8.19	18.26	55.16
37	2825	1	G	2	3	AC	2.488	2.639	4.25	2.85	5.71	16.37	65.15
38	2001	1	G	2	4	AC	2.339	2.410	6.30	2.49	2.93	11.74	75.07

Table A-6. LTPP test section with computed air voids, VMA, and VFA

SC	SHRP_ID	CN	Experiment Type		Layer Number	Layer Type	Average Bulk Specific Gravity	Average Maximum Specific Gravity	Mean Asphalt Content (%)	Aggregate Combined Bulk Specific Gravity	Air Voids (%)	VMA (%)	VFA (%)
41	2002	1	G	2	5	AC	2.390	2.484	5.00	2.52	3.78	9.67	60.96
41	7018	2	G	7S	5	AC	2.182	2.456	4.80	2.47	11.16	15.71	28.96
42	1599	1	G	1	4	AC	2.330	2.553	7.00	2.75	8.71	20.92	58.38
42	1599	1	G	1	3	AC	2.445	2.587	3.95	2.75	5.48	14.59	62.42
45	1008	1	G	1	3	AC	2.391	2.470	4.99	2.66	3.21	14.25	77.47
45	1011	1	G	1	3	AC	2.391	2.488	4.40	2.72	3.89	15.71	75.27
45	1024	1	G	1	3	AC	2.245	2.433	5.45	2.65	7.73	19.63	60.64
46	9106	1	G	2	5	AC	2.234	2.441	5.40	2.55	8.48	17.01	50.15
46	9106	1	G	2	4	AC	2.319	2.479	5.55	2.63	6.44	16.49	60.98
47	1023	1	G	2	5	AC	2.374	2.538	4.85	2.71	6.48	16.47	60.62
47	1023	1	G	2	4	AC	2.431	2.527	4.15	2.71	3.81	13.87	72.56
47	1028	1	G	2	5	AC	2.448	2.525	5.90	2.74	3.05	15.58	80.45
47	1028	1	G	2	4	AC	2.388	2.594	2.75	2.75	7.94	15.49	48.72
47	1029	1	G	2	5	AC	2.331	2.509	4.70	2.68	7.12	16.94	57.95
47	1029	1	G	2	4	TB	2.375	2.495	4.00	2.69	4.81	15.10	68.16
47	2001	1	G	2	5	AC	2.372	2.445	6.20	2.70	3.01	17.29	82.59
47	2001	1	G	2	4	AC	2.434	2.477	4.20	2.71	1.76	13.76	87.24
47	2008	1	G	2	5	AC	2.476	2.523	4.10	2.59	1.86	8.19	77.24
47	2008	1	G	2	4	AC	2.445	2.504	4.00	2.50	2.36	5.98	60.60
47	2008	1	G	2	3	AC	2.407	2.507	3.34	2.70	3.97	13.72	71.05
47	3075	1	G	1	4	AC	2.251	2.529	4.10	2.72	11.01	20.51	46.35
47	3075	1	G	1	3	AC	2.250	2.527	2.55	2.72	10.97	19.34	43.29
47	3101	1	G	2	4	AC	2.374	2.523	4.58	2.70	5.89	16.04	63.26
47	3104	1	G	1	3	AC	2.285	2.481	5.60	2.65	7.91	18.36	56.89
47	3108	1	G	2	5	AC	2.453	2.528	5.20	2.71	2.98	13.97	78.67
47	3108	1	G	2	4	AC	2.505	2.532	4.10	2.71	1.07	11.22	90.50
47	3108	1	G	2	3	TB	2.397	2.585	3.20	2.71	7.27	14.30	49.17
47	3109	1	G	2	4	AC	2.373	2.528	4.05	2.72	6.15	16.15	61.94
47	3109	1	G	2	3	TB	2.326	2.578	2.90	2.72	9.75	16.89	42.27
47	3110	1	G	2	5	AC	2.258	2.680	5.10	2.81	15.72	23.54	33.20
47	3110	1	G	2	4	AC	2.403	2.615	3.90	2.81	8.11	17.69	54.18
47	9024	1	G	2	3	AC	2.421	2.521	4.20	2.70	3.99	14.09	71.71
47	9025	1	G	2	4	AC	2.354	2.546	4.40	2.70	7.53	16.60	54.66
48	1039	2	G	1	4	AC	2.325	2.482	4.35	2.60	6.33	14.16	55.31
48	1047	1	G	1	4	AC	2.380	2.467	3.85	2.64	3.54	13.26	73.31
48	1048	1	G	2	3	AC	2.259	2.349	5.55	2.50	3.81	14.43	73.58
48	1060	1	G	1	5	AC	2.262	2.425	4.75	2.48	6.72	13.00	48.31

Table A-6. LTPP test section with computed air voids, VMA, and VFA

SC	SHRP_ID	CN	Experiment Type		Layer Number	Layer Type	Average Bulk Specific Gravity	Average Maximum Specific Gravity	Mean Asphalt Content (%)	Aggregate Combined Bulk Specific Gravity	Air Voids (%)	VMA (%)	VFA (%)
48	1060	1	G	1	4	AC	2.354	2.456	4.05	2.53	4.17	10.65	60.88
48	1065	1	G	1	4	AC	2.336	2.456	4.40	2.57	4.88	13.01	62.52
48	1068	1	G	1	5	AC	2.296	2.400	4.85	2.57	4.31	14.62	70.52
48	1068	1	G	1	4	AC	2.297	2.411	4.05	2.68	4.75	17.48	72.81
48	1077	1	G	1	3	AC	2.395	2.449	4.35	2.61	2.21	12.19	81.87
48	1123	2	G	1	4	AC	2.303	2.504	3.55	2.60	8.03	14.49	44.61
48	2108	1	G	2	4	AC	2.319	2.456	4.63	2.55	5.57	12.98	57.07
48	2133	1	G	2	6	AC	2.273	2.423	4.90	2.48	6.17	12.72	51.53
48	2176	1	G	2	4	AC	2.304	2.410	5.35	2.61	4.40	16.10	72.67
48	3559	1	G	2	4	AC	2.354	2.494	3.85	2.61	5.61	13.15	57.32
48	3669	1	G	2	5	AC	1.679	1.733	8.60	1.83	3.09	15.31	79.80
48	3669	1	G	2	4	AC	2.255	2.427	6.25	2.57	7.05	17.28	59.17
48	3689	1	G	2	5	AC	2.082	2.441	5.00	2.58	14.73	23.07	36.17
48	3749	1	G	1	5	AC	2.121	2.266	6.00	2.40	6.38	16.70	61.80
48	3835	1	G	1	4	AC	2.282	2.397	4.90	2.56	4.81	14.93	67.80
49	1001	1	G	1	3	AC	2.391	2.395	5.70	2.64	0.15	14.38	98.97
49	1008	1	G	1	3	AC	2.398	2.441	5.65	2.63	1.78	13.72	87.01
51	1002	1	G	1	4	AC	2.338	2.456	5.95	2.66	4.80	17.17	72.01
51	1002	1	G	1	3	AC	2.484	2.596	4.35	2.81	4.34	15.18	71.42
51	1023	2	G	6C	6	AC	2.205	2.424	5.80	2.73	9.02	23.69	61.94
51	1023	1	G	1	5	AC	2.399	2.421	6.05	2.65	0.90	14.62	93.81
51	1023	1	G	1	4	AC	2.407	2.460	4.30	2.75	2.17	16.10	86.53
51	1417	1	G	2	5	AC	2.422	2.667	5.37	2.64	9.20	12.87	28.51
51	1417	1	G	2	4	AC	2.432	2.641	4.80	2.60	7.92	10.60	25.32
51	1419	2	G	6B	4	AC	2.367	2.489	6.05	2.63	4.88	15.04	67.53
51	1419	2	G	6B	3	AC	2.422	2.525	5.30	2.60	4.06	11.40	64.38
51	1464	1	G	1	5	AC	2.307	2.378	6.15	2.64	2.99	17.63	83.06
51	1464	1	G	1	4	AC	2.385	2.495	5.38	2.60	4.41	12.83	65.61
51	2004	1	G	2	4	AC	2.237	2.393	6.04	2.64	6.52	20.02	67.45
51	2004	1	G	2	3	AC	2.336	2.459	4.28	2.60	5.00	13.70	63.51
51	2021	1	G	2	4	AC	2.301	2.445	5.65	2.65	5.89	17.74	66.79
56	1007	1	G	1	3	AC	2.320	2.359	6.85	2.54	1.64	14.51	88.71
56	2017	1	G	2	3	AC	2.320	2.427	5.60	2.58	4.42	14.75	70.04
56	2018	1	G	2	4	AC	2.245	2.379	6.15	2.62	5.63	19.23	70.73
56	2019	1	G	2	5	AC	2.382	2.438	5.65	2.61	2.31	13.66	83.10
56	2020	1	G	2	3	AC	2.356	2.430	6.20	2.64	3.03	15.93	81.00
56	2037	1	G	2	3	AC	2.413	2.464	5.35	2.61	2.07	12.30	83.15

Table A-6. LTPP test section with computed air voids, VMA, and VFA

SC	SHRP_ID	CN	Experiment Type		Layer Number	Layer Type	Average Bulk Specific Gravity	Average Maximum Specific Gravity	Mean Asphalt Content (%)	Aggregate Combined Bulk Specific Gravity	Air Voids (%)	VMA (%)	VFA (%)
56	7772	1	G	2	3	AC	2.252	2.326	6.86	2.45	3.21	13.82	76.80
56	7773	1	G	2	4	AC	2.374	2.466	5.30	2.64	3.73	14.60	74.45
56	7775	1	G	1	4	AC	2.350	2.388	6.40	2.58	1.62	14.44	88.78
81	1805	1	G	1	4	AC	2.290	2.414	6.20	2.58	5.15	16.44	68.68
81	2812	1	G	2	3	AC	2.311	2.377	5.20	2.57	2.76	14.55	81.02
82	1005	1	G	1	4	AC	2.337	2.452	5.15	2.62	4.72	15.25	69.03
82	6007	2	G	6S	5	AC	2.304	2.445	5.70	2.68	5.76	18.61	69.06
82	9017	1	G	2	6	AC	2.431	2.524	4.44	2.72	3.67	14.29	74.34
82	9017	1	G	2	5	TB	2.393	2.519	3.60	2.72	5.02	15.13	66.80
83	6450	2	G	6B	4	AC	2.310	2.540	3.55	2.60	9.07	14.25	36.32
83	6451	2	G	6B	4	AC	2.307	2.516	3.50	2.60	8.31	14.30	41.92
85	1808	1	G	1	4	AC	2.455	2.510	6.50	2.64	2.19	12.63	82.70
88	1645	1	G	1	4	AC	2.336	2.434	5.00	2.60	4.03	14.27	71.74
88	1646	1	G	2	4	AC	2.331	2.371	6.35	2.59	1.72	15.26	88.73
88	1646	1	G	2	3	AC	2.355	2.442	5.05	2.58	3.53	13.23	73.30
88	1647	1	G	2	5	AC	2.434	2.545	6.65	2.67	4.34	14.48	70.01
89	1127	1	G	1	5	AC	2.370	2.427	6.70	2.31	2.37	3.66	35.21
89	1127	1	G	1	4	AC	2.388	2.452	5.00	2.38	2.62	4.40	40.57
90	6410	2	G	6B	5	AC	2.375	2.451	5.35	2.64	3.10	14.46	78.56
90	6412	2	G	6B	5	AC	2.390	2.457	5.60	2.64	2.73	14.11	80.67